ASSESSMENT OF TRANSMISSION LENGTH AND BOND STRENGTH OF PRETENSIONED CONCRETE SYSTEMS WITH SEVEN-WIRE STRANDS

A THESIS

Submitted by

PRABHA MOHANDOSS

for the award of the degree

of

DOCTOR OF PHILOSOPHY

DEPARTMENT OF CIVIL ENGINEERING

INDIAN INSTITUTE OF TECHNOLOGY MADRAS

CHENNAI, INDIA

JULY 2019

THESIS CERTIFICATE

This is to certify that the thesis titled "**ASSESSMENT OF TRANSMISSION LENGTH AND BOND STRENGTH OF PRETENSIONED CONCRETE SYSTEMS WITH SEVEN-WIRE STRANDS**", submitted by **Ms. PRABHA MOHANDOSS**, to the Department of Civil Engineering, Indian Institute of Technology Madras, Chennai, for the award of the degree of Doctor of Philosophy is a bona fide record of research work carried out by her under my supervision. The contents of this thesis, in full or in parts, have not been submitted and will not be submitted to any other Institute or University for the award of any degree or diploma.

Dr. Radhakrishna G. Pillai
Research Guide
Associate Professor
Department of Civil Engineering
Indian Institute of Technology Madras
Chennai - 600 036, India

Chennai, India

July 1, 2019

DEDICATION

To my family and teachers

ACKNOWLEDGEMENTS

I thank IIT Madras for the great opportunity given to me to pursue doctoral studies in the BTCM division. I express my feelings of gratitude to Dr. Radhakrishna G. Pillai for his motivating ideas, constant support, immense patience for long discussions, thoughtful feedback, meticulous comments, and his invaluable guidance throughout the research program.

With great respect, I express my thanks to Prof. Ravindra Gettu for his constructive criticisms, suggestions, words of encouragement, and for inculcating a sense of responsibility and values in me during the various stages of this research program. I am thankful to Prof. Manu Santhanam and Dr. Piyush Chaunsali for their valuable comments and support during the various phases of this research program. Additionally, I express my gratitude to them for their tireless efforts and helpful ideas during the weekly research group meetings.

I would like to express my gratitude to my Doctoral Committee Members Prof. Amlan Kumar Sengupta, for his constant support and refreshing insights about this research program and Prof. Srinivasan Chandrasekaran for his words of encouragement during seminars. I express my sincere thanks to the present Head, Department of Civil Engineering, Prof. K. Ramamurthy, and the former heads Prof. A. Meher Prasad and Prof. S.R. Gandhi for facilitating my academic needs during the pursuit of my Ph.D. programme.

I have been greatly benefitted from Prof. Mark G. Alexander and Prof. Surendra P. Shah with their insightful comments, suggestions, and warm words of encouragement throughout this research program. Discussions with Prof. Vellore Gopalaratnam and Prof. Carmen Andrade during their visit to IIT Madras have been illuminating. I am extremely thankful to all faculty members of BTCM division for their intangible support.

I express my sincere thanks to all the lab staff, especially, Ms. Malarvizhi, Mr. Krishnan, Mr. Subramanian, Mr. Gaseber, and Mr. Soundarapandian, for their help in the experimental work. I thank Mr. R. Murali, Mr. Prince, Mr. Balu, and Mr. Nagarajan, Department workshop facility for their inestimable help in the fabrication of moulds and test set-ups. The support from the BTCM office and Civil Engineering office is gratefully acknowledged. I thank Dr. T. Chellappa for his helpful suggestions in document correction.

I would like to thank Mr. George from Concrete product for sharing his thoughts on precast sleepers and providing materials required for the experiments. I thank Dr. Ganesh from L & T for sharing the design details of a bridge for the case study. I am very delightful to acknowledge the support from all our beloved intern students, especially Sriram K. K., Sree Maheshwari, Nandita Gettu, and Sethuraj for their valuable contributions to this research study. Also, I am thankful to my research assistants Anupama, Sree Anand S., Nirmal Nayak, Rakishma, Rajath, Herry Thomas, who helped me in many ways.

My sincere appreciation to all my friends and fellow researchers at IIT Madras, Dr. Jayachandran K., Dr. Bahurudeen, Dr. Komathi M., Sakthivel, Srinivasan, Sooraj, Sripriya, Swathy, Aswathy, Sundar, Deepak, Vaishnav, Stefie, Sanoop , Rohit, Sachin, Anusha S. B., Menaka, Dyana J., Manu, Sujatha, Divya and all other research scholars for the suggestions, discussions and help rendered during different stages of my research work and for making my stay at IIT Madras the most pleasant and memorable I am grateful to Ms. Dhanya R. for her moral support and encouragement in several ways.

I am grateful to Ram, Shriram and Yuvaraj for cheering me in various phases of my research work. A big thanks to Santhosh for his timly help to get things done at the crucial times of Ph.D.

I thank My cousins Hema and Rajesh for their motivational words during the period of my research. I thank my bestie Aishwarya Srinidhi for being my constant companion and sacrificed many trips for early completion of thesis. My appreciation to Mr. Kumaresh for all the conversation and discussions to keep me going. I express my profound thanks to Vigneswari, Umesh, Nivethitha, Vinoth, Anandhi, Priya, Vaishu, Jeeva, and Vivek for their favours, especially the delicious home food.

With deep respect, I express gratitude to my beloved parents Mohandoss and Kalavathi for their understanding and motivational words of courage to achieve my ‘Ph.D. dream’. Many thanks are due to my brother Arvind for his constant support. I am grateful to my grandmother for her blessings. I appreciate all my relatives for their continuous encouragement.

My special thanks to my love Ganesh for his abundance support, care, and patience in achieving my dream.

Prabha Mohandoss

ABSTRACT

In the PTC systems, the bond between the strand and concrete plays a vital role in transferring the prestress from the strand to the surrounding concrete. The length of the strand (near the ends) required to transfer or transmit the prestress from the strand to the surrounding concrete is defined as 'transmission length (L_t)'. If the bond is inadequate, the prestress would not be transferred effectively. This could reduce the shear and flexural performance of the PTC members, especially in the transmission zone, where transverse cracks in concrete could develop due to the poor bond. Hence, an accurate estimation of the L_t and the bond strength (τ_b) between the strand and concrete is necessary to obtain the rational shear design in the transmission zone.

Many factors (especially the properties of strand and concrete) influence the L_t and τ_b. However, the existing design formulations for the L_t do not consider these major factors in the estimation of the L_t. Many standards consider only the diameter of the strands to estimate the L_t. Consideration of only the d_s could lead to the overestimation or underestimation of the L_t. Both overestimation and underestimation of the L_t are unsafe, especially for shear performance of the PTC systems. In the PTC systems, the determination of the bond strength is a challenging task due to the applied prestress and required embedment length of strand to transfer the stress to the surrounding concrete unlike the conventional reinforced concrete (CRC) systems. The existing test methods to determine the strength of Strand-Concrete (S-C) bond in the PTC systems are ASTM A1081 (2012), Moustafa's method, and ECADA's test method. However, these methods suggest a pre-defined slip of 2.5 mm to determine the S-C bond strength (τ_b), which may lead to erroneous results and significant scatter.

This thesis presents a comparative study of the formulations of transmission length (L_t) given in various codes such as AASHTO, ACI, AS, BIS, CSA, EN2, IRC, and *fib* and other literature. A comprehensive experimental study was carried out in order to determine the L_t of the PTC members. Totally, 12 prism specimens [(100 ×100 × 2000) mm] with a seven-wire strand at the centre were cast using four different compressive strengths of concrete. An initial prestress of $0.75f_{pu}$ (where, f_{pu} = ultimate tensile strength of strand) was applied. The average compressive strength of concrete at transfer (f_{ci}) was 23, 28, 36, and 43 MPa, respectively.

Then, the L_t was measured using DEMEC gauges and compared with the L_t calculated using the various available formulations in literature. Moreover, the challenges involved with the measurements of DEMEC measurements and possible human errors in the measurements are discussed. The results indicate that when the f_{ci} increases from about 23 to 43 MPa, the L_t could decrease by about 34%. Based on this data, a new bilinear formulation is proposed to determine the L_t as a function of f_{ci} and it is expected to help achieve more rational structural designs. Further, in order to understand the significance of time on the L_t, measurements were taken at different ages. Additionally, case studies indicate that lower and higher estimates of L_t as per the available formulations, will lead to lower shear resistance in the transmission zone of the PTC members and lower estimate of bursting tensile stress in concrete, respectively. This could lead to poor shear performance and failures of the PTC systems.

To overcome the challenges associated with the determination of the bond strength of pretensioned strands in concrete, this thesis puts forward a new procedure to determine the bond strength of strands in concrete. This examines the effects of the compressive strength of concrete (f_c), the prestress level (f_{ps}), and the embedment length of strands (l_e) on the determined bond strength of strand. Pull-out specimens with a 12.7 mm dia. strand embedded in concrete prisms (100×100 mm cross-section) were used for the study. Two prestress levels of 0.1 f_{pu} and 0.7 f_{pu} (taut and stressed strands, respectively), two l_e of 450 and 950 mm, and two f_c of 43 and 62 MPa were used. There were significant variations on the bond stress slip behaviour between the stressed and taut strands in concrete with different l_e. In the PTC systems, unlike the CRC systems, the transmission length (L_t) plays a vital role in deciding the required embedment length of strands in concrete. Therefore, the l_e should be at least more than twice the L_t of the specimens. A total of 24 specimens were tested, and the $\tau - s$ curves indicated that the conventional way of defining the τ_b as the stress corresponding to 2.5 mm slip at the free end is not suitable for the PTC specimens. Based on these, this thesis proposes a new method to determine the τ_b as an S-C interface parameter that is independent of l_e and f_{ps} and provides results with less scatter. In this method, τ_b is defined as the bond stress corresponding to the yield point of the τ-s curve. Due to the relatively less cumbersome procedures to prepare the test specimens with taut strands (instead of fully stressed strands), this method can be used as a quality control test in the field.

TABLE OF CONTENTS

LIST OF FIGURES

LIST OF TABLES

NOTATIONS AND ABBREVIATIONS

NOTATIONS

α	Proportionality constant and coefficient used in the L_t equation by Barnes et al. (2003) and Pellegrino et al. (2015)
α_1	Factor to account for the releasing method
α_2	Factor to account for the type of strand in EN 2 (2004) and the action effect in *fib* MC (2010)
α_3	Factor to account for pretensioned strand in *fib* MC (2010)
η_1	Upper, mean, and lower bound value of τ
η_2 and η_3	Experimental constants
η_{p1}	Factor to account for the type of tendon in *fib* MC (2010)
η_{p2}	Factor to account for the position of the tendon in *fib* MC (2010)
β,γ,δ	Coefficient used in the L_t equation Pellegrino et al. (2015)
λ	Factor to account for low-density concrete
θ	Helical angle of the strand (°)
ε_{ce}	Effective strain on the concrete surface (mm/mm)
ε_{pi}	Strain in the strand due to initial prestress before losses (mm/mm)
ε_{pe}	Effective strain in the strand (mm/mm)
$\varepsilon_{ps(x)}$	Strain in strand at *x* distance after transfer (mm/mm)
$\varepsilon_{c(x)}$	Strain on the concrete surface at *x* distance (mm/mm)
$\varepsilon_{c,\,max}$	Maximum strain on the concrete surface (mm/mm)
$\varepsilon'_{c(x)}$	Smoothened strain on the concrete surface at *x* distance (mm/mm)
$\Delta\varepsilon_p$	Strain difference in the strand with adjacent concrete (mm/mm)

Δl	Change in length (mm)
Δl_{nc}	Elastic deformation of strand portion outside the concrete (mm)
τ	Bond stress (MPa)
$\tau_{01}/\tau_{2.5}$	Average bond stress corresponding with the pull-out force @ 0.1 in/2.5 mm slip (MPa)
τ_b	Bond strength between the strand and concrete (MPa)
$\tau_{b,\ taut}$	Bond strength of the taut strands in concrete (MPa)
$\tau_{b,\ stressed}$	Bond strength of the stressed strands in concrete (MPa)
τ_{yield}	Bond stress at the yield point on τ-s curve (MPa)
φ_c	Resistance factor for concrete
φ_p	Resistance factor for prestressing tendons
b_w	Width of the cross section at the centroid (mm)
d	Effective depth of the member (mm)
d_o	Diameter of outer wire of the strand (mm)
d_s	Diameter of prestressing strand (mm)
f_{bpt}	Bond stress at the time of releasing (MPa)
f_c	Compressive strength of concrete at pull-out testing (MPa)
f_{ci}	Compressive strength of concrete at release (MPa)
f_{ck}	Characteristic compressive strength of concrete (MPa)
f_{cp}	Concrete stress due to effective prestress at centroid (MPa)
f_{ctd}	Design tensile strength of concrete (MPa)
f_t	Maximum principal tensile stress (MPa)
f_{pe}	Effective stress in prestressing steel after allowance for all prestress losses (MPa)
f_{pi}	Initial prestress of strand before losses (MPa)

f_{ps}	Applied prestress (MPa)
f_{pu}	Ultimate tensile stress in strand (MPa)
f_v	Transverse tensile stress at the centroid of the end face (MPa)
l	Length of strand at LE (mm)
l_e	Length of embedded strand in concrete (mm)
l_{bb}	Length of bonded breaker in concrete (mm)
l_{nc}	Length of strand portion outside the concrete – not in contact (mm)
l_x	Distance of section considered from the starting point of the L_t (mm)
k	Risk factor
k_1	Factor to account for the distance of section considered from L_t
p	Circumference of the strand (mm)
s	Bond slip (mm)
$s_{01}/s_{2.5}$	Bond slip at 0.1 in/2.5 mm
$s(x)$	Bond slip at any load 'x'(mm)
A	Cross-sectional area of the concrete (mm^2)
A_{ps}	sum of cross-sectional areas of seven wires in a strand (mm^2)
A_{sv}	Area of vertical steel required (mm^2)
D	Overall depth of the member (mm)
F_{bat}	Transverse tensile force (kN)
F_b	Bearing force at the S-C interface (kN)
F_s	Shear force at the S-C interface (kN)
I	Moment of inertia of gross cross section (mm^4)
K_t	Factor to represent the type of tendon in BS 8110 (1997)
L	Length of the specimen (mm)

L_b	Bond length (mm)
L_d	Development length (mm)
L_t	Transmission length (mm)
$L_{t,\ code}$	L_t value obtained using codal equations (mm)
$L_{t,\ estimated}$	Calculated L_t based on the proposed model (mm)
$L_{t,\ n}$	L_t measured at n^{th} day (mm), where n = 0, 7, 28, 120, 180, 270, 300, 360 days
N	Normal force at the S-C interface (kN)
M	Internal moment due to prestress (N mm)
P	Axial pull-out force (kN)
P_0	Applied pre load before slipping (kN)
P_{max}	Maximum axial pull-out force (kN)
P_s	Applied load at s mm slip (kN)
P_T	Axial prestressing force at transfer (kN)
Q	Moment of the area (mm^3)
V_c	Shear capacity contributed by the concrete (kN)
V_{ci}	Ultimate shear resistance of cracked section in flexure (kN)
V_{cw}	Ultimate shear resistance of uncracked section (kN)
V_n	Nominal shear resistance of concrete (kN)
V_p	Vertical component of the effective prestress (kN)
V_s	Shear capacity contributed by stirrups (kN)
$V_{n,\ max}$	Maximum shear resistance (kN)

ABBREVIATIONS

AASHTO	American Association of State Highway and Transportation
ACI	American Concrete Institute
AMA	Anchorage Measurement System
AMS	Average Maximum Strain
AS	Australian Standard
ASTM	American Standard Test Method
BS	British Standard
CRC	Conventional Reinforced Concrete
CSA	Canadian Standard Association
DEMEC	Demountable Mechanical Gauge
ECADA	Ensayo para Caracterizar la Adherenciamediante Destesado y Arrancamiento
FE	Free End
HCC	Hollow Core Concrete
IRC	Indian Road Congress
IS	Indian Standards
JE	Jacking End
LE	Live End
LVDT	Linear Variable Differential Transducer
NASP	North American Strand Producers
PTC	Pretensioned Concrete
RE	Releasing End
S-C	Strand-Concrete
SCC	Self-Compacting Concrete

1 INTRODUCTION

1.1 PROBLEM STATEMENT

Pretensioned concrete systems (PTC) with seven-wire strands are widely used as girders in bridges/buildings and hollow-core slabs in buildings. In the PTC elements, the prestress from the strand is transferred to the surrounding concrete through the bond between the strand and concrete, say Strand-Concrete (‘S-C bond’, herein). If the prestress is not adequately transferred within a particular distance from the free end of strands, the shear critical sections, near the support, may not have the required prestress to resist the applied shear stresses. The length of a strand required to develop the effective prestress (f_{pe}) from the strand to concrete is defined as L_t. An inadequate transmission length (L_t) could result in shear cracks under the external loading (Elliott, 2014). Figure 1.1 shows a classic case of inclined shear cracks observed in highway bridge girders, in Mumbai, India - necessitating a standard quality control test for the τ_b of the PTC systems. Such shear cracks can occur due to (i) low strength concrete, (ii) poor construction practices, (iii) low bond strength, and (iv) inadequate design provisions for L_t. Similar kind of failure can be observed in slabs/beams used in buildings under loading conditions. Figure 1.2 shows an instance of shear failure of precast pretensioned hollow core slab due to inadequate L_t under loading (Elliot, 2014).

The shear demand is usually high in the transmission zones, say near the support regions of the PTC systems. The underestimation of L_t can lead to less conservative shear designs. Therefore, a realistic estimation of the L_t is essential for achieving an adequate shear capacity, especially for the precast pretensioned hollow-core slabs which do not have shear reinforcements. Various factors associated with concrete and strand properties can influence the L_t. However, some design standards do not account for these factors and they could result in an inadequate L_t. This research work examines the existing formulations for estimating the L_t, their limitations, and the experimental observations on the influence of the compressive strength of concrete and time on the L_t. Both underestimation and overestimation of the L_t have their significance on the structural performance of the PTC members that are addressed in this study.

(a) A pretensioned concrete bridge on an elevated highway

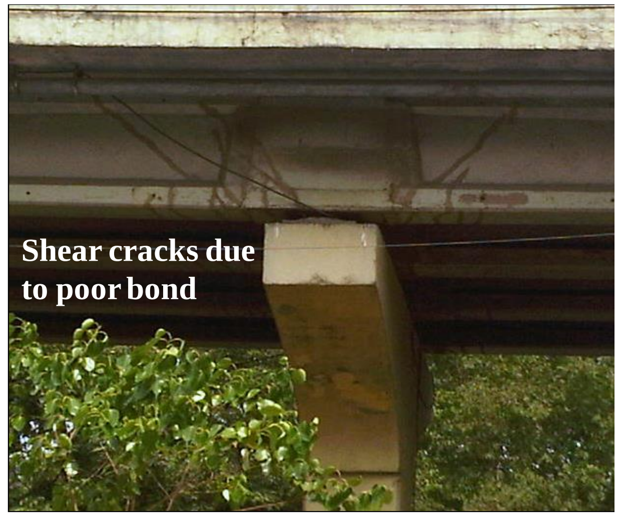

(b) Shear cracks near the support regions of the pretensioned girders

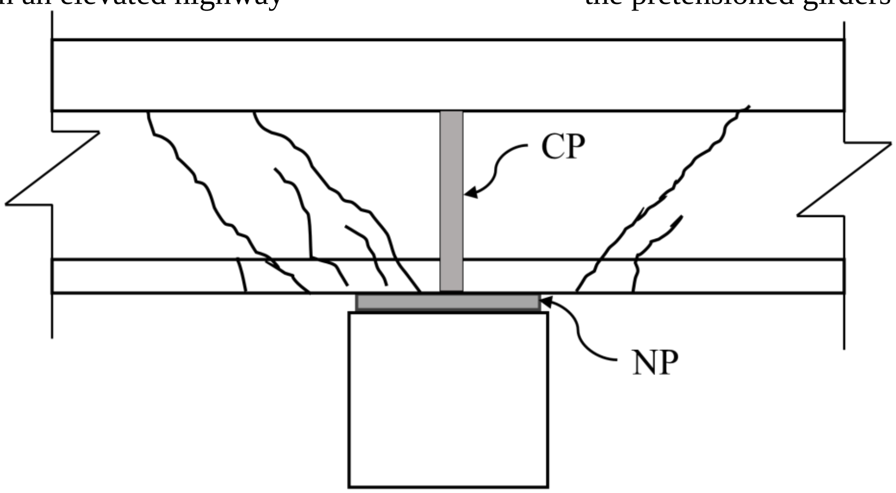

CP: Closure pour; NP: Neoprene pad

(c) A schematic illustration of the inclined shear cracks on the girder

Figure 1.1 Shear cracks observed on the girders of highway bridges in India

(a) Use of hollow-core slabs in a commercial building; Courtesy: https://infogram.com

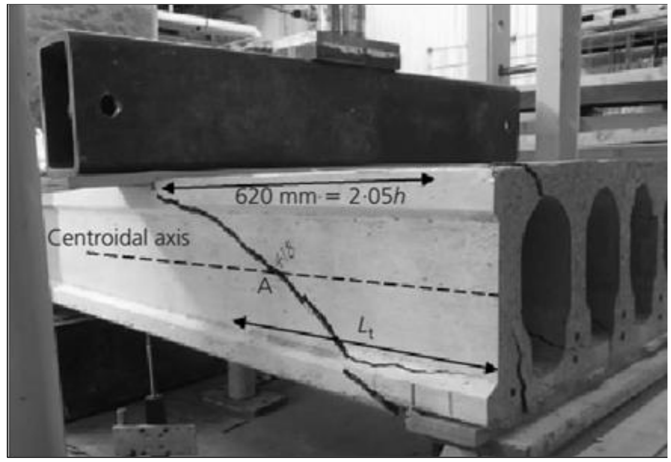

(b) Occurrence of shear crack due to the inadequate L_t

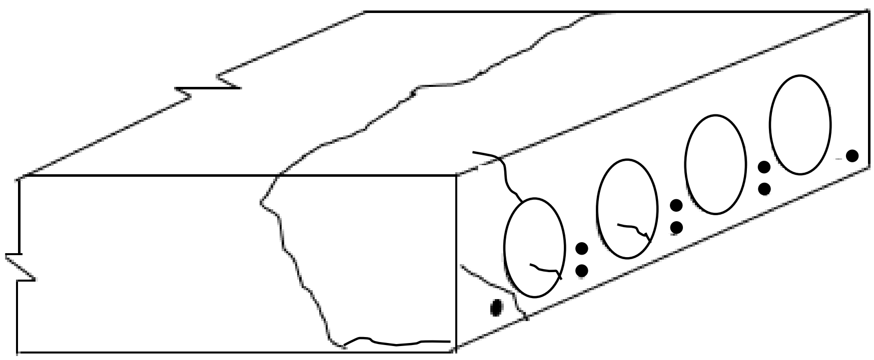

(c) A schematic representation of the inclined shear cracks in the HCS member

Figure 1.2 Shear cracks in the hollow-core slab member (Elliot, 2014)

The transmission length of the PTC members depends on the bond between the pretensioned strand and concrete. If the bond of the PTC members is inadequate, then it could substantially reduce the structural performance. Eventually, this could cause shear failure at the ends and flexural cracks in the members. The bond action is not only necessary to provide an adequate safety by allowing the strand and concrete to work together, but also to control the structural behaviour by offering an adequate level of ductility (*fib* Bulletin 10, 2000). The failure of the S-C bond can lead to structural cracks, which can provide easy access for the deleterious elements causing premature and localized corrosion of the embedded strands. Therefore, ensuring the sufficient S-C bond strength (τ_b) is essential to achieve the desired safety and service life for the PTC structures. State-of-the-art design procedures and construction materials/practices are available to ensure the adequate S-C bond. Also, very limited information is available on the bond stress-slip behaviour of the PTC systems unlike the conventional reinforced concrete (CRC) systems, which is important to define the bond strength of the PTC systems. Also, many standards and literature follow the same bond strength definition or failure condition of rebar for strands using 2.5 mm slip method. However, these conditions may not be valid for strands. This research work presents the laboratory tests conducted at IIT Madras. Based on this study, a relatively easy-to-prepare pull-out test specimen and an evaluation procedure that minimizes the effects of the embedment length (l_e) and prestress applied (f_{ps}) on the determined τ_b is proposed to use as a quality control measure at the site.

1.2 DEFINITIONS

This section catalogues the definitions of some keywords used in this thesis work.

i. 7-wire strand: Six outer wires wound helically around a king wire.

ii. Bond length (L_b): Length of embedded pretensioned strand, required to develop the ultimate prestress from the effective prestress when the member is loaded (see Figure 2.4).

iii. Bond slip (s): The relative axial movement between strand and concrete.

iv. Bond strength (τ_b): The maximum bond stress that a strand-concrete system can sustain before failure.

v. Bond stress (τ): Shear stress experienced by the strand-concrete interface

vi. Development length (L_d): Length of the embedded pretensioned strand, required to develop the design strength of steel at a critical section under service.

vii. Effective prestress (f_{pe}): Stress remaining in the prestressing strand after losses due to elastic shortening and seating just after transmission of prestress.

viii. Embedment length (l_e): Embedded length of strand in the concrete or cement grout specimens or length of strand in contact with the surrounding concrete/cement grout.

ix. Free end (FE): The end of pull-out specimen, where the strand is not gripped and kept free.

x. Initial prestress (f_{pi}): The initial stress applied to tension the strand before casting of concrete.

xi. Live end (LE): The end of pull-out specimen, where the strand is gripped to apply load during pull-out test.

xii. Stress adjusting system: A plate welded with three hexagonal nut-bolt used as stress adjusting system to stress/release the stress in the strand.

xiii. Stressed strands: Strands experiencing an initial prestress of about $0.7f_{pu}$.

xiv. Taut Strands: Strands experiencing an initial prestress of about 0.1 f_{pu} (to keep the strands straight).

xv. Transmission length or Transfer length (L_t): Length of embedded pretensioned strand required to transfer the effective prestress from strand to concrete.

1.3 RESEARCH QUESTIONS

i. Are the existing formulations for the design transmission length of the PTC systems conservative? What does the overestimation/underestimation of L_t imply on the structural performance of the PTC systems? – See Chapter 5 for results

ii. Does the compressive strength of concrete at transfer influence the length needed to transfer the prestress from the strand to concrete? If so, should it be considered to determine the transmission length? – See Chapter 5 for results

iii. Does the transmission length of pretensioned concrete systems change as a function of age or exposure period? – See Chapter 5 for results

iv. Do the existing test methods to determine the bond strength between the strand and concrete represent the true conditions of PTC systems? – See Chapter 6 for results

v. Is the conventional method of determining the bond strength based on an absolute slip of 2.5 mm at free end valid for the PTC systems? – See Chapter 6 for results

vi. Do prestress level and embedment length of strand influence the performance of strand-concrete bond? – See Chapter 6 for results

1.4 OBJECTIVES AND SCOPE

Following are the objectives of this research work. The points following each objective indicate the scope of the work.

1. To determine and model the effect of compressive strength at transfer (f_{ci}) on the transmission length (L_t) of pretensioned concrete systems.

    - Initial prestress: 0.75 f_{pu}
    - Compressive strength of concrete at transfer (f_{ci}): 23, 28, 36, and 46 MPa.
    - Cross section of specimen: (100 × 100) mm
    - Time effect: 3 to 360 days

2. To develop a simplified procedure and determine the bond strength of strand in concrete as a function independent of the embedment length and prestress level.

    - Applied prestress (f_{ps}): 0.1 f_{pu} and 0.7 f_{pu}
    - Compressive strength of concrete at testing (f_c): 40 and 60 MPa
    - Embedment length of strand (l_e): 450 and 950 mm
    - Cross section of specimen: (100 × 100) mm

1.5 RESEARCH METHODOLOGY

An experimental research methodology designed to meet the objectives is formulated as shown in Figure 1.3. The experimental programs that are developed to achieve the research objectives are discussed in Chapter 4.

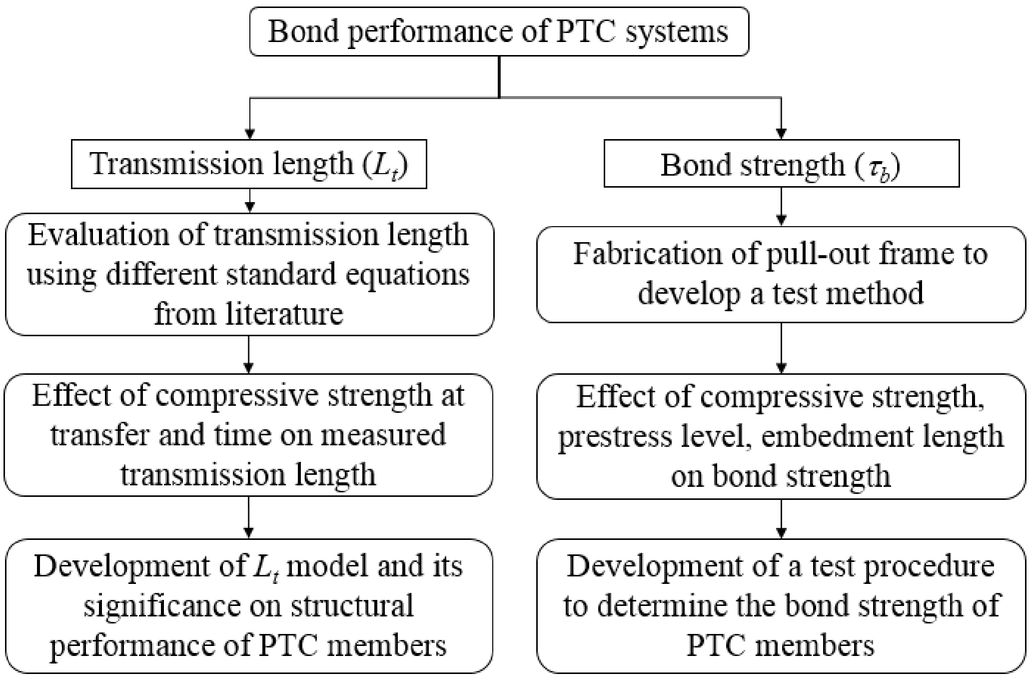

Figure 1.3 A chart showing the research methodology

1.6 ORGANIZATION OF THE THESIS

This thesis comprises seven chapters and two appendices. Following is a brief explanation of the components of the thesis.

Chapter 1 presents the research problem which the thesis attempts to address. This chapter defines the terminology used in the study, highlights the research questions and hypothesis, and frames the objective and scope of the work. An overview of the research methodology formulated to address the objectives are also presented.

Chapter 2 considers a critical review on factors affecting the transmission length and bond strength of the PTC members, the available test methods and their limitations in determining the transmission length and bond strength. Also, it reviews the available codal/literature formulations to determine the transmission length and bond strength, and the significance of bond strength on the structural behaviour of the PTC systems to identify the research gap to be addressed.

Chapter 3 emphasises the research needs and significance of the thesis.

Chapter 4 consists of the details of materials, geometry of the specimens, experimental design, and methods used in the experimental program to achieve the objectives of this study.

Chapter 5 evaluates the transmission length using different standard equations from literature and describes the result and discussion of the experimental investigation on transmission length. It highlights the significance of the compressive strength of concrete at transfer and time on the transmission length of the member. It also provides two case studies to understand the significance of transmission length on the shear capacity of the PTC members.

Chapter 6 elaborates the results and discussions on the bond performance of the PTC members. It details the challenges associated with the bond measurements and explains the bond slip behaviour of different embedment length of strand in concrete under different applied prestress levels. Based on the experimental study, this chapter proposes a new method to determine the bond strength of the PTC members.

Chapter 7 summarizes the conclusions of each objective drawn from this study and also recommends the scope for future research.

Appendix A explains the procedure to determine the transmission length of the PTC members.

Appendix B details the technique to determine the bond strength of strands in concrete.

Appendix C provides the load – slip response at LE and FE of the specimens.

Appendix D provides the bond stress – slip response at LE and FE of the specimens.

2 LITERATURE REVIEW

2.1 INTRODUCTION

This chapter provides a critical review on the transmission length and bond performance of the pretensioned concrete systems. The chapter starts with a discussion on the bond mechanisms in the steel-concrete systems. Then, various factors affecting the transmission length (L_t) and bond strength (τ_b) of the PTC systems are reviewed. Next, the challenges in the measurement of L_t is mentioned. Following this, a review on the existing codes and empirical equations available in the literature to calculate the L_t and τ_b of the PTC systems is presented. This is followed by a review of existing test methods and its limitations to determine the L_t and τ_b of the PTC systems. Then finally, the effect of bond and its influence on the structural performance of the PTC systems and failure modes of strand-control bond are reviewed.

2.2 BOND MECHANISMS IN STEEL-CONCRETE SYSTEMS

The bond allows the strand and concrete to work together as a composite material under service loading. When the load is applied, the strand tends to move in the applied load direction. This relative movement between the strand and concrete is prevented by the bond. If the bond is inadequate to prevent the movement, bond failure will occur due to excessive slip of the prestressing strand. Based on the relative movement between strand and concrete, bond mechanisms are mainly contributed by three factors: adhesion, mechanical interlock, and friction. However, these bond mechanisms are significantly different in conventionally reinforced concrete (CRC) and the pretensioned concrete (PTC) systems that are explained in the following sections.

2.2.1 Conventional reinforced concrete (CRC) systems

In the CRC systems, the bond between the steel and concrete is achieved by the following three mechanisms; 1) Chemical adhesion between the steel bar and the concrete; (2) Frictional forces arising from the roughness of the interface, and 3) Mechanical anchorage or bearing of the ribs against the concrete surface (Pillai and Menon, 2009; ACI 318, 2014). Figure 2.1 shows the bond mechanism of the CRC systems. The bond strength was initially contributed by adhesion mechanism due to the presence of chemicals on the steel surface, but the resistance by this mechanism is destroyed once the strand slips. Then, friction contributes to bond. However, this becomes inefficient with increasing slip between the rebar and concrete. Further, the bond resistance is majorly contributed by the bearing stress due to mechanical interlock.

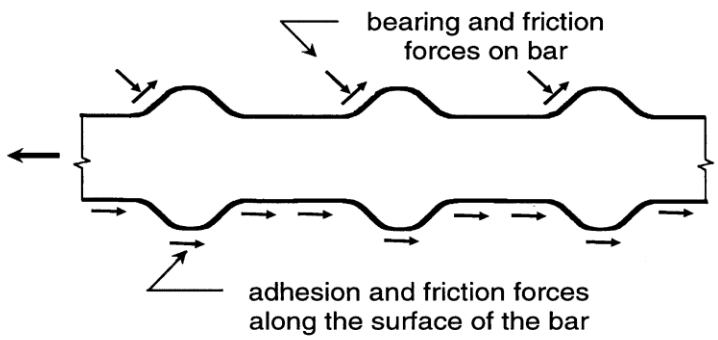

Figure 2.1 Bond mechanism in conventional reinforced concrete systems (adapted from ACI 318-11)

The S-C bond in the CRC systems is well studied and many bond-slip models have been derived based on the experimental test results (Mirza and Houde, 1979; Alsiwat and Saatcioglu, 1992; Song et al., 2015). *fib* MC10 proposes a general bond stress-slip model to calculate the bond stress subjected to monotonic loading. Also, AS 3600 (2009) and ACI 318 (2011-2014) propose a bond model to calculate the bond stress of deformed steel bar in concrete. The following section explains how different these mechanisms are in the PTC systems.

2.3 BOND MECHANISMS IN PRETENSIONED CONCRETE (PTC) SYSTEMS

The S-C bond mechanisms in the PTC systems are also contributed by adhesion, mechanical interlock, and friction (Janney, 1954; Hanson and Kaar, 1959). The forces induced by these mechanisms at the S-C interface in the PTC systems are shown in Figure 2.2.

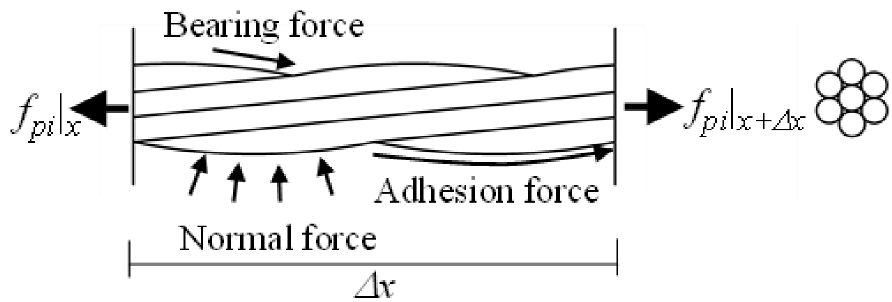

Figure 2.2 Bond mechanisms in pretensioned concrete systems

Adhesion plays a minimal role in transferring the prestress as the slipping of the strand with respect to the hardened concrete during the stress transfer can destroy the adhesive bond (Barnes et al., 2003). At the ends of the members, this effect would be lost at transfer. Then, the friction and mechanical interlock mechanisms play a significant role in the PTC systems. The friction is developed by the Hoyer effect and confinement of concrete. During prestressing, the strand is elongated and when the prestress is transferred to the surrounding hardened concrete, the strand tries to shorten longitudinally and expand laterally due to Poisson's effect. However, the surrounding confined concrete provides wedge action and induces compressive stresses perpendicular to the S-C interface. As a result, the frictional force is increased, which in turn enhances the bond. This phenomenon is known as the Hoyer effect (Hoyer and Friedrirch, 1939). Therefore, in the PTC systems, the Poisson's effect plays a key role in influencing the bond stress, particularly when the strand is in the elastic stage as it induces the wedging action at the S-C interface (*fib* Bulletin 10, 2000).

Normal pressure and bond stress are high at the end of the member and gradually get decreased over the L_t and become negligible at the end of the transmission zone (Abdelatif et al., 2015). However, at loading or service conditions, the increase in the prestressing strand stress could counteract the Hoyer effect by decreasing the strand diameter due to the Poisson's effect. This phenomenon could reduce the frictional bond mechanism and consequently, increases the significance of the mechanical bond mechanism [Hanson and Kaar, 1959 and Gustavason, 2004]. The mechanical interlock occurs due to the spiral twisting of the outer wires that form the strand. This helical shape of the strand results in the bearing stress between the strand and concrete which contributes to the bond stress development.

Figure 2.3 provides the bond slip relationship of plain wire and seven-wire strands. The bond resistance of a strand does not drop after a small slip unlike the plain wire, where bond resistance is dropped after a small slip (*fib* Bulletin 10). This indicates that the frictional mechanism is lost and then the mechanical mechanism is responsible after a small slip.

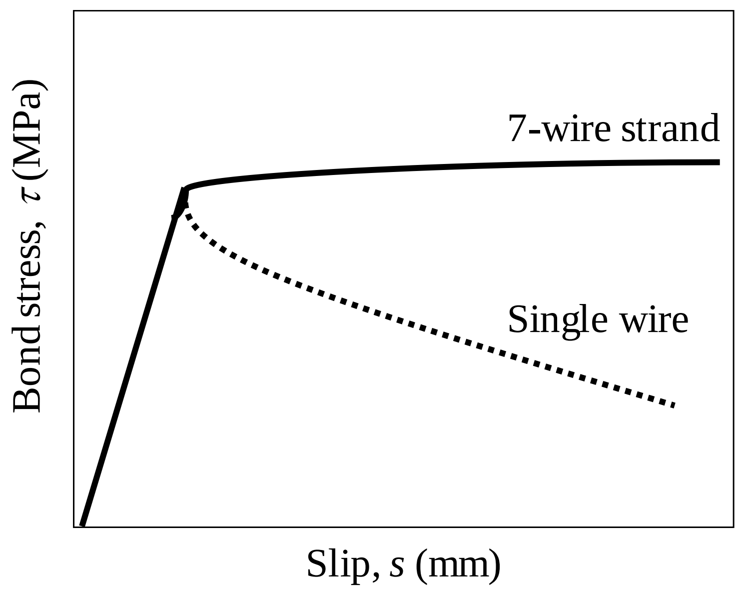

Figure 2.3 The bond stress-slip behaviour of plain wire and seven-wire strands

2.3.1 Prestress transfer mechanism from strand to the concrete

Figure 2.4(a) shows the idealised bilinear curve exhibiting the development of stress in the strand along the distance '*x*' from the end of the member. As shown, by Line 1, stress at the end of the member (at $x = 0$) is zero and gradually it increases to f_{pe} at the end of the transmission zone (at $x = L_t$) (ACI 318, 2014; AASHTO, 2012).

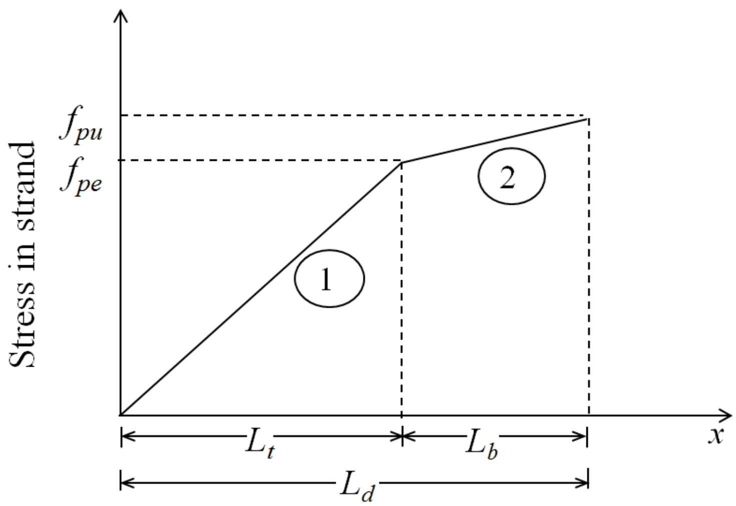

(a)

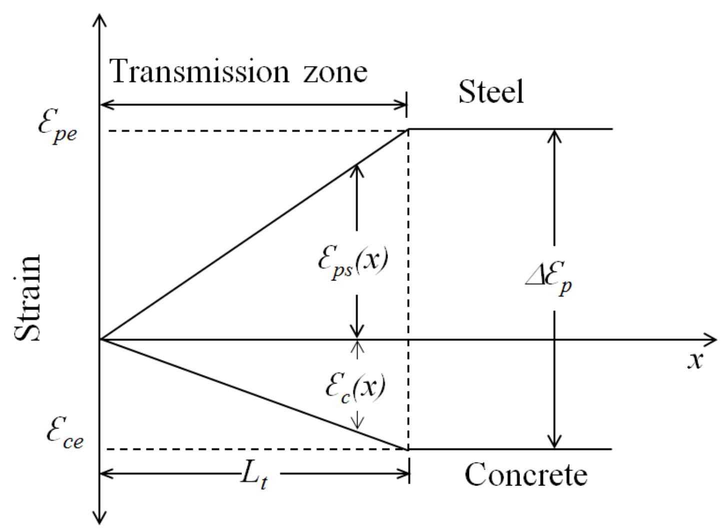

(b)

Figure 2.4 (a) Idealized stress development in the strand; (b) Strain development in the steel and concrete at the transfer of prestress

Further, as depicted by Line 2, under ultimate loading conditions, the stress along the strand increases linearly from f_{pe} (at $x = L_t$) to the ultimate stress (f_{pu}) (at $x = L_d$). The length required to increase the stress in the strand from f_{pe} to f_{pu} is defined as the bond length (L_b), which is the difference between L_d and L_t. The bond existing along the L_t and L_d is called transmission and development bond, respectively. Figure 2.4 (b) shows the strain in the strand (ε_{ps}) and strain on the concrete surface (ε_c) at prestress transfer. The ε_{pe} and ε_{ce} are effective strains (after the initial losses) in the strand and on the concrete surface, respectively. The sum of ε_{pe} and ε_{ce} is equal to the $\Delta\varepsilon_p$ - strain difference in the strand with adjacent concrete.

2.4 Bond strength definitions and formulations from literature

The stress developed at the S-C interface is called bond stress and it is expressed in terms of the tangential force per unit surface area of the strand (Pillai and Menon, 2009). As per ASTM A1081, the bond strength (τ_b) can be determined by measuring the pull-out force corresponding to 2.5 mm slip at the free end (FE) of the strand. Many researchers have used this method to determine the bond strength (Riding et al., 2016; Dang et al., 2014a). Table 2.1 provides the formulae for determining the bond stress (τ) of the PTC systems from literature. EN 2 (2004) and *fib* MC (2010) codes present the formulations for τ_b that could be used for both CRC and PTC systems. In addition to the formulations, *fib* MC (2010) considers the load vs slip relationship using which, τ between the concrete and reinforcing steel can be calculated as a function of slip (s). Several analytical works were carried out to understand the bond mechanisms of the PTC systems (Baláz, 1992; Oh et al., 2006; Martí-Vargas, 2012a; Dang et al., 2015). Based on the load vs slip relationship from the *fib* code, Balaz (1992) proposed an analytical equation for the S-C bond stress along the L_t. Similarly, Dang et al. (2015) adapted the τ-s model for rebars from *fib* MC (2010) by incorporating a coefficient 'k_b' to calibrate the τ_b for strands with and without stress. Martí-Vargas (2012b) proposed a bond stress equation along the length of the L_t based on the compatibility conditions. However, the effect of applied prestress (f_{ps}) on τ-s behaviour for the PTC systems is not well addressed in the literature (ACI 318, 2014; CSA A23, 2004; *fib* MC, 2010; IS 1340, 2012; Martí-Vargas et al., 2006; Shin et al., 2018). The conventional way of determining τ_b using 2.5 mm slip method found not valid for the PTC conditions and that are explained later in Chapter 6

Table 2.1 Bond equations from standards and literature

Reference	Bond equation
fib MC (2010), EN 2 (2004)/IRC 112 (2011)	$$\tau_b = \eta_{p1}\,\eta_{p2} f_{ctd}$$ η_{p1} – 1.2 and 3.2 for *fib* MC and EN/IRC, respectively η_{p2} – 1 for bond conditions
Baláz (1992)	$$\tau_b = \eta_1\,\eta_2 f_{ci}^{0.5}\left(\frac{s}{d_s}\right)^{\eta_3}$$ η_1 – 1.35, 1, 0.65 for the upper, mean, and lower bound of τ η_2 and η_3 – 2.055 and 0.25 experimental constants
Martí-Vargas (2012b)	$$\tau_b = \frac{P_T}{{}^4\!/_3\,\pi d_s L_t}$$ P_T – Prestressing force transferred L_t – Transmission length d_s – Nominal diameter of the strand
Dang et al. (2015)	$$\tau(x) = k_b \tau_{01}\left(\frac{s(x)}{s_{01}}\right)^{\alpha}$$ k_b – Calibration coefficient τ_{01} – Bond stress corresponding to the pull-out force of P_{01} s_{01} – Free end slip of 0.1 in. (2.5 mm) $\tau(x)$ – Bond stress at any location x $s(x)$ – Strand slip at any location x α - Exponential factor of bond stress-slip model

2.5 FACTORS AFFECTING THE BOND STRENGTH AND TRANSMISSION LENGTH OF THE PTC SYSTEMS

The transmission length of the PTC members depends on the bond strength between the strand and concrete. If the S-C bond is adequate, the length required to transfer the prestress would be less – hence, the L_t would be less. Therefore, the factors affecting the bond strength would also influence the L_t of the members. This section discusses the influence of these factors on the τ_b and L_t of the PTC members. Several factors like the compressive strength of concrete (f_c), cement content, water to cement ratio, embedment length of strand (l_e), applied prestress level (f_{ps}), diameter of the strand (d_s), texture and surface condition of the strand, confinement due to the presence of stirrups, method of prestress transfer (gradual or sudden), and other time-dependent effects (creep and shrinkage) can affect the L_t and bond strength of the PTC members (Mitchell et al., 1993; Zia and Mostafa, 1997; Rose and Russell, 1997; Oh and Kim, 2000; Oh et al., 2006; Martí-Vargas et al., 2012; Martí-Vargas et al. 2013a; Dang et al., 2014a; Dang et al., 2014b; Abdelatif et al., 2015; Dang et al., 2015; Ramirez-Garcia et al., 2017; Dang et al., 2016a). The influence of these factors on τ_b is well established for the CRC systems (Desnerck and Khayat, 2014; Mousavi et al., 2017; Shen et al., 2016; Sulaiman et al., 2017; Yalciner et al., 2012; Zhao et al., 2016). However, limited works are available for the PTC systems. Following is the discussion on these factors.

2.5.1 Compressive strength of concrete (f_c)

In practice, the prestress is transferred when the concrete attains about 60% of its target characteristic compressive strength (f_{ck}). The increase in stiffness of the concrete improves the S-C bond by providing more resistance to the slip (Barnes et al., 2003). Generally, bond resistance is proportional to $(f_c)^{\kappa}$, where κ is the variable ranges between 0.5 and 0.67 for the CRC systems (Harajli et al., 1995). A few literature data have been collected and plotted as shown in Figure 2.5 to understand its significance on the bond stress of the PTC members. It indicates that with the increase of f_c, the τ_b increases. However, a lot of scatter was observed between the results in various literature (Abrishami and Mitchell, 1993; Brearley and Johnston, 1990; Cousins et al., 1990; Haq, 2005; Martí-Vargas et al., 2012 and 2013b). The scatter could be due to the difference in the geometry, the applied prestress levels, and test methods used for the determination of τ_b. The test methods used to determine the τ_b and their limitations are explained in the later section. There is a need to develop a test method that provides an estimate of τ_b as a parameter that is independent of the geometry and prestress levels of the test specimen.

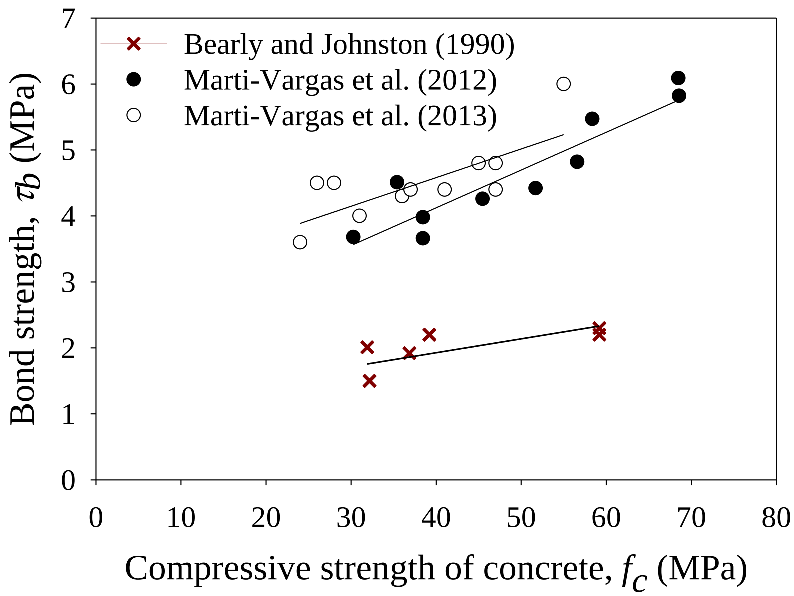

Figure 2.5 Bond stress as a function of the compressive strength of concrete

In the PTC systems, due to the Hoyer effect, the induced radial compressive stresses at the interface depend on the tensile strength of the strand. Thus, as the compressive strength of concrete increases, the resulting frictional stresses also increase. This results in shorter L_t due to improved bond (Oh and Kim, 2000 and Martí-Vargas et al., 2012). Table 2.2 provides the details of materials and geometry used in the literature. It was observed that the length of the specimems used to determine the L_t typically varied from 2 to 5 m. The table also provides the experimentally obtained L_t from literature. The L_t was significantly decreased by about 30% when the f_{ci} increases from 35 to 70 MPa (Martí-Vargas, 2012b) – similar to the observations obtained in the current study.

Based on the experimental results, several empirical equations are developed to determine the L_t as a function of the f_{ci} and other parameters, as shown in Table 2.5 and discussed later. From the experimental observations, using low strength concrete prevailing in the 1950s, Hanson and Kaar (1959) found no relationship between the L_t and f_{ci} – similar to some of the findings in this thesis. However, several studies after that indicated that the L_t decreases with increase in f_{ci} (Zia and Moustafa, 1977, Cousins et al., 1990, Mitchell et al., 1993, Lane, 1998; Barnes et al., 2003, Martí-Vargas et al., 2006; Kose and Burkett, 2007, Ramirez and Russell, 2008, Pellegrino et al., 2015; Ramirez-Garcia et al., 2016). Significant variations of L_t with respect to f_{ci} from the literature are collected and plotted as shown in Figure 2.6. A huge scatter in data was observed for the same f_{ci}, which could be due to the difference in the geometry and materials used for their study. Also, Ramirez-Garcia et al., 2016 reported that the significance of f_{ci} on L_t is up to a certain level of 55 MPa, beyond that increase in L_t is not critical.

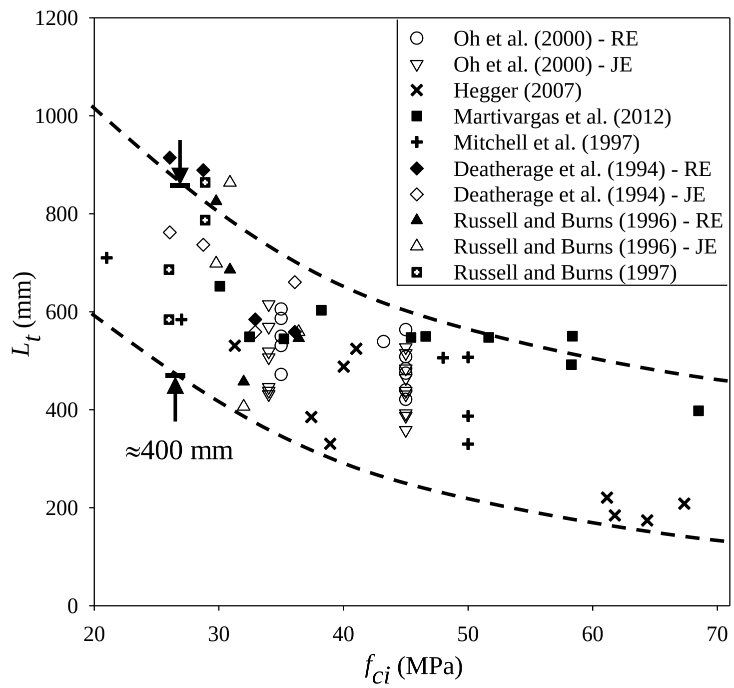

Figure 2.6 L_t of the PTC members as a function of f_{ci} from literature data

In addition to the lateral confinement provided by the concrete matrix, the closed stirrups also provide confinement and reduce the L_t (Vázquez-Herrero et al. 2013; Floyd et al., 2015). Russell and Burns (1996), Akhnoukh (2008), Song et al. (2014), and Kim et al. (2016) reported that the effect of stirrups/confinement reinforcement on the L_t is negligible.

On the other hand, Swamy and Anand (1975) reported that both the addition of stirrups and maturity of concrete controlled the L_t and the effective transfer of prestress considerably. They observed about 15% reduction in the L_t due to the addition of stirrups, especially in the light-weight concrete members which experience the structural failure due to split cracks after prestress release. These split cracks along the prestressing strand affect the durability of the systems and could reduce its service life due to other durability related issues (Vázquez-Herrero et al., 2013). Therefore, it is important to consider the f_{ci} in the design estimation of L_t. It should be noted that considering size effect, correlating the L_t of laboratory specimens with single-strand and a few stirrups with that of structural elements with multi-strands and many stirrups is challenging and is not a focus of the current study.

Table 2.2 Effect of compressive strength of concrete on the measured transmission length

Reference	$f_{ci,\ avg}$ (MPa)	$L_{t,\ avg}$ (mm) LE	$L_{t,\ avg}$ (mm) DE	Influence in L_t (%)	Geometry ($b \times h \times l$) (mm)
Kaar et al. (1963)	24	1010		-6	150 × 200 × 2400
	34	950			
Over and Au (1965)	38	890			75 × 75 × 2000
Dorsten et al. (1984)	28	670			89 × 114 × 2440
Cousins et al. (1990)	28	1270			102 × 102 × 1000
Mitchell et al. (1993)	21	70		-45	100 × 200 × L (L = 650 – 1600)
	50	390			
Russell and Burns (1996)	30	745	760	-28	100 × 125 × 3000
	32	560	545		
	36	540	545		
Oh et al. (2000)	35	549	521	-15	100 × 100 × 3000
	45	490	444		
Hegger et al. (2007)	39	432			150 × 250 × 2000
Martí-Vargas (2012b)	34	587		-32	100 × 100 × 2000
	48	548			
	58	521			
	68	398			
Floyd et al. (2015)	23	696	665	-28	170 × 300 × 5500
	30	697	573		
	33	537	680		
	43	510	462		
Ramirez-Garcia et al. (2016)	28	733		-31	165 × 305 × 2750
	42	520			
	64	506			

2.5.2 Diameter of strand (d_s)

The bond strength of the PTC systems gets reduced with an increased diameter of the strand (d_s). τ_b is inversely proportional to d_s or the surface area of the strand. During the pull-out test, the larger the diameter of the strand, the higher the load acting on it and thus results in significant reduction in diameter of strand due to the Poisson's effect. This affects the S-C bond and reduces the confinement due to the compressive strength of concrete and results in lower bond strength (Shin et al., 2018). Adhesion force is proportional to the amount of adhered surface at the S-C interface – it is directly proportional to the diameter of the strand. Also, the frictional force could be affected due to the increase in the normal force due to the increase in d_s. As the grooves between the outer wires of the strand become larger with increased strand diameter – the bearing force also tends to increase due to mechanical action (Deatherage et al., 1994).

Consequently, the L_t of the PTC members depends on the available surface area of strands. As the d_s increases the effective force to be transferred also increases, which results in longer L_t. The AASHTO LRFD (2012), ACI 318 (2014), AS 3600 (2009), CSA 23 (2014), EN 2 (2004), IRC 112 (2011), *fib* MC (2010), and IS 1343 (2012) codes consider this in an empirical way - by using the diameter of the strand (d_s) and a multiplier in the equation for L_t. It is to be noted that, the pitch of the helical outer wires influences the S-C bond mechanism – longer the pitch, the lesser will be the angle between the outer and centre wires – leading to lower bearing and mechanical interlock provided. Table 2.4 provides the formulations of the L_t. It should be noted that the AASHTO LRFD (2012), ACI 318 (2014), AS 3600 (2009), CSA A23 (2004), EN 2 (2004), IRC 112 (2011), *fib* MC (2010), and IS 1343 (2012) consider a linear relationship between L_t and d_s. It should also be noted that many codes consider only the d_s as a variable, which indicates its significance on L_t.

2.5.3 Embedment length (l_e)

The bond stress (τ) depends on the surface area ($l_e \times p$) of the strand in concrete. Furthermore, the τ at any instant during the test varies non-linearly along the length of the member (Abrishami and Mitchell, 1996; *fib* Bulletin 10, 2000; Dang et al., 2014b). Therefore, to avoid this non-linearity and obtain reasonably uniform bond stress along the l_e, a short l_e has been used in many pull-out tests on CRC systems (Khayat, 1998). However, for the PTC systems, the l_e of the strand in concrete should be long enough to accommodate the transmission length, L_t (Martí-Vargas et al., 2006; Martí-Vargas et al., 2013; Naito et al., 2015; Mohandoss and Pillai, 2017). As l_e increases, the resistance to bond failure also increases. Therefore, more load acts on the longer member and reduces the confinement effect of the surrounding concrete due to Poisson's effect (Hegger and Bertram, 2008). Hence, the l_e plays a critical role in the PTC systems. Martí-Vargas et al. (2006) studied the effect of l_e varied from 600 to 1000 mm by considering L_t. Mohandoss and Pillai (2017) suggested that l_e should be more than $2L_t$ for studying bond strength in PTC systems. It is found that using short/inadequate l_e for the PTC systems cannot provide a reliable τ_b. The challenges associated with this is explained later in Chapter 6.

2.5.4 Surface conditions of the strand

Although, not within the purview of this work, it can be mentioned that the surface conditions could affect the τ_b of S-C interface (Abrishami and Mitchell, 1993; Brearley and Johnston, 1990; Cousins et al., 1990; Deng et al., 2015; Girgis and Tuan, 2005). The surface condition of the strand could directly influence the frictional mechanism of the S-C bond. A rough surface due to the weathering of the strand or indented strands could enhance the friction between the strand and concrete, which in turn results in increased bond and reduced L_t (Martin and Scott, 1976; Barnes et al., 2003).

During strand manufacturing, the pre-treatments of strands, wire-drawing processes, use of lubricants (calcium salts of fatty acids, sodium stearate, etc), and cleaning process can alter the surface properties (Rose et al.1997; Dang et al., 2014b). Moreover, the thickness of the residual lubricant film on the strand surface can vary from one strand manufacturer to the other. All these conditions make the strand surface to be smooth and shiny. If the surface of the strand is smooth due to the presence of lubricants and the application of coating, then adhesion and frictional resistance would be less – thus resulting in reduced bond strength and increased L_t.

2.5.5 Applied prestress (f_{ps}) and releasing method

The initial prestress level applied in the S-C bond plays a crucial role contributing to the Hoyer effect. Naito et al. (2015) found that the bond stress computed using the stressed strands resulted in higher τ_b than that of the unstressed strands. Shin et al. (2018) investigated the effect of initial prestress on the τ_b by considering the two f_{ps} (0.8 and 0.9 f_{pu}) with about 10% difference and reported a negligible change in τ_b. It is cumbersome and expensive to prepare test specimens with high prestress levels. Hence, a relatively simplified test procedure with taut specimens is needed. However, the correlation between the τ_b of specimens with significantly different stress levels is not reported in the literature and is the focus of this thesis.

The method of prestress releasing (say, sudden release or gradual release) can influence the L_t. The gradual and sudden methods of transfer of prestress can have different dynamics of energy at stress transfer (Belhadj et al., 2001; Moon et al., 2010). In a sudden release of the stressed strand, the end portion of the strand does not get enough time to transmit the energy - resulting in longer L_t than that is achieved in a gradual release method (Barnes et al., 2003; Rose and Russell, 1997). The sudden release by flame cutting could result in L_t of about 6 to 60% greater than that is obtained for similar strands using the gradual releasing method (Kaar et al., 1963; Cousins et al., 1986; Rose and Russell, 1997; Oh and Kim, 2000). Russell and Burns (1997) also reported that the effect due to the releasing method becomes less significant as the length of the PTC elements increases. Also, the sudden release method in practice could increase the scatter in results (Floyd et al., 2015). Therefore, the gradual release method is recommended for the laboratory studies on the PTC specimens with less than 3 m. Hence, in this study also, the gradual release method was adapted.

2.5.6 Time-dependent effect

The bond in the PTC systems depends on the confinement provided by the concrete. The prestress is transferred when the compressive strength of concrete is about 60% of its design characteristic strength. The continued increase in concrete strength can enhance the S-C bond and could help in counteracting the possible adverse effects due to the long-term creep, shrinkage, and relaxation (*fib* Bulletin 10, 2000 and Barnes et al., 2003). Also, the PTC specimens would experience prestress losses over time due to shrinkage and creep which could also affect the L_t (Caro et al., 2013a). Kaar et al. (1963) and Bruce et al. (1994) had reported that for seven-wire, 12.7 mm diameter strands embedded in concrete with f_{ci} = 34 MPa, could increase L_t by approximately 10% during the first 28 days. After 28 days till 365 days no significant changes were reported, only 3% increment was observed. Also, for seven-wire, 12.7 mm diameter strands embedded in concrete with f_{ci} = 27 MPa, the L_t can increase by up to 20% in 14 months (Dorsten et al., 1984).

Table 2.3 presents the past work done on time variation on the L_t in chronological order. Several researchers had monitored the effect of time on L_t from the time of transfer to several days, months, and years (Kaar et al., 1963; Mayfield, 1970; Swamy and Anand, 1975; Dorsten et al., 1984; Cousins, et al., 1990; Lane, 1998; Roller et al., 1993; Issa et al., 1993; Mitchell et al., 1993; Bruce et al., 1994; Logan, 1997; Oh and Kim, 2000; Peterman, 2007; Larson et al.,2007; Ramirez and Russell, 2008; Pozolo and Andrawes, 2011; Floyd et al., 2015). A few researchers found that the L_t increases with time, whereas other researchers reported that the L_t decreased with time and in some cases, no significant change was observed on the L_t. Also, the reason for this difference in behaviour was not well understood.

Table 2.3 Changes in L_t with time (from literature)

References	Avg. f_{ci} (MPa)	Time interval after transfer	Change in L_t (%)	Remarks/Observations
Kaar et al. (1963)	11, 17, 23, 29, 34	1 year	+ 6% (avg.) +19% (max.)	No significant change
Mayfield (1970)	52	10 months	+5 to 44%	Significant increase in L_t
Swamy and Anand (1975)	31-36	6 to 14 months	+11.5 % +16%	No trend in the change in L_t; In some cases, L_t at two ends were significantly different
Dorsten et al. (1984)	28	14 months	+20 %	Change was observed for uncoated strands; no change was observed for coated strands.
Cousins, et al. (1990)	30	12 months	+15.4% (coated) +5.4% (uncoated)	Change in L_t was significant in the first 90 days after release; More changes have been observed for coated strands.
Lane (1998)	32	12 months	---	No trend in change in L_t
Roller et al. (1993)	62	18 months	---	No significant change
Issa et al. (1993)	33 and 40	20 months	+20 %	Significant increase in L_t
Mitchell et al. (1993)	21, 27, 50	21 days	+9% (avg.) +53% (Max)	Decrease of L_t have also been observed in some specimens
Bruce et al. (1994)	60	28 days	+10%	No significant change
Logan (1997)	30	21 days	+30 to 67%	Significant increase in L_t
Oh and Kim (2000)	35 45	7 days 90 days	~3% ~6%	No significant change
Larson et al. (2007)	25 - 35.	21 days	+10 to 45%	Significant increase of L_t was observed while using SCC
Ramirez and Russell (2008)	28 and 42	240 days	+190% (max) +62% (avg)	Significant difference between L_t at the two ends of the same specimen
Pozolo and Andrawes (2011)	34	28 days	-14%	Significant difference between L_t at the two ends of the same specimen

Note: The sign (+)/(-) indicate an increase/a decrease in L_t, respectively

2.6 Measurement of transmission length

The L_t of the PTC specimens is determined based on strain distribution along the length of the PTC members due to prestress transfer. The strain on the strand or concrete surface along a line parallel to the strand can be measured to determine the L_t. The strain measurements can be obtained by using electrical strain gauges or demountable mechanical strain gauges or Laser speckle method. The L_t of the PTC specimens can also be obtained by stress acting on the strand using the ECADA method. These methods are discussed in detail in the following sections. Also, the transmission length of the PTC members can be determined by measuring the strand end slips using empirical equations. However, this method often results in longer L_t than the strain method as it is calculated using an empirical equation and bond stress distribution coefficient (Dang et al., 2016b). Hence, determining the L_t using the strand slip is not within the purview of this study. This study is focused to determine the strain variation along the length to estimate the L_t of PTC members.

2.6.1 Demountable mechanical (DEMEC) strain gauges

Researchers have developed a way to indirectly determine the strain on the strand surface by measuring the strain on the concrete surface using demountable mechanical (DEMEC) strain gauge. A small stainless or brass discs of size 10 mm dia. with a centre hole of about 1 mm dia. would be pasted on the concrete surface along the strand line with a gauge length of 50 to 150 mm. The distance between the discs would be measured using the DEMEC gauge before and after prestress release. Then the strain on the concrete surface would be calculated using the change in distance between the discs with respect to the gauge length. It should be noted that the measurement of strain using the DEMEC gauge is highly sensitive to the pressure applied, the angle of holding, posture etc. – leading to a significant experimental/human error. If the concrete surface is good enough, then this would give a reliable L_t measurement. Else, reading would be affected due to improper bonding between the disc and concrete surface. As multiple DEMEC measurements are made across overlapping the measurement regions, the strain on the concrete surface is obtained by a smoothening technique using the average maximum strain method (known as AMS method) (Russell and Burns, 1997). This procedure is adapted in this study and it is explained in Chapter 4. However, obtaining strain using this method is time-consuming and requires a skilled operator as the reading could vary with the personal skills of the operator. The challenges associated with the L_t measurements would be discussed later in Chapter 5. As far as long-term measurement is concerned, this is one of the best methods to monitor the strain on the concrete surface.

2.6.2 Electrical strain gauge

Electrical strain gauges would be placed on the surface of the strand or concrete using adhesives to determine the strain profile. However, the placement of strain gauges on the helical shaped outer wires of the 7-wire strand and the calculation of corresponding axial strain in the strand are technically challenging. Also, pasting multiple gauges along the strand surface would affect the S-C bond (Park et al., 2013). These factors could result in erroneous L_t measurement. Therefore, the measurement of strain on the concrete surface would be preferable. However, proper surface preparation has to be done to paste the electrical strain gauges on the concrete surface to ensure good bonding. If the strain gauges are not bonded well, it could lead to erroneous reading or the strain gauges could come off from the surface, especially in long-term studies. Also, placing strain gauges on the concrete surfaces along the length of members would cost high. In addition, a sophisticated data acquisition system would be required to monitor the reading. Therefore, this method is not commonly used due to its high cost and less durability.

2.6.3 ECADA method

The ECADA test method determines the L_t by measuring the strand force in a series of specimens with different embedment lengths (Martí-Vargas et al., 2006). The L_t is determined as the length where the effective prestress is attained after loses and becomes constant. For the L_t measurement, the specimen should at least have twice the expected L_t from both ends. Therefore, it would require at least 2 to 3 m long specimens. In order to reduce the length of the member, this method uses a virtual part concept where a certain portion of the member could be replaced using anchorage-measurement-access (AMA). The AMA is designed by simulating the stiffness of the member to be replaced to match with the existing member. However, matching the stiffness of the member is not possible in reality – hence, the AMA would be overdesigned. Thus, this results in overestimated L_t. This method uses a series of specimens with different l_e to determine the L_t of one particular grade or variable. Also, if the grade or geometry of the specimen is changed, then the AMA has to be modified accordingly. Each specimen requires individual AMA system and AMA cannot be reused if the member is monitored for long-term effect. Therefore, this method consumes more material and cost. Moreover, with the AMA system (virtual concept) it does not represent the real scenario in the field. From the above discussions, the measurement of the L_t using the DEMEC is reliable especially for a long-term measurement of the L_t. Hence, in this study the traditional method of measuring the L_t using DEMEC gauge would be used.

2.6.4 Laser-speckle imaging

Laser-speckle imaging is an advanced method, developed to measure the strain distribution along the length of the members rapidly. A thin layer of paint is speckled on the concrete surface to measure the strain on it at the transfer of prestress. A laser is used on the traversable rail to take the readings before and after the prestress release (Murphy et al., 2012). This method determines the L_t by calculating strain using the change in distance captured by the images. Using this method, the accuracy of less than 10 micro-strain could be measured. However, this method is not suitable for long-term studies as the speckle pattern or paint could change or fade which could lead to erroneous readings. Hence, this method could be useful for the L_t measurement of large number of specimens at the time of prestress transfer.

2.7 Existing codes and empirical equations for calculating the transmission length of the PTC systems

Different standards provide different design equations for calculating the L_t using various factors that can influence the L_t and these are listed in Table 2.4.

2.7.1 ACI 318 (2014)

As discussed in Section 2.5, many factors can affect the L_t. However, ACI 318 (2014) considers only the f_{pe} and d_s to compute the L_t. The compressive strength of concrete at release (f_{ci}) is one of the factors which significantly influences the L_t and that was not considered in the ACI codal equation. The number '21' in the design equation represents the characteristic compressive strength of concrete in MPa (Tabatabai and Dickson, 1993; Zia and Mostafa, 1997). The design equation of L_t in ACI 318 (2014) is based on the experimental work by Kaar and Hanson in 1959, which was adapted by ACI 318 (1963). However, this equation was not updated from 1963 to date (ACI 318, 2011; ACI 318, 2014). The materials used in those days were different and the same equation could not be used for the advanced materials being used in the current construction practices. Hence, there is a need to revise the L_t equation for the current construction materials and practices for a realistic estimation of the L_t.

2.7.2 AASHTO (2012), AS 3600 (2009), CSA A23 (2014), and IS 1343 (2012)

AASHTO LFRD (2012), AS 3600 (2009), CSA A23 (2014), and IS 1343 (2012) codes have considered only the diameter of the strand (d_s) to calculate the L_t. However, calculating the L_t based on only the d_s does not represent the actual L_t of the PTC systems that could be affected by other variables also. AASHTO LFRD (2012) and AS 3600 (2004) suggest 60 times d_s to calculate the L_t which is almost close to the L_t value based on ACI equation if the strands are stressed to $0.75f_{pu}$ (L_t = ~ 62-65 times d_s depending on the prestress loss at transfer). CSA and IS codes suggest 50 and 30 times d_s, respectively to calculate the L_t which is about 80 and 50 % of the L_t values based on the AASHTO and AS codes, respectively. These design values of L_t based on CSA and IS could underestimate the actual value of L_t of the PTC systems as these consider only the d_s. The provision of L_t in IS 1343 was based on the contemporary code of UK (CP 110, 1972). The British standard has been revised subsequently to meet the current practices. However, the provision of L_t in Indian code is not updated - indicating the need to revise the code to meet the modern construction practices.

2.7.3 BS 8110 (1997)

BS 8110 (1997) suggests an equation as a function of d_s and f_{ci}, also it includes a constant representing the tendon type for calculating the L_t, and it does not consider the prestress level in the strand. Typically, in the PTC construction practices, strands are stressed to $0.75f_{pu}$. In practice, controlling the applied initial stress is crucial. If the strands are less stressed then the design value will be conservative as the L_t required is less to transfer the applied prestress and vice-versa. On the other hand, overstressing the strand is not common in construction practices as the strand could yield and break. However, if the strands are overstressed that could result in longer L_t than the required. Therefore, for a realistic estimation of L_t, prestress is one of the important parameters to consider. Later, the use of this code became obsolete and BS has adapted the European standards EN 2 (2004).

2.7.4 EN 2 (2004)/IRC 112 (2011) and *fib* MC (2010)

EN 2 (2004) and *fib* MC (2010) consider many variables that could affect the L_t and proposed an equation as a function of the area of strand, the diameter of the strand, stress in strand, bond stress and other factors (α_1, α_2, α_3, η_{p1}, and η_{p2}). Mainly these two codes consider f_{ci} indirectly to compute the bond stress between the strand and concrete. In EN code, the factors α_1 and α_2 are provided to account for the releasing method and type of strand, respectively. The factor α_1 = 1 and 1.25 for gradual and sudden release; α_2 = 0.25 and 0.19 for wires and strands (3 and 7-wire strands).

In *fib* MC code, the factors α_1, α_2, α_3, η_{p1}, and η_{p2} are provided to account for the releasing method, action effect, bond situation, type of strand, and position of the strand, respectively. The factor α_1 = 1 for gradual release and 1.25 for sudden release; α_2 = 1 for calculation of L_t when the moment and shear capacity are considered and 0.5 for verification of transverse stress; α_3 = 0.5 and 0.7 for strands and indented or crimped wires, respectively; η_{p1} = 1.4 and 1.2 for indented/crimped wires and 7-wire strands, respectively; η_{p2} = 1 for all the horizontal tendons and 0.7 for all other cases. Since these codes consider the possible factors affecting the L_t they could provide a conservative design. In addition, these codes consider lower and upper bound values for an accurate prediction of L_t.

Table 2.4 L_t formulations from standards

Code	Transmission length equation (SI units)
ACI 318 (2014)	$L_t = \left(\frac{f_{pe}}{20.7}\right) d_s$
AASHTO (2012)	$L_t = 60 d_s$
AS 3600 (2009)	
BS 8110 (1997)	$L_t = \frac{K_t d_s}{\sqrt{f_{ci}}}$
CSA A23 (2004)	$L_t = 50 d_s$
fib MC (2010)	$L_t = \alpha_1 \alpha_2 \alpha_3 \frac{A_s}{\pi d_s} \frac{f_{pi}}{\eta_1 \eta_2 f_{ctd}}$
EN 2 (2004)	$L_t = \alpha_1 \alpha_2 \alpha_3 d_s \frac{f_{pi}}{\eta_1 \eta_2 f_{ctd}}$
IRC 112 (2011)	
IS 1343 (2012)	$L_t = 30 d_s$

2.7.5 Other empirical models to determine the L_t

Several researchers had worked on to develop the formulations to determine the transmission length of the PTC systems. Table 2.5 presents the empirical and analytical formulations to determine the L_t. Hanson and Kaar (1959) had initiated the experimental work on the determination of transmission length and proposed an equation as a function of effective prestress and diameter of the strand considering the numerical value of 20.3 which represent the characteristic compressive strength of concrete used.

Table 2.5 Empirical and analytical formulations to determine L_t from literature

Year	Reference	Equation for transmission length, L_t
1959	Hanson and Kaar	$\frac{f_{pe}}{20.3} d_s$
1969	Marshall and Krishna Murthy	$\sqrt{\frac{\sqrt{f_{ci}} \times 10^3}{\beta}}$
1976	Martin and Scott	$80d_s$
1977	Zia and Mostafa	$1.5 \frac{f_{pi}}{f_{ci}} d_s$-117
1990	Cousins et al.	$0.5 \left[\frac{U_t^{'} \sqrt{f_{ci}}}{B}\right] + \left[\frac{f_{pe} A_{ps}}{\pi d_s U_t^{'} \sqrt{f_{ci}^{'}}}\right]$
1992 1994 1995	Shahawy et al. Deatherage et al. Buckner	$\frac{f_{pi}}{20.7} d_s$
1993	Mitchell et al.	$\frac{f_{pi}}{20.7} d_s \sqrt{\frac{20.7}{f_{ci}^{'}}}$
1997	Russell and Burns	$\frac{f_{pe}}{13.8} d_s$
1998	Lane	$\left[\frac{4f_{pi}}{f_{ci}^{'}} d_s\right]$ -127
2003	Barnes et al.	$\alpha \frac{f_{pi}}{\sqrt{f_{ci}}} d_s$
2006	Martí-Vargas et al.	$\frac{2.5 A_{ps} f_{pi}}{P f_{ci}^{2/3}}$
2005	Kose and Burkett	$0.045 \frac{f_{pi} (25.4\text{-}d_s)^2}{\sqrt{f_{ci}}}$
2008	Ramirez and Russell	$\frac{315}{\sqrt{f_{ci}}} d_s \geq 40 d_s$
2013b	Caro et al.	$\xi . \lambda . \left[\chi . \left(\frac{f_{pe}^n A_{ps}}{(k_1 \pi d_b) U_t}\right) + k_2\right]$
2015	Pellegrino et al.	$e^{\alpha + \beta d_s + \gamma f_{pi} + \delta f_{ci}}$
2016	Ramierz-Garcia et al.	$25.7 \left(\frac{f_{pi}}{f_{ci}} d_s\right)^{0.55}$

In 1969, Marshall and Krishna Murthy proposed an empirical formula to estimate the L_t by considering cube compressive strength at transfer and a constant to account for the type of strand. $\beta = 0.058$ for 12.7 mm dia. 7 wire strands. Some researchers, Shahawy et al. (1992), Deatherage et al. (1994), Bucker (1995) had suggested L_t equations similar to ACI 318, considering f_{pi} instead of f_{pe}, and not considering f_{ci}. Zia and Moustafa (1977), Cousins et al. (1990), Mitchell et al. (1993), Lane (1998), Barnes et al. (2003), Martí-Vargas et al. (2006), Kose and Burkett (2007), Ramirez and Russell (2008), Pellegrino et al. (2015), and Ramirez-Garcia et al. (2016) had proposed different L_t equations with f_{ci} as a variable. As L_t depends on the bond strength of strand in concrete, Cousins et al. (1990) and Caro et al. (2013b) considered the bond strength of the member to estimate the L_t. In addition, Caro et al. (2013b) considers a factor to account for the effect of time. These formulations were evaluated later in Chapter 5 and compared with the codal formulations.

2.8 EXISTING TEST METHODS FOR DETERMINING THE BOND STRENGTH OF THE PTC SYSTEMS

Typically, the bond strength between strand and concrete is determined by the pull-out test. Many test methods were developed to determine the S-C bond. However, each method suggested the use of different geometry, materials, and stress levels. Figure 2.7 presents the details of the test specimen and set-up used in those test methods. Table 2.6 gives the details of the materials and methods used in the three widely reported bond test methods (Moustafa pull-out test, ASTM A1081, and ECADA test method). The details and limitations of these test methods are discussed in the following sections.

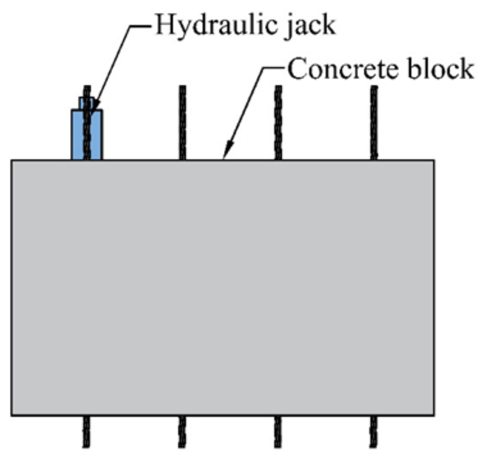

(a) Moustafa Method (Unstressed strands in block: 600 × 1200 × 900)

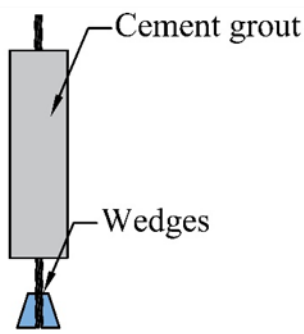

(b) ASTM A1081 (Unstressed strands in cylinder: 125 × 450)

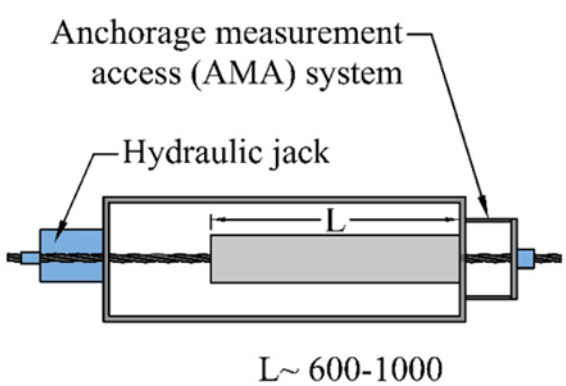

(c) ECADA Method (Stressed strands in prism: 100 × 100 × L)

Figure 2.7 The schematic representation of specimen geometry and set-up used in the existing pull-out test methods

Table 2.6 Materials, prestress effect, and pull-out test method considered in the existing test methods

<table>
<tr><th rowspan="2">Test methods</th><th rowspan="2">Type of specimen geometry*</th><th colspan="2">Materials</th><th rowspan="2">Prestressing and transfer of prestress</th><th colspan="2">Pull-out test using</th></tr>
<tr><th>Cement mortar</th><th>Concrete</th><th>Jack</th><th>Universal testing machine</th></tr>
<tr><td>ASTM A1081</td><td>Cylindrical</td><td>✓</td><td>×</td><td rowspan="2">×</td><td>×</td><td>✓</td></tr>
<tr><td>Moustafa</td><td>Large block</td><td rowspan="2">×</td><td rowspan="2">✓</td><td rowspan="2">✓</td><td rowspan="2">×</td></tr>
<tr><td>ECADA</td><td>Prism</td><td>✓</td></tr>
</table>

* Refer Figure 2.7 for more details on the geometry of the specimen

2.8.1 Moustafa test method

The Moustafa pull-out (reported in Rose and Russell, 1997) was one of the earliest test methods used to quantify the τ_b of strands used for lifting loops. In this method, unstressed strands were pulled out from the large concrete block size of (1200 × 1200 × 600) mm using a hydraulic jack. The use of unstressed strands in the concrete block cannot represent the PTC systems. Therefore, the bond strength obtained using this method cannot be used to quantify the bond strength of the PTC systems.

2.8.2 ASTM A1081 test method

Post-Tensioning Institute (PTI) bond tests and North American Strand Producers (NASP) were also developed bond test methods using unstressed prestressing strands. The reliability of these methods was tested and the results from different laboratories showed that the NASP bond test is the most reproducible method (Russell and Paulsgrove, 1999). The contemporary version of the NASP method was modified and adapted by ASTM A1081 (2012). This method suggests the use of 450 mm long unstressed strand in 125 mm dia. cylindrical cement mortar. This test is considered as an indicator of the bondability of strands; but, did not recommend any qualifying criteria. Later, based on NASP test method, Dang et al. (2014a) established the minimum thresholds for qualifying prestressing strands. Dang et al. 2015 reported that when the mortar is used, the friction bond formed between the strand and mortar becomes insignificant. Therefore, using the cement grout/mortar instead of concrete and unstressed strands cannot be helpful to determine the bond strength of the PTC systems as those could not represent the actual bond mechanisms of the PTC systems.

2.8.3 ECADA Pull-out test method

The ECADA pull-out test method is developed to determine the bond strength of stressed strands in concrete (Martí-Vargas et al., 2006). Performing a pull-out test for the pretensioned members is tedious as it requires long member length to account for the transmission length while transferring the stress. Therefore, the test set-up required to perform has to be designed such that it can accommodate the longer pull-out specimens.

Researchers have worked on to develop a suitable test method to determine the S-C bond and Martí-Vargas et al. (2006) had proposed an ECADA method which means in Spanish Ensayo para Caracterizar la Adherenciamediante Destesado y Arrancamiento (Test to characterize the bond by release and pull-out). This method considers the virtual part concept using an anchorage measurement access (AMA) in order to reduce the required long l_e for the PTC members. This AMA system designed such that the stiffness of the AMA should match the stiffness of the concrete portion that has to be replaced. So that the stiffness matched AMA system could represent the virtual part of the concrete member length (say about ~2 m depending on the l_e).

2.8.4 Limitations of the existing test methods to determine the bond in the PTC systems

The aforementioned Moustafa and ASTM A1081 test methods suggest the use of unstressed strands and cement mortar/concrete. The unstressed strands in the specimens may not be perfectly straight and while being pulled-out they tend to straighten; in this straightening process, they would compress the grout on one side and lose contact with the grout on other side. Such uncontrolled mechanisms could induce more scatter in the test results than those observed with specimens with stressed and straight strands (Dang et al., 2015).

Martí-Vargas et al. (2006) had proposed the ECADA test method using prestressed strands (say, $0.7f_{pu}$) to represent the real conditions at the S-C interface of the PTC systems. However, this method adopts a virtual part concept with a system designed to match the stiffness of the concrete portion that would be replaced to reduce the length of the member. Note that the stiffness of this system is designed to be higher than that of concrete. As a result, this method overestimates the τ_b of PTC systems (Martí-Vargas et al. 2013), which may underestimate the transmission length resulting in reduced shear capacity in the transmission zone (Mohandoss et al. 2018). Therefore, there is a need for a simplified test specimen and method to determine the τ_b of S-C systems, which is the focus of this thesis.

2.9 EFFECT OF BOND AND ITS INFLUENCE ON THE STRUCTURAL BEHAVIOUR OF THE PTC SYSTEMS

The S-C bond could influence the performance of concrete structures in several ways. At the serviceability limit state, the bond influences the width and spacing of transverse cracks, tension stiffening, and curvature. Similarly, at the ultimate limit state condition, the bond is responsible for the strength of end anchorages. In CRC, the bond characteristics of reinforcement could influence the cracking and deflection of the member at the serviceability limit state. Also, the strength of anchorage depends on bond at the ultimate limit state. The rotation capacity of plastic hinges is also influenced by the bond characteristics of the reinforcement (*fib* Bulletin 10, 2000). Bond could also influence the ductility – by withstanding the steel strain along the embedded reinforcement which controls the bending cracks and formation of secondary cracks. In the PTC systems in addition to the above functions, bond plays a major role at the stage of prestressing and transfer of prestress before subjecting to service loads (Dang, 2015). Therefore, the L_t could be significantly influenced by the S-C bond. Consequently, L_t influences the bending and shear strength of the members particularly short members supported within the L_t (Swamy and Anand, 1975). Therefore, an adequate L_t is critical especially in hollow-core slab units without shear reinforcements.

Hence, in the following sections, the effect of bond is discussed in terms of the significance of the L_t on the shear performance and critical shear regions of the PTC members.

2.9.1 Effect of transmission length on the shear capacity of PTC systems

The L_t of prestressed strands plays a crucial role in achieving the desired shear capacity ($V_{n, max}$) within the shear-critical region, especially when the elements do not have shear stirrups. To ease the placement of concrete and casting, it is common not to use stirrups in the pretensioned hollow-core slabs (HCS) and rely on the prestressed strands to achieve the desired shear resistance. The shear force required to cause an inclined crack can be calculated as the shear force required to cause a principal tensile stress equal to the tensile strength of the concrete at the centroid of the beam. The nominal shear resistance of the PTC systems is computed as given in Eq. 2.1 (Nawy, 2003):

Eq. 2.1

$$V_n = V_c + V_s + V_p$$

where, V_n is the nominal shear force; V_c, V_s, and V_p are the shear capacity contributed by the concrete, steel stirrups, and prestressed strands (vertical component only), respectively. For the HCS systems without shear reinforcement and with horizontal strands, the V_s and V_p can be considered to be zero. For being conservative, V_c is taken as the lower among the V_{cw} and V_{ci} (the ultimate shear resistance of sections uncracked and cracked in flexure, respectively). HCS systems can be considered as simply supported systems and, in such systems, V_{cw} is found to be lower than V_{ci}, especially near the supports. Hence, V_c can be considered to be equal to V_{cw}. Based on the principles of classical mechanics and Mohr's circle, V_{cw} is given as follows (Eq. 2.2) (Navy, 2003).

Eq. 2.2

$$V_c = V_{cw} = \frac{Ib_w}{Q}\sqrt{f_t^2 + f_{cp}f_t}$$

where,
I – Moment of inertia of gross cross section; b_w – Width of the cross section
Q – Moment of area; f_t – Maximum principal tensile stress ; f_{cp} – compressive stress due to effective prestress at centroid

Table 2.7 presents the various codal equations for calculating V_{cw}. It may be noted that for achieving a conservative design, the ACI 318 (2014), EN 2 (2004), *fib* MC (2010), and IS 1343 (2012) consider different resistance factors for the parameters in Eq. 2.2.

Table 2.7 Equations provided in various codes/standards for web shear capacity

Code	Web shear capacity (SI units)
ACI 318 (2014)	$V_{cw}=\left(0.29\lambda\sqrt{f_c'}+0.3f_{cp}\right)b_w d$
AS 3600 (2009)	$V_{cw}=\frac{0.8Ib_w}{Q}\sqrt{f_{ctd}^2+\alpha_1 f_{cp}f_{ctd}}$
CSA 23 (2004)	$V_{cw}=\beta_p\lambda\phi_c\sqrt{f_c'}\sqrt{1+\frac{\phi_p f_{cp}}{0.33\lambda\phi_c\sqrt{f_c'}}}$
EN 2 (2004)	$V_{cw}=\frac{Ib_w}{Q}\sqrt{f_{ctd}^2+k_1 f_{cp}f_{ctd}}$
fib MC (2010)	$V_{cw}=\frac{0.8Ib_w}{Q}\sqrt{f_{ctd}^2+\alpha_1 f_{cp}f_{ctd}}$
EN 2 (2004)	$V_{cw}=\frac{Ib_w}{Q}\sqrt{f_{ctd}^2+k_1 f_{cp}f_{ctd}}$
IS 1343 (2012)	$V_{cw}=0.67b_w d\sqrt{f_t^2+0.8f_{cp}f_t}$

2.9.2 End region reinforcement

In the transmission zone of the PTC beams, transverse reinforcement is necessary to prevent the concrete cracking due to large radially outward stresses. The crack occurs when the maximum stresses exceed the tensile strength of the concrete. Figure 2.8 shows the idealised distribution of tensile stress in the transmission zone (Raju, 2011). At the end of the member, the transverse tensile stress is maximum and gradually gets reduced along the length in the transmission zone (Murthy, 1971). However, for the design of end reinforcement, this transverse tensile stress was approximated as a linear variation over half the L_t. The transverse tensile force and area of the vertical reinforcement are computed as follows using Eqs. 2.3 and 2.4.

$$F_{bat} = \frac{1}{2} f_{v(max)} \frac{L_t}{2b_w} \quad \text{Eq. 2.3}$$

$$A_{sv} = \left[\frac{2.5M}{f_s D}\right] \quad \text{Eq. 2.4}$$

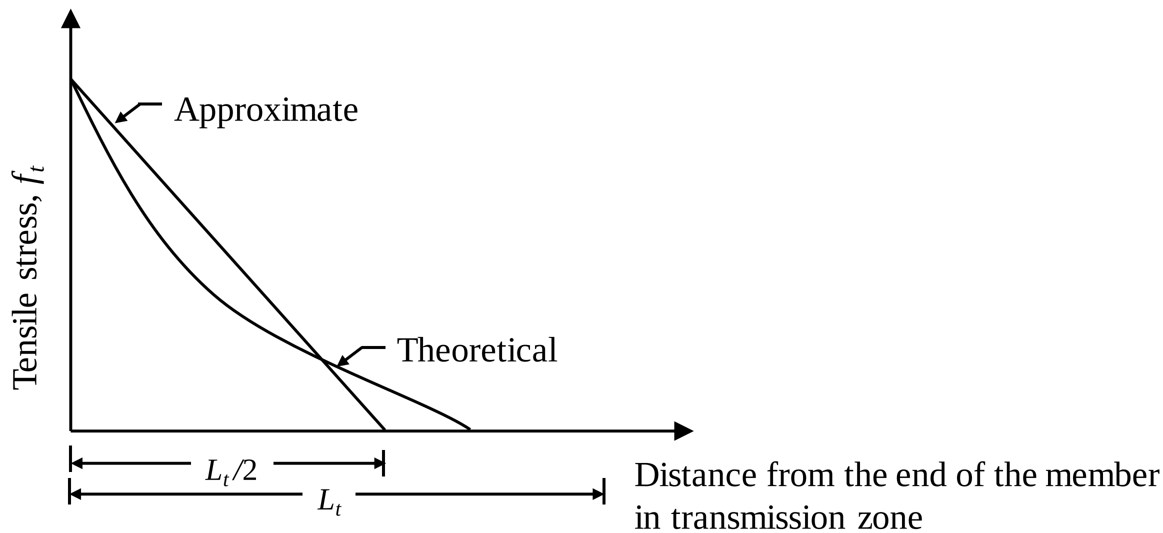

Figure 2.8 Theoretical distribution of tensile stress in the transmission zone (adapted from Raju, 2011)

On the other hand, some researchers had developed an empirical equation based on a laboratory test to calculate the required total stirrup force (F) and it is given as follows in Eq. 2.5. From this equation, the area of reinforcement required for the transmission zone along the L_t can be obtained as shown in Eq. 2.6 (Nawy, 2003).

$$F = 0.0106 \left(\frac{P_i h}{L_t}\right) \quad \text{Eq. 2.5}$$

$$A_t = 0.021 \left(\frac{P_i h}{f_s L_t}\right) \quad \text{Eq. 2.6}$$

As the L_t influences the amount of shear reinforcement in the transmission zone, it is essential to estimate the L_t correctly. An overestimation or underestimation of the transmission length would result in inadequate transverse reinforcement. If the L_t is overestimated then the amount of steel in the transmission zone would be lesser than the required. The members like bridge girders, end shear reinforcement could be provided by calculating the amount of force using the given equations. The members like hollow core slab, where end shear reinforcements are not provided, the available prestress itself has to take care of the shear along the transmission length. Hence, it is vital to calculate the realistic L_t of the PTC systems.

2.9.3 Critical sections for shear

The maximum shear force occurs at the face of the support, which is the critical section for shear and gradually reduces with increasing distance from the support. However, under the concentrated load the shear force remains high in the region between the support and first concentrated load. The shear strength of this region is enhanced when the support reactions introduce the transverse compression at the end of the members. Therefore, inclined cracks do not develop near the face of the support (Pillai and Menon, 2009). In such a case, the code allows a section at a distance *d* from the face of the support to be treated as shear critical region where maximum shear force was expected, where *d* is the depth of the member. Figure 2.9 shows a schematic illustration of shear critical regions specified by ACI 318 (2014) and IS 1343 (2012).

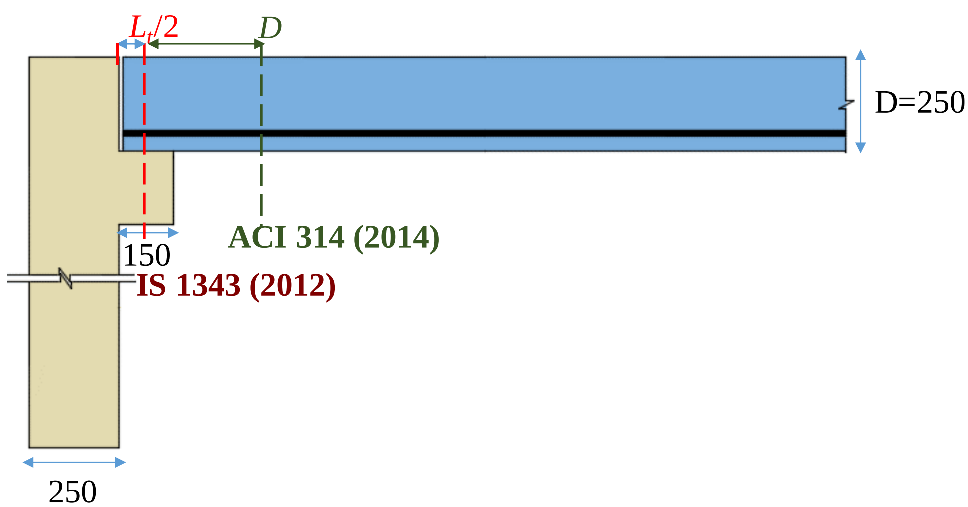

Figure 2.9 The schematic illustration of critical shear regions specified by ACI 318 (2014) and IS 1343 (2012)

ACI code does not provide a shear critical region for the PTC systems by considering the L_t. However, it has a general specification suggesting that the shear critical region should be within the distance of h (depth of the member) from the face of the support. The specifications for the PTC systems from IS code says that half of the L_t should be achieved at the face of support so that the L_t would be avoided in the clear span. Therefore, determination of L_t plays a vital role in shear critical region also. Again, this necessitates the rational determination of L_t.

2.10 MODES OF FAILURE IN THE S-C BOND SYSTEM

The S-C bond could fail either by the deformation of steel bar/strand or concrete. The failure could occur due to any one or combination of the following actions (Pillai and Menon, 2009):

- Break-up of adhesion between the steel and concrete.
- Longitudinal splitting of the concrete around the steel.
- Shear of the concrete keys between the ribs/surface of the steel at the S-C interface.
- Rupture of the strand

Break up of adhesion at the S-C interface is not a major failure mode in the PTC systems as the adhesion mechanism has a minimal role on the S-C bond. The commonly observed failure modes are: pull-out (shearing of concrete), splitting, and rupture of strands. These failure modes are discussed as follows.

(i) Pull-out failure

Concrete is sheared at the interface across the tops of the bar ribs. This type of failure occurs when resistance is offered by thick concrete cover or the confining effect of secondary reinforcement. It generally occurs when the concrete cover is exceeding 3 times the diameter of the strand/bar. However, this could also occur due to insufficient embedment length to develop the stress (Mahmoud et al., 1999). This failure is related to a local mechanism where only interface collapse would be observed.

(ii) Splitting failure

When the concrete cover was not adequate to provide the required confinement, then the concrete fails by longitudinal splitting. Typically, this failure could occur when the concrete cover is less than 2 times the diameter of the bar (*fib* Bulletin 10, 2000). This type of failure is related to structural collapse.

(iii) Strand rupture

As the embedment length increases the resistance to bond failure also increases. Hence, the strand experiences the maximum load of its breaking strength and – strand ruptures. Typically, this type of failure is observed when the embedment length was longer than the required length to develop the stress (Mahmoud et al., 1999; Martí-Vargas et al., 2013).

2.11 SUMMARY

The detailed literature review presented in this chapter helps to understand the bond mechanisms and various factors influencing the L_t and τ_b. The L_t and τ_b formulations from the literature were discussed. The various methods to determine the L_t and τ_b and the limitations associated with those methods were also presented. Finally, the significance of bond performance on the structural behaviour and its mode of failure were discussed. Based on the literature review, the need for this research work is presented in the forthcoming chapter.

3 RESEARCH NEEDS AND SIGNIFICANCE

3.1 RESEARCH NEEDS

The underestimation or overestimation of the L_t can lead to less conservative shear designs as it influences the available prestress in the transmission zone to resist the external load. Therefore, a realistic estimation of the L_t is important for achieving adequate shear capacity. However, the estimation of the L_t has certain challenges in obtaining strain on the steel/concrete surface. Also, the L_t parameter of the PTC systems depends on several factors. The major factors that could influence the L_t are the diameter of the strand, the prestress level, and the compressive strength of concrete at transfer. Therefore, for a rational estimation of the L_t, these parameters should be considered. However, many standards available for the PTC systems do not consider the compressive strength at transfer in the design L_t equations. Also, a lot of studies have been done on the effect of the compressive strength of concrete at transfer and a huge scatter has been observed in the collected literature data. This is because, different studies have used different geometry, materials, and methods to determine the L_t. Thus, it indicates a need to study the effect of the compressive strength on the L_t and for standardising the procedure to determine the L_t.

As mentioned in Chapter 2, the L_t of the PTC systems depends on the S-C bond. Hence, the determination of the bond strength (τ_b) of the pretensioned strands in concrete is also a vital parameter. The existing test methods that determine the bond strength are the Moustafa test, ASTM A 1081 pull-out test, and the ECADA test. Among these methods, ASTM A 1081 and the Moustafa tests suggest the use of unstressed strands in cement grout/ concrete block. The use of unstressed strands in cement grout/concrete block does not represent the S-C bond of the PTC systems. Later, the ECADA test method was developed for stressed strands. However, this method has led to more complexity by considering the virtual part concept to reduce the length of the member. One of the challenges in the PTC systems in determining the S–C bond is the embedment length of the member by considering the transmission length from both ends of the member. The conventional method of using a 2.5 mm slip to determine the bond strength could not be valid for long PTC specimens. Therefore, a suitable test procedure is required to determine the bond strength. The research significance of this work is as follows.

3.2 RESEARCH SIGNIFICANCE

A significant number of pretensioned, precast girders and hollow-core concrete (HCC) slabs are used in bridge construction and high-rise and industrial buildings, respectively. As mentioned above, the shear performance of the member depends on the available stress in the transmission zone. This transmission zone becomes critical, especially in the case of HCC slabs which do not have shear reinforcement or stirrups. Hence, the L_t is one of the important design parameters to ensure the PTC members' shear performance. However, it is found that significant discrepancy exists among the design L_t equations in the various codes and literature. Some codes provide empirical formulations to estimate L_t as a function of only the properties of strands and do not consider that of concrete. This thesis highlights the influence of f_{ci} on L_t. Also, the influence of seemingly simple, but complex test procedures on the determined L_t and its scatter are explained. Based on the experimental results with various strength grade concretes, a bilinear model for L_t as a function of the properties of both strand and concrete is developed. It is anticipated that the proposed equation would be incorporated in the design codes to achieve more rational estimates of L_t, and hence, more refined structural designs for the end zone reinforcements of PTC members. As aforementioned, the transmission of prestress depends on the bond between the pretensioned strand and concrete. Failure of the S-C bond has been observed in pretensioned concrete (PTC) bridges, indicating the poor bond between the strand and concrete. The available test methods to determine the bond strength, τ_b, in PTC systems have limitations in terms of (i) complexity in the preparation of test specimens, (ii) the method of evaluation, and (iii) dependency on the length of the test specimen. For frequent quality assurance tests, a simplified test method by eliminating these limitations is required. Based on a comprehensive experimental work, this thesis proposes a bond test method with simplified pull-out specimen containing a taut strand and a method to estimate τ_b based on bond yield stress approach.

4 EXPERIMENTAL PROGRAM

4.1 INTRODUCTION

Based on the research objectives and scope two different experimental programs have been developed. This section enumerates the details of the materials and methodology adapted for each experimental program. The properties of the materials used are discussed first, which is followed by the details of experimental design, and test methodology for Objectives 1 and 2. The test set-up and the instrumentation required for the transmission length and bond strength test are also specified in this section.

4.2 MATERIALS USED IN THE EXPERIMENTAL PROGRAMS AND THEIR PROPERTIES

This section deals with the characteristics of the materials used in the experimental programs.

4.2.1 Prestressing strand properties

A low relaxation seven-wire strand of 12.7 mm diameter was used. Note that the strands are kept inside the material storing room to prevent the surface damage or other environmental efforts. A uniaxial tensile test was performed as shown in Figure 4.1 for 1 m long specimen to obtain its mechanical properties. Figure 4.2 shows the stress-strain behaviour of the prestressing strands. Three specimens were tested. The average modulus of elasticity of the strand (E_s) was 198 ± 3 GPa (CoV was 2%). The average ultimate tensile strength with of the strand (f_{pu}) was 1877 ± 3 MPa (CoV was 0.2%) conforming to IS 6000 (1983). The symbol ± indicates the standard deviation. Table 4.1 provides the chemical composition of the strand obtained using optical emission spectroscopy.

Table 4.1 Chemical composition of the prestressing strand

Elements	C	Si	Mn	P	Cr	Ni	Al	Co	Cu	S	Fe
Concentration (%)	0.72	0.21	0.94	0.02	0.27	0.02	0.01	0.02	0.02	0.002	Remaining

Figure 4.1 Uniaxial tensile test setup for prestressing strands

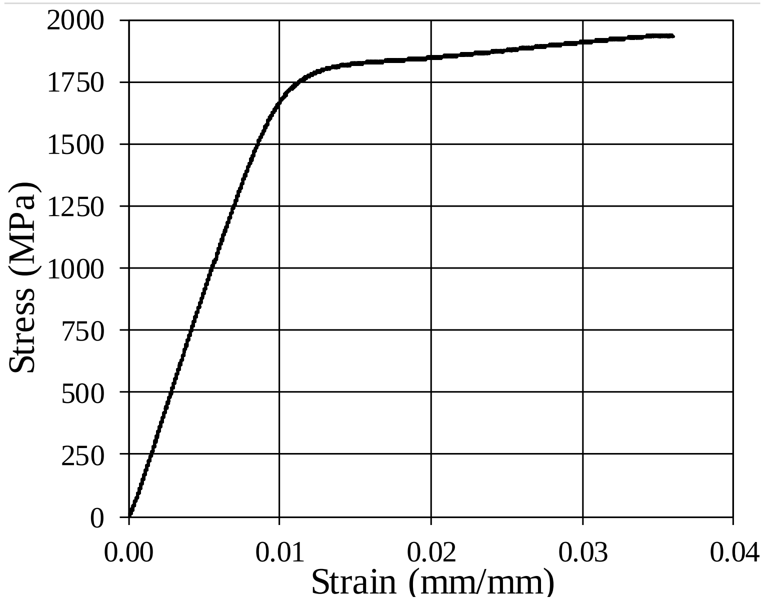

Figure 4.2 Stress-strain behaviour of prestressing strand

4.2.2 Cement properties

The Ordinary Portland Cement (OPC) 53S sleeper grade was used. This finely ground cement helps to achieve early compressive strength gain to transfer the prestress (IS 269, 2015). Table 4.2 provides the chemical composition of the OPC obtained using X-ray fluorescence. The physical properties of cement were obtained conforming to IS 4031(1988-1999) and ASTM C204 (2016) and provided in Table 4.3

Table 4.2 Chemical composition of Ordinary Portland Cement 53S

Chemical composition	**Al_2O_3**	**CaO**	**Fe_2O_3**	**K_2O**	**MgO**	**Na_2O**	**SiO_2**	**SO_3**
Concentration (%)	5.74	63.07	4.94	0.60	1.40	0.20	16.29	3.11

Table 4.3 Physical properties of Ordinary Portland Cement 53S

Characteristics	Values obtained	Relevant standard
Specific gravity	3.17	IS 4031 (Part 11) - 1998
Fineness (m^2/kg)	380	IS 4031 (Part 2) - 1998 ASTM C204 - 2016
Consistency (%)	30	IS 4031 (Part 4) - 1998
Initial setting time (min)	64	IS 4031 (Part 5) - 1988
Final setting time (min)	435	IS 4031 (Part 5) - 1988

4.2.3 Aggregate properties

The crushed granite and natural sand were used as coarse and fine aggregates conforming to IS 378 (2016). The physical properties of the aggregates used were determined as per IS 2383 (2007) and they are given in Table 4.4.

Table 4.4 Physical properties of the aggregates

Properties	Coarse aggregate (20 mm)	Coarse aggregate (10 mm)	Fine aggregate
Specific gravity (SSD)	2.77	2.74	2.54
Water absorption	0.30	0.44	0.67

4.2.4 Superplasticizer

Master Glenium 8233, a polycarboxylate (PCE) based superplasticizer was used to attain the required workability. The appearance was in a reddish-brown colour liquid. The density of the liquid content was 1080 kg/m^3 and it has 33% solid content. The specific gravity and pH were 1.08 and 6.0, respectively

4.2.5 Concrete

The experimental program has four types of concrete mixes (M) designed for M35, M45, M55, and M65 grades. The mix design was done as per IS 10262 (2009) specifications. The details of the mix proportions are presented in Table 4.5. The mixes were designed to achieve the targeted slump of 100 ± 20 mm by adding superplasticizer. The mechanical properties were tested and the average compressive strength and static modulus of elasticity with standard deviation (SD) are detailed in Table 4.6. The compressive strength and static modulus of elasticity of concrete were obtained as per the standards IS 516 (1959 - Reaffirmed 2018) and ASTM C469 (2014) were used for obtaining, respectively. The concrete mix would be referred using their average compressive strength instead of its design grades, i.e. the concrete id would be $f_{ci}23$, $f_{ci}28$, $f_{ci}36$, and $f_{ci}43$ at 3-days for L_t specimens and f_c43 and f_c62 at 28 days for pull-out specimens.

Table 4.5 Details of concrete mix proportions

Ingredients	**Concrete strength**			
	M35	**M45**	**M55**	**M65**
Cement (kg/m^3)	380	380	420	420
Water (kg/m^3)	190	171	168	147
Water – cement ratio	0.50	0.45	0.40	0.35
Aggregate 10 mm (kg/m^3)	432	436	428	433
Aggregate 20 mm (kg/m^3)	648	655	641	649
Sand 4 mm (kg/m^3)	750	758	743	752
Superplasticizer (% bwoc) MasterGlenium SKY 8233	0.8	0.3	0.6	0.5

Table 4.6 Properties of concrete

Concrete grades	**Average compressive strength ± SD (MPa)**		**Average static modulus of elasticity ± SD (GPa)**
	3-days	**28-days**	**28-days**
M35	23 ± 1.00	45 ± 1.42	30 ± 0.62
M45	28 ± 0.87	53 ± 1.14	33 ± 0.39
M55	36 ± 1.76	62 ± 0.52	35 ± 0.50
M65	43 ± 0.73	74 ± 0.47	39 ± 0.68

4.3 OBJECTIVE 1: DETERMINATION OF THE TRANSMISSION LENGTH (L_t) AND ITS EFFECT ON SHEAR CAPACITY OF THE PRISTINE PTC SYSTEMS

This section puts forward a detailed description of the geometry of specimens, experimental variables, preparation of L_t specimens, and the strain measurements used for Objective 1.

4.3.1 Experimental design

The main experimental variable for this objective was the compressive strength of concrete at transfer (f_{ci}). f_{ci} of 23, 28, 36, and 43 MPa were used. Then, three L_t specimens of each variable were cast. Totally, 12 specimens were tested to obtain the L_t of the PTC systems as a function of f_{ci}. Later, to understand the influence of time dependent effects, the transmission length was monitored upto 360 days. Table 4.7 presents the experiment design used for Objective 1.

Table 4.7 Experimental design for Objective 1

Specimen ID	f_{ci} (MPa)	No. of specimen	Duration (days)								
			3	7	28	120	150	200	250	300	360
f_c23	23	3	✓			✓	✓	✓	✓		✓
f_c28	28	3	✓	✓							
f_c36	36	3	✓				✓	✓	✓	✓	
f_c43	43	3	✓		✓						

Note: Prestress is transferred at 3rd day.

4.3.2 Specimen geometry

A prismatic specimen with a 12.7 mm diameter strand at the centre, as shown in Figure 4.3 was used. The cross section of the concrete prism was 100 × 100 mm and length of the specimen was 2000 mm. The DEMEC inserts were placed on both sides of the concrete surface along the length of the specimen at 50 mm interval to obtain strain on it. The details of the DEMEC inserts are set forth in the following sections.

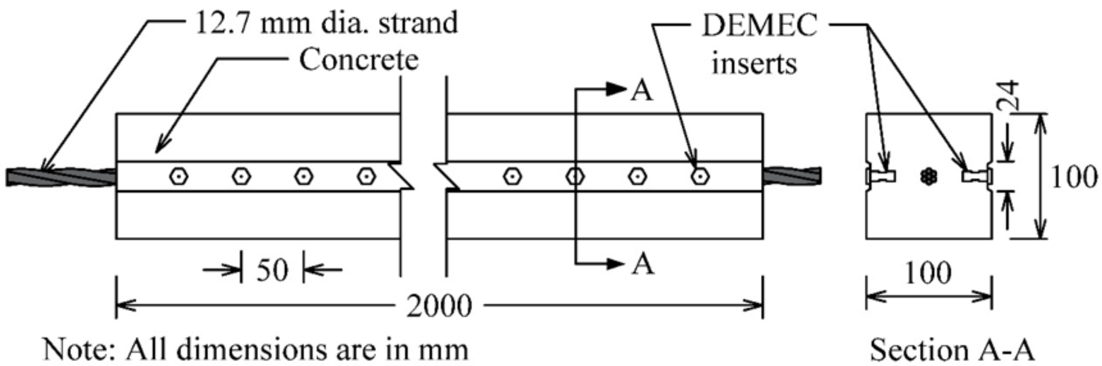

Figure 4.3 The schematic representation of transmission length specimen geometry

4.3.3 Preparation of L_t specimens

The specimen preparation involves three stages (i) prestressing the strand, (ii) concreting and curing, and (iii) prestress releasing.

4.3.3.1 Stage 1: Prestressing the strand

Figure 4.4 shows the prestressing bed and the PTC specimen. The prestressing bed consisted of a hollow steel section and two end brackets. A 5.5 m long seven-wire strand was inserted in the through-holes of the end brackets. Then, an initial prestress of about 0.75 f_{pk} was applied. As indicated in the zoomed portions 1 and 2 of Figure 4.5 (a) and (b) at the jacking end (JE), a hydraulic jack (300 kN capacity) was placed to apply the stress. Steel chair, wedges and barrels, and load cell were also kept to, activate the stress reaction, lock the stress, and monitor the load applied, respectively. The wedge & barrel placed outside the load cell was initially kept loose and while stressing the load was activated between the two outer wedges placed at both ends. After stressing, the wedge & barrel placed outside the load cell would be locked tightly using the ring holder and then, the outer wedge & barrel and hydraulic jack were removed. Now the stress would act between the two end brackets of the bed. While removing the hydraulic jack, some amount of stress would be lost due to the seating of wedge placed outside the load cell. However, the loss of prestress was negligible by about 5%. The load cell reading indicating the applied prestress of about 0.7 f_{pu} would be recorded as effective stress acting on the strand.

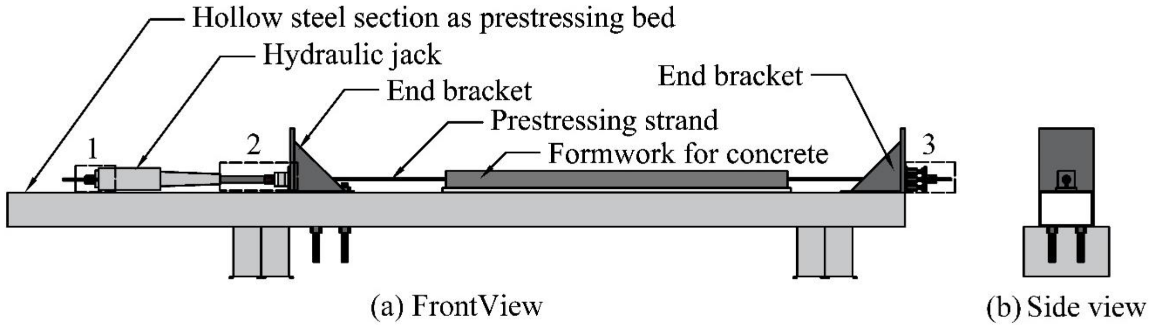

(c) Photograph of prestressing bed

Figure 4.4 The schematic representation and photograph of prestressing bed with the PTC specimen

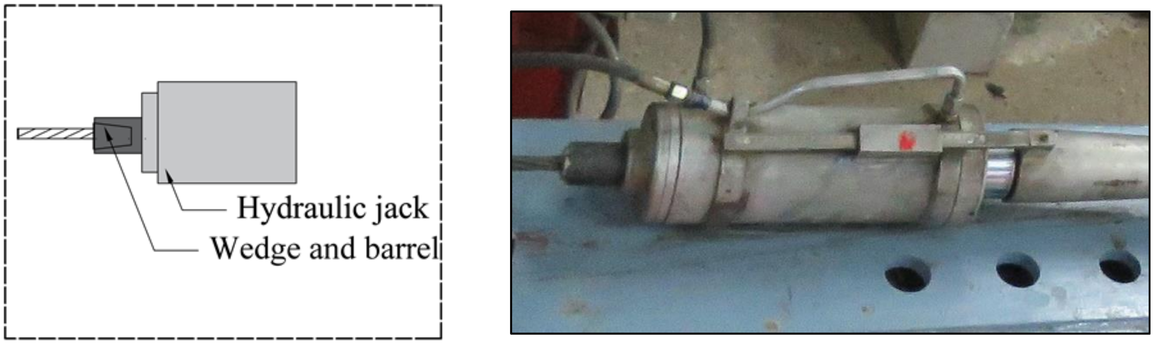

(a) Zoomed Portion 1

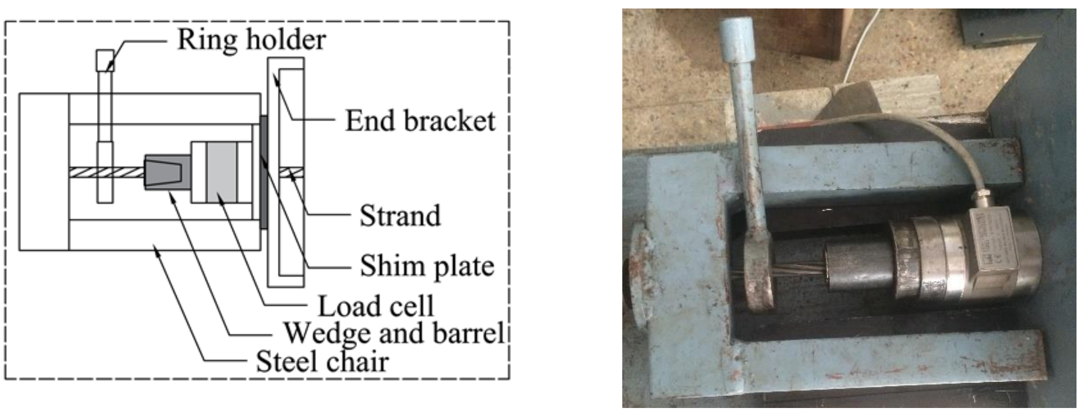

(b) Zoomed Portion 2

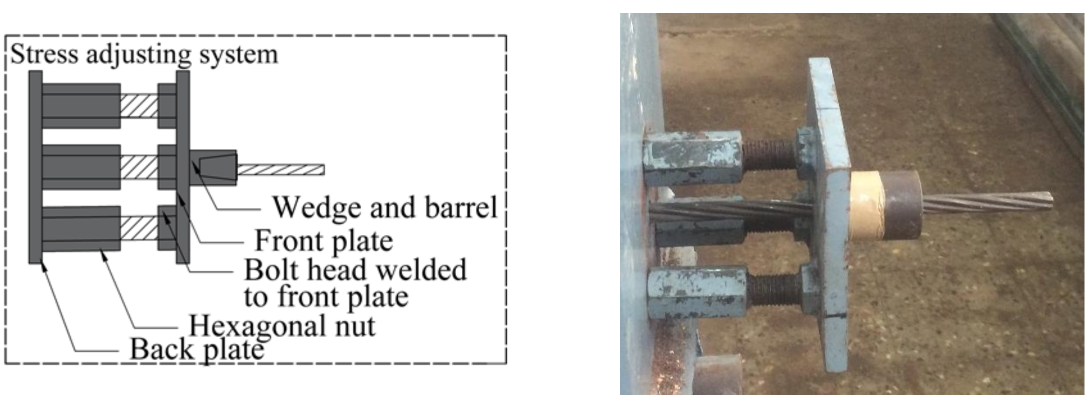

(c) Zoomed Portion 3

Figure 4.5 Zoomed portions of various arrangement to apply and release the prestress

4.3.3.2 Stage 2: Concreting and curing

After stressing the strand, a custom-designed PVC mould was placed around the strand (on the prestressing bed) to place the concrete. Hexagonal brass inserts with bolt/head and nut/base were designed and fabricated for the strain targets (Mohandoss et al., 2018). These were affixed to acrylic strips with pre-defined holes (50 mm c/c spacing) for accurate spacing and alignment. These strips with brass inserts were then placed along the centre line of the two opposite, vertical surfaces on the inside faces of the PVC mould as shown in Figure 4.6. Figure 4.7 provides more details on these brass inserts. It should be noted that achieving uniform compaction of concrete along the strand was crucial for the study. To achieve this, concrete in the PVC mould was placed in a single layer of 100 mm height and compacted uniformly (25 tampings for every 100 mm length). After 24 hrs, the L_t specimen and the accompanying cube specimens were demoulded. Then, the acrylic strips were removed from the concrete surface (by unscrewing the bolt/head of the inserts). Then, the bolt/head of the inserts was threaded again to the nut/base - to facilitate DEMEC gauge measurements. The specimens were cured (by covering with wet burlap and plastic sheet) until 3 days or when the concrete attained about 60% of the target compressive strength, whichever was earlier.

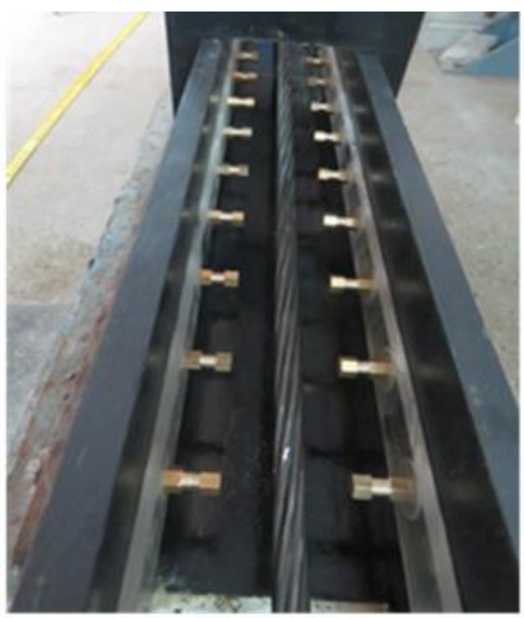

Figure 4.6 DEMEC insert arrangement for the preparation of the L_t specimens

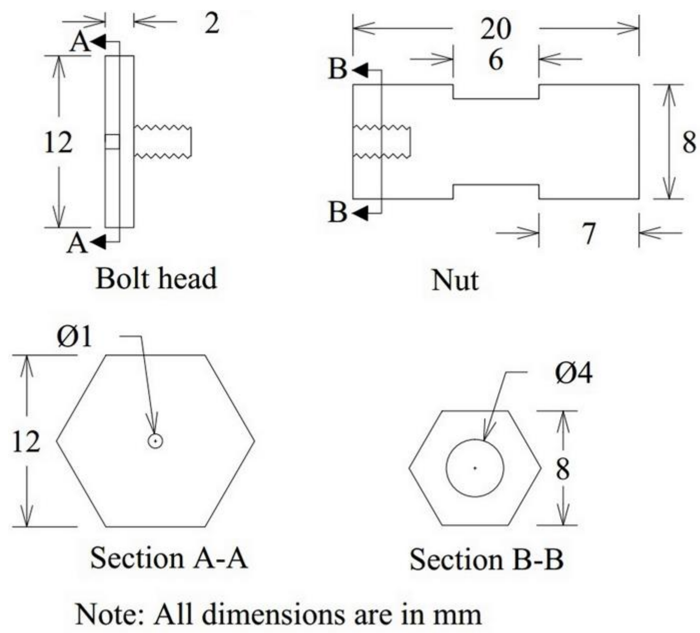

Figure 4.7 The schematic illustration of the DEMEC inserts used

4.3.3.3 Stage 3: Prestress releasing

At the releasing end (RE) as shown in Figure 4.5 (c), a hexagonal nut and bolt arrangement was used as a stress adjusting system (SAS) - to gradually transfer the prestress from the strand to the hardened concrete. Once the concrete had attained its sufficient strength, say about 60% of its target compressive strength in about 3 days, the prestress was gradually transferred. The SAS consists of three hexagonal bolts welded with a steel plate of (150 × 150 ×15) mm in size as shown in the zoomed portion 3. The L_t was obtained by measuring the change in distance between the inserts before and after prestress transfer. The average f_{pe} was about 1215 MPa. Figure 4.8 shows the photograph of the L_t specimen after prestress release.

Figure 4.8 The photograph of transmission length specimen

4.3.4 Strain measurements and instrumentation

The L_t of the PTC member is determined based on the strain development on the strand or concrete surface. Measuring strain on the strand surface is difficult as placing multiple strain gauges on the strand surface could affect the S-C bond. In addition to this, the strain gauge could be damaged during compaction and prestress transfer. Hence, in this study, strain measurement on the concrete surface was used to obtain the L_t. Researchers have also proved that there is no significant change in the strain measurement between the strand and concrete surfaces (Russell and Burns, 1996).

Figure 4.9 The photograph of the DEMEC gauge used to take measurements

Demountable mechanical (DEMEC) gauge as shown in Figure 4.9 was used to measure the distance between the inserts before and after prestress transfer. The gauge length of DEMEC was 150 mm. Inserts were typically placed at 50 mm gauge length. Initially, surface-mounted DEMEC discs were glued on the concrete surface using Anabond adhesive. Then, it was experimentally observed that these discs were not suitable for long-term measurements. Sometimes even while taking measurements, these pins might come off. Therefore, to avoid this issue, brass inserts were used to obtain quality data, especially for long-term measurements. These inserts were custom-designed and fabricated as nut bolt system using hexagonal brass rods and the details are provided in Figure 4.7. Initially, the inserts were designed without grooves and then later it was found that these inserts were not gripped properly and could come off from the concrete. In order to fix the inserts properly, grooves are made on the inserts.

Figure 4.10 shows the details of the DEMEC gauge readings using a 150 mm gauge. The DEMEC readings were taken with reference of 150 mm gauge length and the strain $(\varepsilon_c)_x$ is assigned to the midpoint of the gauge length, which is the distance between every $(n\text{-}1)^{th}$ to $(n+1)^{th}$ point (see Figure 4.11). Consequently, readings were taken for all the points on the concrete surface. The measured strain data was smoothened by averaging the strain data over the three consecutive and overlapping 150 mm gage lengths. Therefore, the smoothened strain at x^{th} point $(\varepsilon'_c)_x$ was calculated as follows using Eq. 4.1:

Figure 4.10 Length change being measured using the DEMEC gauge

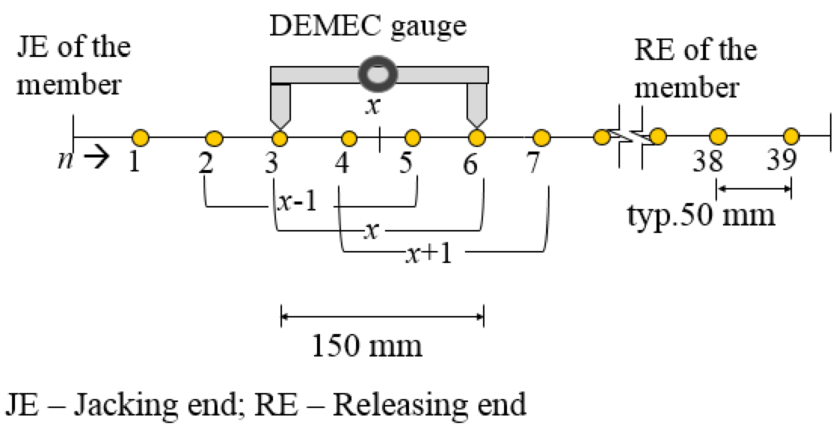

Figure 4.11 Strain measurement using the DEMEC gauge on the concrete surface

$$(\varepsilon'_c)_x = \frac{(\varepsilon_c)_{x-1} + (\varepsilon_c)_x + (\varepsilon_c)_{x+1}}{3} \qquad \text{Eq. (4.1)}$$

The average of $(\varepsilon'_c)_x$ observed at the left and right sides of the specimen was calculated and the average strain profile along the length of the specimen was plotted (with a plateau at the center portion). Then, the average maximum strain (AMS), as defined by Russell and Burns (1997), was computed by averaging all the strain measurements on the plateau. The L_t is defined as the distance from the end of the member to the point with average strain equal to the 95% of AMS. In this way, the L_t at both ends of the specimen was calculated and the average was defined as the L_t of the specimen.

4.4 OBJECTIVE 2: DETERMINATION OF BOND STRENGTH BETWEEN THE PRESTRESSED STRANDS AND CONCRETE

4.4.1 Specimen geometry

As per the experimental design, 24 pull-out specimens were cast and tested. Figure 4.12 shows the geometry details of bond test specimens with strands embedded in a concrete prism of cross section 100×100 mm. A 50 mm long PVC pipe was placed as a bond breaker as shown to avoid stress concentration during testing.

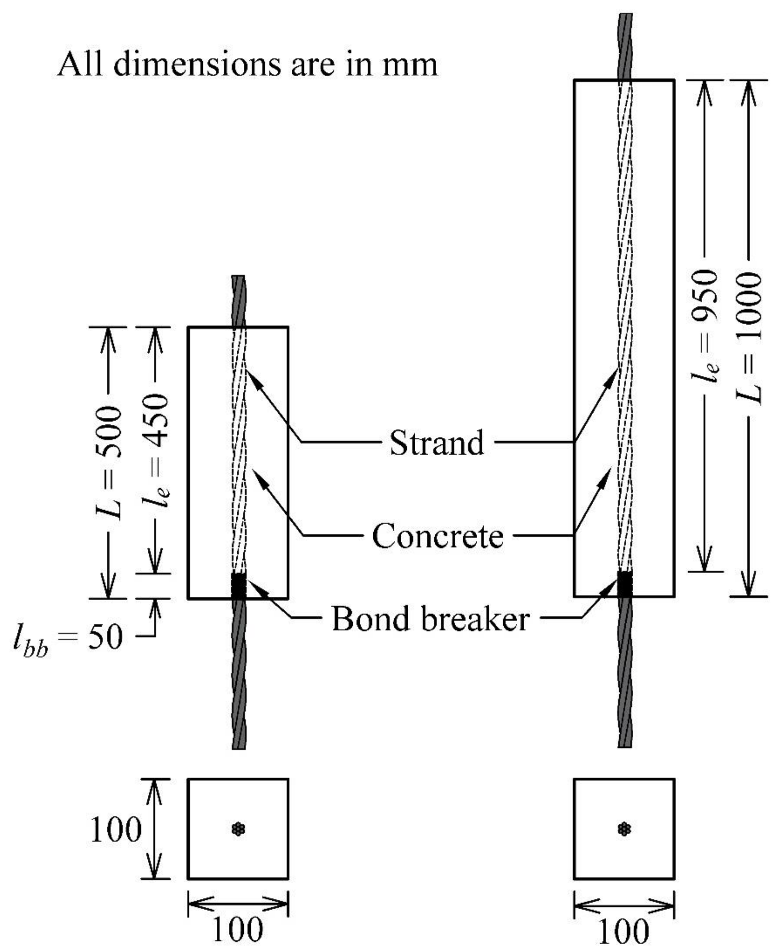

Figure 4.12 The schematic diagram of bond test specimen configuration

4.4.2 Experimental design

The main experimental parameters for this objective were compressive strength of concrete, embedment length of the member, and prestress level. Six numbers of specimens were cast for each group. A total of 24 specimens were cast and tested to determine the bond strength of the PTC members. Table 4.8 provides the test variables and number of test specimens for each variable combination studied.

Table 4.8 Experimental design showing the test variable and its combination

Specimen ID	**Experimental variables**						**Number of specimens**
	Concrete strength		**Embedment length**		**Prestress level**		
	$f_c = 43$	$f_c = 62$	$l_e = 450$	$l_e = 950$	$f_{ps} = 0.1f_{pu}$	$f_{ps} = 0.7f_{pu}$	
f_c43-T-S	✓		✓		✓		6
f_c62-T-S		✓	✓		✓		6
f_c62-T-L		✓		✓	✓		6
f_c62-S-L		✓		✓		✓	6

Note: Specimen ID; $f_c$xx – compressive strength; T/S – taut (0.1 f_{pu})/stressed (0.7 f_{pu}); S/L – short l_e (450)/long l_e (950)

Two typical compressive strength of concrete (f_c = 43 and 62 MPa) used in the PTC applications was selected for the experimental work. The l_e was chosen by considering the transmission length (L_t) for the applied prestress level. As mentioned in Chapter 2, the l_e should be at least more than twice the L_t. Specimens with taut and stressed strands were prepared. For the taut strand specimens, the minimum stress of about 0.1 f_{pu} was applied to avoid the wobbling of the strands, and two strengths of concrete (f_c = 43 and 62 MPa) were used with l_e = 450 mm. For the stressed strand specimens, the maximum stress of about 0.7 f_{pu} was applied and the length of the specimen (L) was 1000 mm so that l_e is more than twice the L_t. For a stress of ~0.7 f_{pu}, the L_t in concrete with f_c = 62 MPa is about 440 mm (Mohandoss et al., 2018).

The pull-out specimens with a maximum of 1000 mm long specimens can only be tested using the available MTS machine at IIT Madras. As the height of the universal testing machine (UTM) limits the available space to mount the frame. Therefore, for the stressed strands f_c = 43 MPa could not be used as it requires l_e more than 1000 mm. Also, the stressed strands with short l_e of 450 mm could not be designed as in the taut strands due to inadequate L_t to transfer the prestress. Thus, to compare the τ_b of stressed strands with that of taut strands, similar specimens (l_e of 950 mm and f_c of 62 MPa) with taut and stressed strands were cast and tested.

4.4.3 Casting of concrete and precautions

A 5 cm long PVC pipe was kept around the strand near the live end (as a bond-breaker). The bond breaker was placed to avoid the stress concentration during the pull-out test. The wedges and barrels were placed outside the end brackets of the prestressing bed so as to lock and maintain the applied prestress. A stress adjusting system with a nut-bolt arrangement was placed at the releasing end to facilitate the gradual release of the prestress. The prestressing and release methods are similar to L_t specimens discussed in Section 4.3.3

Concrete was prepared and placed inside the prism moulds that are placed on the prestressing bed. Also, it was ensured that the mould-releasing oil, if any, on the surface of the strand was removed. The concrete was hand-compacted as per IS 1199 (1959) and ASTM C192 (2016) to obtain adequate and uniform compaction, especially along the strand-concrete interface. This helped in reducing the scatter in the test results. Three companion cube specimens were also cast and the f_c at the time of pull-out test was determined. The taut specimens were demoulded and the prestress was released after 24 hours. However, the stressed specimens were demoulded and the prestress was released only after third day after casting. This was delayed so that the concrete attains sufficient strength (say, about 60% of its target strength) to withstand the stress transferred. Figure 4.13 shows the photograph of the specimens cast for the pull-out test.

Figure 4.13 The photograph of the pull-out specimens

The compaction of concrete plays a critical role in the preparation of pull-out specimens as it could affect the S-C interface. Therefore, it has to be done properly to achieve uniformity by avoiding voids. Care was taken to attain proper compaction as per IS 1199 (1959) and ASTM C192 (2016). Since the depth and width of the specimens were 100 mm, concrete was placed in a single layer for a section length of about 100 mm (to avoid separation at the S-C interface) and it was hand compacted. Each section was given 25 strokes and distributed uniformly along the length of the moulds. After compacting the layers, the outsides of the mould were tapped for about 10 to 15 times to release the trapped large air bubbles. The surface of the strand should be clean without any rust formation and oil while placing the concrete. Also, the end faces of the specimens were finished and maintained perpendicular to the axis of the strand.

4.4.4 Pull-out test set-up and procedure

Figure 4.14 shows the details of the pull-out test set-up used. A pull-out frame of 1.4 m long was designed and fabricated to perform the bond test. 40 mm thick top and bottom hardened steel plates of the frame are connected using four tension members (1.4 m long and 36 mm diameter steel rods). The top plate of the frame was connected to a rod (with swivel joint), which was gripped at the top wedge of the universal testing machine (UTM). The bottom steel plate of the frame has a hole of 16 mm diameter at the centre. The strand protruding from the live end of the specimens were inserted through this centre hole and gripped using the V-grooved wedges at the bottom of the UTM. The top portion of the specimen was free and that end is known as the free end (FE). Two LVDT's were placed, one at the LE and the other at the FE of the strand to measure the slips. The load was applied at a displacement rate of 2 mm/min. The applied load and slip at both LE and FE were continuously monitored using a data acquisition system. Figure 4.15 shows the photograph of the pull-out frame with a specimen mounted on the MTS machine.

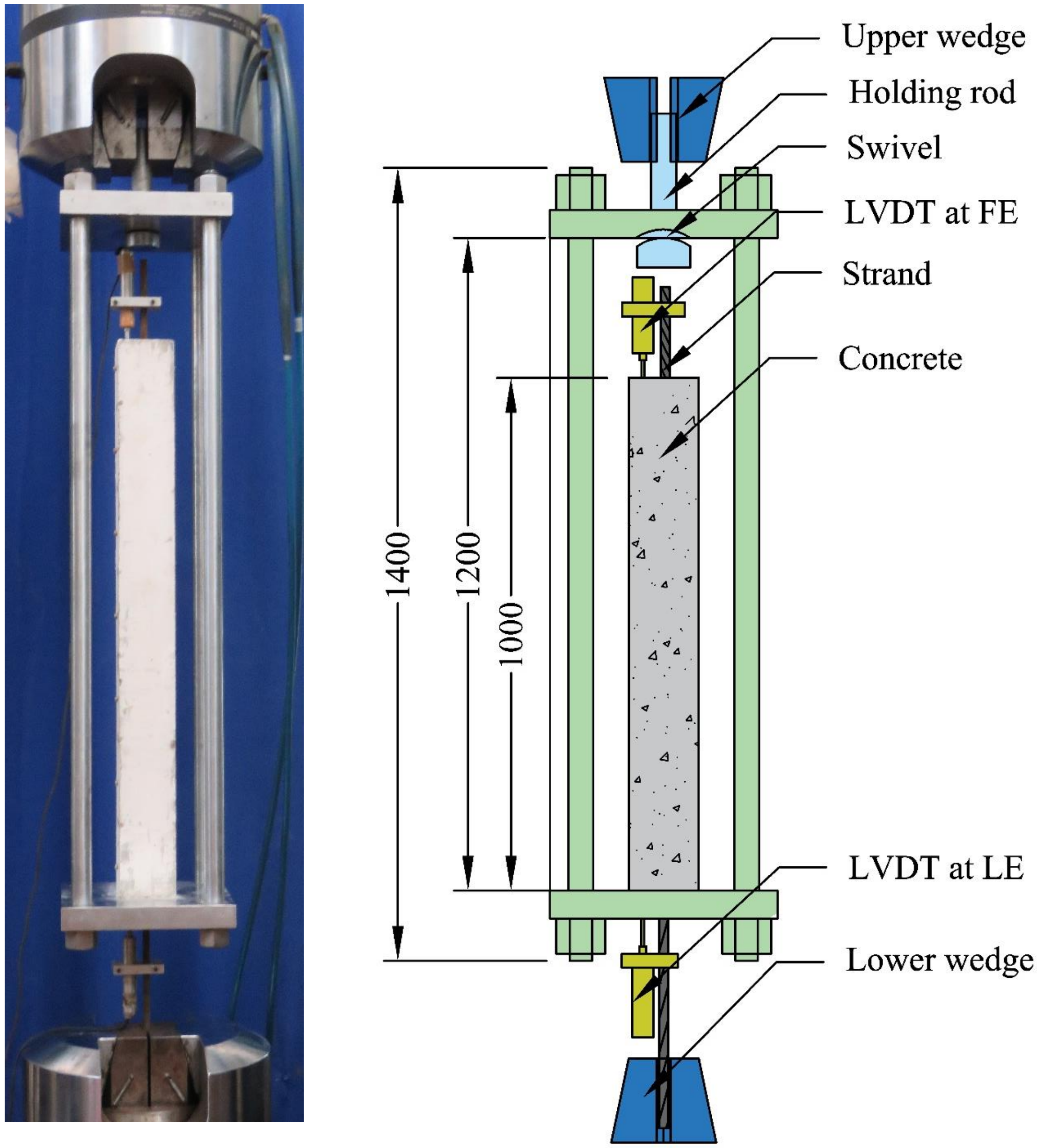

All dimensions are in mm

Figure 4.14 The details of the pull-out test set-up

Figure 4.15 The photograph of the experimental set-up used for the pull-out test

4.4.5 Instrumentation

Two LVDT's of 50 mm travel length (AEP transducers) were used. One was placed at the live end and the other was placed at the free end of the strand, as shown in Figure 4.14 - to measure the slip of the strand with respect to the concrete during testing. An L-shaped smooth plate surface was placed on the surface of concrete at the free end to place the LVDT in a position to get a uniform reading. A QuantumX (MX 1615B model) data acquisition system (DAQ) was used for measuring the test parameters. Two LVDTs, displacement of actuator and load cell of the UTM machine were connected to the DAQ system to record the LVDTs' reading, displacement of actuator, load, and elapsed time.

4.5 SUMMARY

In sum, this chapter delineated the experimental method adapted for the study which provides the details of materials, configuration of specimens, experimental variables, and specimen preparations for L_t and bond studies. Also, the methods adapted and instrumentations used to measure the L_t and the bond-slip behaviour of the PTC systems in detail. The results obtained from the experimental programs would be enumerated in the following chapters.

5 RESULTS AND DISCUSSIONS – TRANSMISSION LENGTH (L_t)

5.1 INTRODUCTION

This chapter presents and discusses the results obtained from the experimental investigations to achieve Objective 1, which addressed the effect of compressive strength of concrete at transfer and time on transmission length. The challenges associated with the transmission length measurements were discussed to reduce the error in the DEMEC measurements. Based on the experimental results, this chapter proposes an L_t model as a function of the f_{ci} and compares that with the available standard L_t models. Also, the consequences of the underestimation and overestimation of the L_t are disputed by conducting case studies which emphasise the significance of the L_t on the shear performance of the PTC members in the transmission zone.

5.2 OBJECTIVE 1: EFFECT OF COMPRESSIVE STRENGTH AT TRANSFER (f_{ci}) ON TRANSMISSION LENGTH (L_t)

Objective 1 has the following three sub-targets: 1) Evaluation of the suitability of various codes for estimating the transmission length, 2) Determination of effect of compressive strength of concrete at transfer on L_t, and 3) Effect of L_t on the shear capacity of the pristine PTC systems and transverse tensile stress distribution along the transmission zone. The first part of the objective is a comparative study to identify the differences and limitations existing in the standard design equations. Then, the following section sets forth the experimental observations on the effect of compressive strength at transfer and time on the L_t and case studies were discussed to highlight the significance of L_t on the shear capacity of the PTC members.

5.3 EVALUATION OF THE EXISTING TRANSMISSION LENGTH MODELS

The available equations to calculate the L_t (discussed in the literature chapter) are evaluated to understand the differences existing between the standard and empirical equations. Many factors could influence the L_t of the member, however, the effect of compressive strength at transfer on the transmission length is the focus of the study. The results indicated that some of the codes over/under estimate the required transmission length, especially the codes that do not consider the f_{ci}. This highlights the need for considering the f_{ci} in the design transmission length.

5.3.1 Comparison of available L_t models

Based on the available codal and literature equations, the L_t was calculated (denoted as $L_{t,\ code}$) and compared to analyse the difference existing among each other. Generally, in the precast PTC systems, 12.7 mm diameter strands are used and stressed to 0.75 f_{pu}. M55 and M65 are the commonly used concrete grades in the PTC systems and as per IS 1343 (2012) the minimum grade of concrete should not be less than M45. Therefore, for the comparative analysis, concrete grades of M35, M45, M55, and M65 were used and the same grades were considered for the experiments also. Figure 5.1 presents the $L_{t,\ code}$ based on ACI, AASHTO, AS, CSA, IS, BS, EN, and *fib*-MC standards for 12.7 mm diameter, 1860 MPa grade, low relaxation strand embedded in concrete with f_{ci} of 23, 28, 36, and 43 MPa. The design equations provided in the standards are discussed in Chapter 2.

Table 5.1 summarises the different parameters considered to compute the design of the L_t in different standards. As ACI, AASHTO, AS, CSA, and IS do not consider f_{ci} as one of the variables in their design L_t equation, L_t is not changed when f_{ci} is increased from 23 to 43 MPa. Based on these standards, $L_{t,\ code}$ for 12.7 mm dia. strand stressed to 0.75f_{pu} is 718, 762, 635, and 381 mm for ACI, AASHTO & AS, CSA, and IS, respectively for all grades of concrete. These codal provisions using empirical formulation based on the diameter of the strands without considering the properties of the concrete may result in less conservative or less rational shear design near the supports (Barnes et al., 2003; Mohandoss et al. 2015).

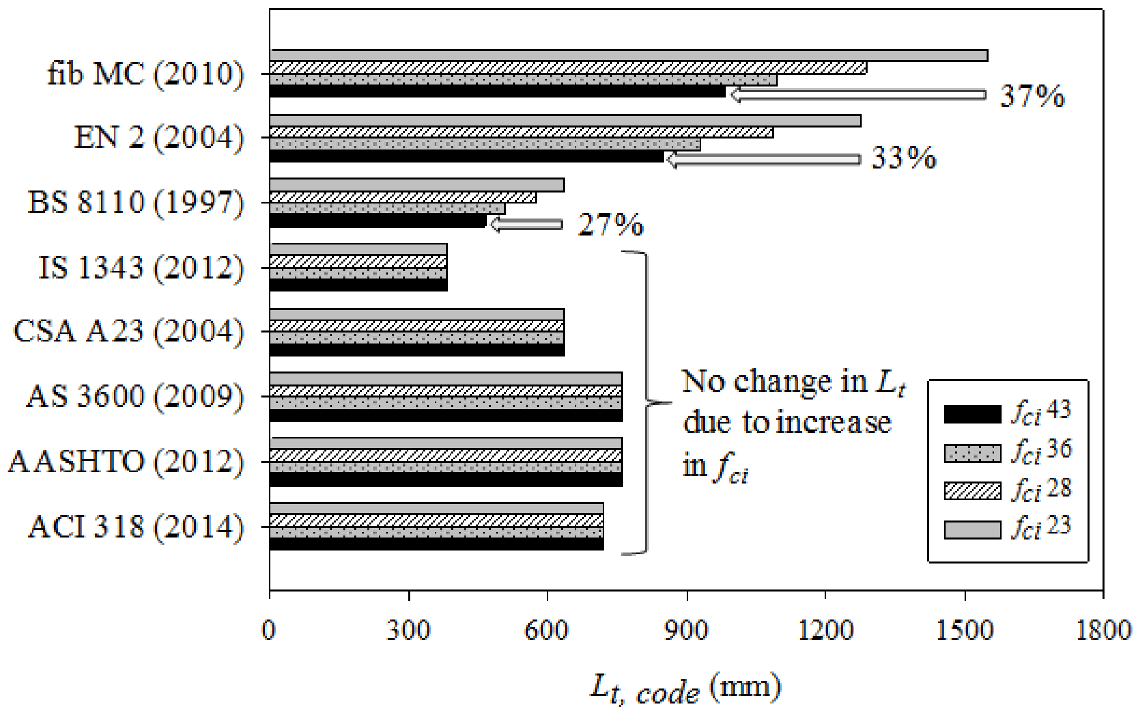

Figure 5.1 Design L_t based on standards for different strengths of concrete at transfer

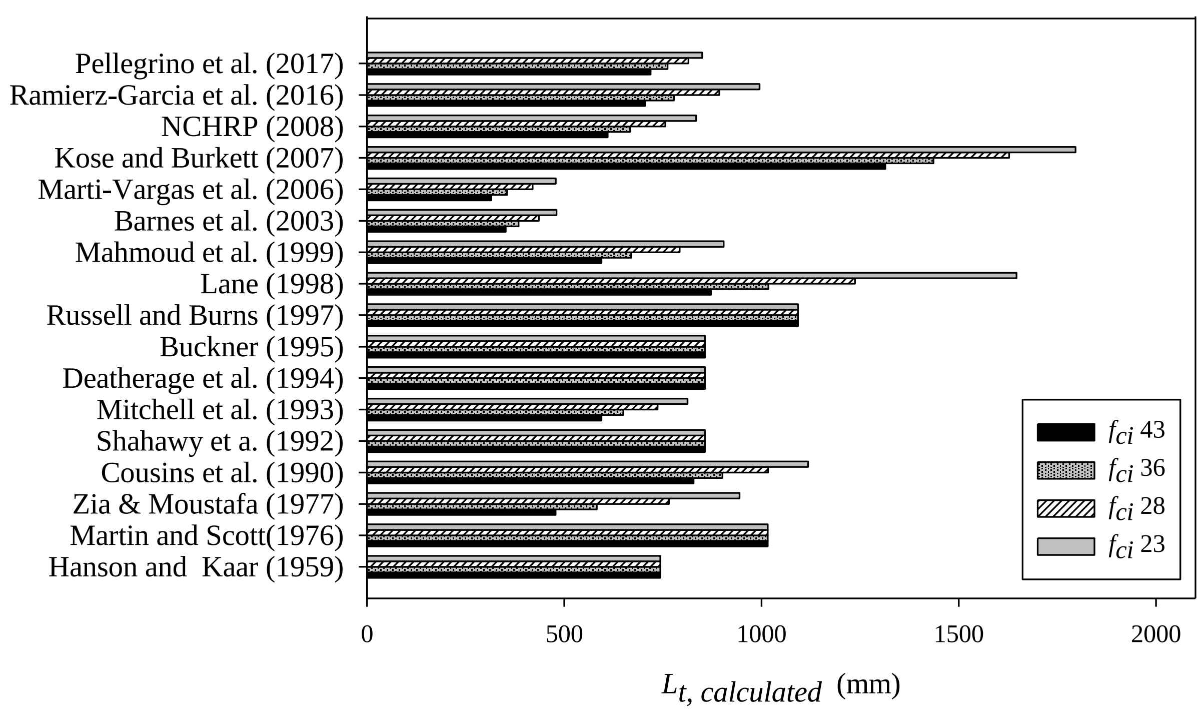

Figure 5.2 Calculated L_t using the empirical model equations from literature

Table 5.1 Parameters considered in different standard L_t equations

Codes	Applied prestress	Strand diameter	Concrete strength at release	Bond stress / condition	Type of tendon	Releasing method
AASHTO (2012)	✗	✓	✗	✗	✗	✗
AS 3600 (2009)	✗	✓	✗	✗	✗	✗
CSA (2004)	✗	✓	✗	✗	✗	✗
IS 1343 (2012)	✗	✓	✗	✗	✗	✗
ACI 318 (1963-2014)	✓	✓	✗	✗	✗	✗
BS 8110 (1997)	✗	✓	✓	✗	✓	✗
EN 2/ IRC (2004)	✓	✓	✓	✓	✓	✓
fib MC (2010)	✓	✓	✓	✓	✓	✓

✓ - Considered in the codes; ✗ - Not considered in the codes

On the other hand, the design value of the L_t based on EN 2 and *fib* MC 10 decreases significantly as the f_{ci} increases thus representing a realistic behaviour. From the plots, it can be seen that the value of the L_t based on the *fib* MC (2010), EN 2 (2004), and BS 8110 (1997) was increased by about 37, 33, and 27%, respectively. The European code overestimates the L_t value by considering many factors that could influence the L_t. Since the values are over predicted, the number of underestimated cases are lower in EN codes than the ACI and AASHTO codes (Martí-Vargas and Hale, 2013).

Figure 5.2 illustrates the calculated values of L_t for different selected concrete strength using the empirical equations proposed by several authors. The values of L_t by Hanson and Kaar (1959), Martin and Scott (1976), Deatherage et al. (1994), Buckner (1995), and Russell and Burns (1997) are 745, 1015, 855, 855, 1090 mm, respectively for all the four f_{ci} as these equations do not consider the f_{ci}. The experimental work and results of Hanson and Kaar (1959) is the fundamental study for the L_t model, and the equation developed based on this study was adapted by ACI 318 (1963). Even today, the same equation is being used by ACI 318 (2014). The number at the denominator indicates the compressive strength of concrete used in those study in the 1960's. The concrete strength and strand used in today's modern construction practices are different from those used in the olden days. Hence, the codal equations should be revised to meet the current construction practices.

Zia and Moustafa (1977), Cousins et al. (1990), Mitchell et al. (1993), Lane et al. (1998), Mahmoud et al. (1999), Barnes et al. (2003), Martí-Vargas et al. (2006), Kose and Burkett (2007), NCHRP (2008), Ramierz-Garcia et al. (2016) and Pellegrino et al. (2017) proposed an empirical equation to calculate the L_t by considering the f_{ci}. However, a huge scatter was observed on the calculated L_t using these empirical equations. For instance, the value of $L_{t,\ calculated}$ for f_{ci} = 43 MPa varied from 315 mm to 1314 mm. Some of these values of $L_{t,\ calculated}$ resulted lesser or higher than that of the $L_{t,\ code}$. This indicates that the design values could underestimate/overestimate the required L_t.

As explained earlier, a realistic estimation of transmission length is important for a pretensioned concrete structural design, especially in the precast PTC industry where obtaining a product within a short duration is essential. So, it is necessary to attain the required f_{ci} as early as possible so that the member can have adequate length to transfer the prestress at release. As explained in Figure 2.4, the L_t is the part of development length (L_d) and therefore, the estimation of L_t influences the stress in the prestressing strand under service. Incorrect estimation of L_t can affect the shear capacity in the end zones of the member at prestress release (Ramirez-Garcia et al., 2016). The under or overestimation of the L_t could lead to the following consequences. Accordingly, a design engineer should address the implications of these effect on the design of PTC members (Martí-Vargas and Hale, 2013).

5.3.2 The significance of transmission length

5.3.2.1 Overestimation of transmission length

If the design L_t is longer than the required L_t, the resulted shorter L_t could increase the stress in the end zone. This could lead to the risk of cracking by concrete splitting and bursting and could result in spalling of concrete in the end regions. Accordingly, this could affect the bond at the transmission zone if the members do not have confinement or shear reinforcement (den Uijl, 1998). Kasan and Harries (2011) reported that if the bond is lost in the transmission zone, an effective prestress could redevelop by bond at a distance from the damaged location. It is critical, especially for the design of precast hollow core slabs, where the members do not have shear reinforcements (Vázquez-Herrero et al., 2013). Hence, proper design checks should be taken to avoid such issues.

5.3.2.2 Underestimation of transmission length

If the design/estimated L_t is shorter than the required L_t, the resulting longer L_t could reduce the available member length to resist bending moment and shear. This will eventually affect the serviceability of the member and result in an unconservative design for shear and flexural. This situation would be worse in the case of hollow core slabs, where prestress transfer plays a major role in shear capacity of the member. The detailed discussion on the significance of transmission length on performance of PTC members is provided in the later sections.

5.4 DETERMINATION OF L_t USING DEMEC GAUGE

As mentioned in Chapter 5, the L_t is determined by obtaining the strain profile on the concrete surface. The strain on the concrete surface is determined by measuring the change in distance between the target points placed on the concrete surface using the DEMEC guage. The measurement of DEMEC gauge readings could seem simple; but it is highly sensitive to the posture of the person taking the measurements, the way of holding the gauge, the speed of taking the reading, etc. The measurement of L_t involves multiple and overlapping gauge lengths, the measurement across which needs to be taken uniformly in a short period (say, a few minutes), adding the difficulties in obtaining reproducible results. Therefore, the DEMEC readings can vary when taken by different persons. To understand this human error and its sensitivity to the L_t calculations, a blind test was conducted and discussed in the following sub-section.

5.4.1 Human error on the DEMEC measurements

In the blind test, three persons (denoted as P1, P2, and P3) measured the length of a standard reference rod (150 mm long invar rod) using the same DEMEC gauge and at the measurement rates of 1.5, 3, and 2 readings/min, respectively. P1 was an undergraduate student and P2 and P3 were graduate students. Figure 5.3 shows the box plot with possible human error in measurement (or the deviation from 150 mm) in the four cases. Vide footnote of Figure 5.3 for the definition of four cases, C1, C2, C3, and C4 with different persons positioning the gauge and reading the data. In the C4, to check the sensitivity of DEMEC measurements, P3 took 100 readings blindly (i.e., without looking at the display of the gauge) to avoid any bias on reading.

The mean (μ) and standard deviation (σ) of C1 and C2 are significantly larger than those of C3 and C4. From the results, it is observed that P1 did not hold the gauge properly and hence, could not obtain consistent and/or reproducible results. Also, significant variation was observed in P2's reading (who has more experience than P1 in DEMEC measurements and hence measured faster than P1 and P3). Person P3 with proper control and moderate speed could control the reading and obtain reproducible results with less error. Hence, in the blind test for Case C4, P3 could take reading with an acceptable error and obtained reproducible results. This study showed that human error could be significant and with appropriate procedures, the variation in the error could be controlled and reproducible results could be obtained. It is to be noted that the other errors such as instrument error are not considered in this study.

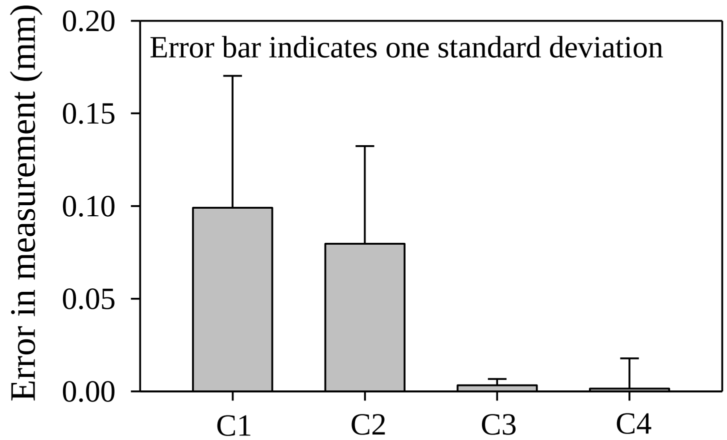

C1- Gauge positioned & data read by P1; (1.5 readings/min)
C2- Gauge positioned & data read by P2; (3 readings/min)
C3- Gauge positioned & data read by P3; (2 readings/min)
C4- Gauge positioned by P3 and data read by P1; (2 readings/min)

Figure 5.3 Variation in DEMEC reading with different persons

5.4.2 Difference in DEMEC measurement using inserts and discs

Strain measurements on concrete surfaces is heavily dependent on the type of gauges used and bond conditions, especially for long-term measurements. In this study, initially DEMEC discs were glued onto the concrete surface using acrylic based adhesive. It was observed that this glue could not provide sufficient bond between these discs and concrete – probably due to the moisture curing practices and/or smooth/machined surfaces of the discs. Also, the force exerted by the technician while placing the gauge onto the DEMEC disc could lead to debonding. To avoid such issues, custom-made brass inserts were used to obtain the quality data, especially for long-term measurements. A brass insert was profiled with a 6 mm wide groove to ensure adequate bond/grip, as shown in Figure 4.7.

For a comparative study, the strain measurements were taken using discs and inserts placed on the same surface of an L_t specimen. As shown in Figure 5.4, inserts were placed along the mid-depth on opposite side faces of the specimen (indicated as I and I$^{/}$) and the discs were placed adjacent to the inserts (indicated as D and D$^{/}$); and companion readings were taken. The two curves with filled and unfilled markers in Figure 5.5 indicate the strain measurements using discs and inserts, respectively. The result proved that discs can significantly underestimate the strain measurements, when above 300 $\mu\varepsilon$. For example, at about 600 mm from the end of the member, the strain values obtained using inserts and discs were about 550 and 400 $\mu\varepsilon$, respectively – indicating a reduction of about 25%. The strain values calculated using Hooke's law, applied prestress, and the measured elastic modulus of concrete were closer to the strains obtained using the inserts than those using the discs. Hence, the inserts were used in the remainder of this study.

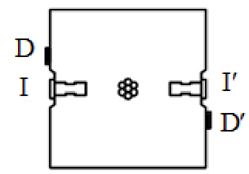

(a) Front view of the L_t specimen (b) Section view

Figure 5.4 Placement of DEMEC inserts and pins on the concrete surface

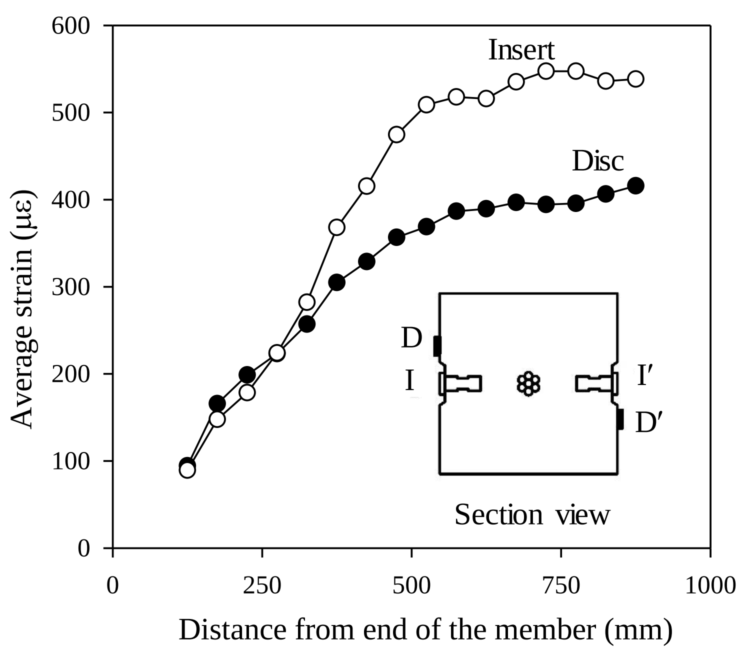

Figure 5.5 Strain values using DEMEC inserts and pins

5.5 EFFECT OF COMPRESSIVE STRENGTH OF CONCRETE ON TRANSMISSION LENGTH

Table 5.2 provides the f_{ci}, f_{pe} at transfer, and measured L_t (denoted as $L_{t,\,measured}$) at both releasing and jacking ends for all the specimens. Figure 5.6 - Figure 5.9 show the average smoothed variation of strain, $(\varepsilon'_c)_x$ along the length of the specimens. At transfer, the strain on the concrete surface increased along the length of the member from the end and became constant. The average strain for all the strengths of concrete at transfer was about 530 με. As the stress is transferred from the strand to concrete at 3 days, the strain variations between the different specimens could be in the range of 5 to 20 microstrains, which could not be exactly captured by DEMEC gauge. Based on the 95% AMS method, a horizontal line has been drawn to 95% of the maximum average strain. The distance at which the line intersects the strain profile is considered as the L_t as explained in the AMS method in Chapter 4.

Table 5.2 Experimental parameters at transfer and measured L_t

Specimen ID	f_{ci} (MPa)	f_{pe} (MPa)	$L_{t,\,measured}$ (mm)			$L_{t,\,avg}$ (mm)	Standard deviation (mm)
			JE	RE	Average		
f_{ci}23 – S1	23.50	1270	630	565	600	580	32
f_{ci}23 – S2	22.80	1189	520	570	545		
f_{ci}23 – S3	22.10	1230	625	580	600		
f_{ci}28 – S1	28.00	1179	550	570	560	565	17
f_{ci}28 – S2	29.00	1209	540	560	550		
f_{ci}28 – S3	28.70	1220	565	600	585		
f_{ci}36 – S1	37.10	1148	480	500	490	465	28
f_{ci}36 – S2	36.00	1179	460	470	465		
f_{ci}36 – S3	36.80	1120	430	445	435		
f_{ci}43 – S1	43.40	1169	385	370	375	385	9
f_{ci}43 – S2	42.56	1189	390	405	395		
f_{ci}43 – S3	43.72	1108	400	375	390		

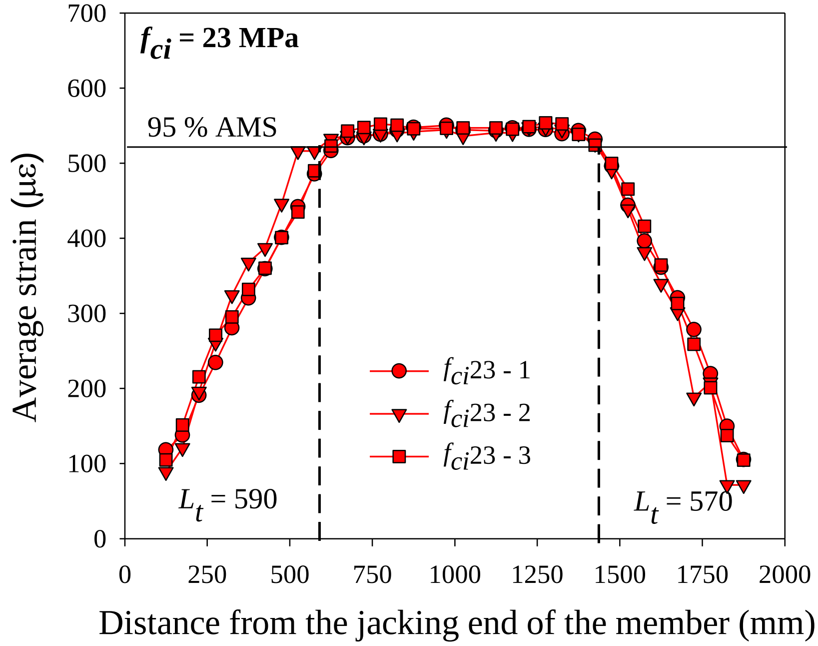

Figure 5.6 Average strain on the concrete surface for f_{ci} = 23 MPa

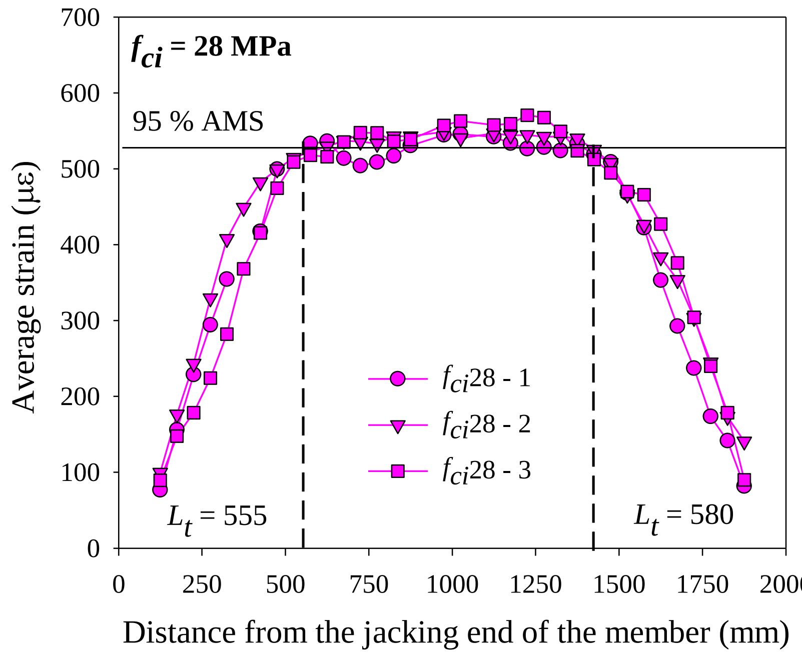

Figure 5.7 Average strain on the concrete surface for f_{ci} = 28 MPa

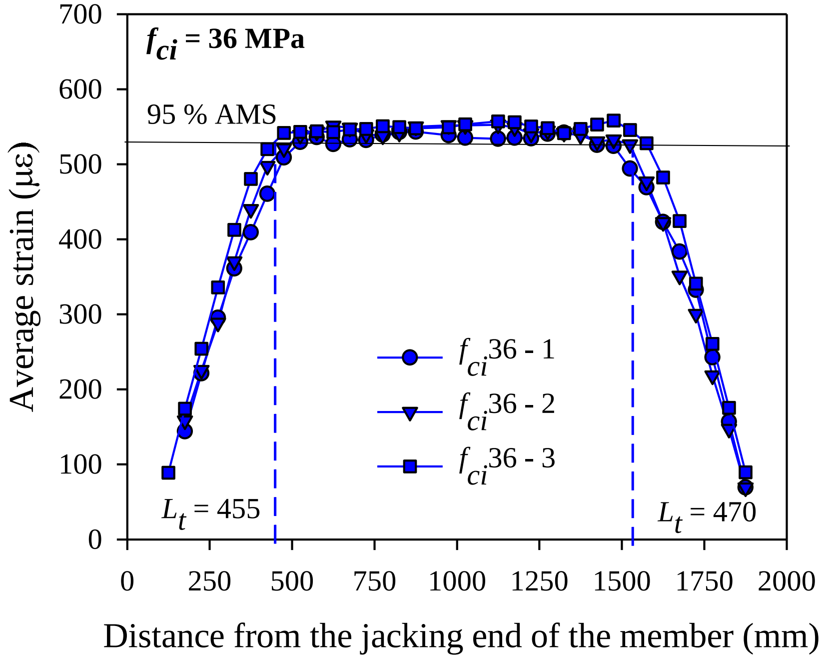

Figure 5.8 Average strain on the concrete surface for f_{ci} = 36 MPa

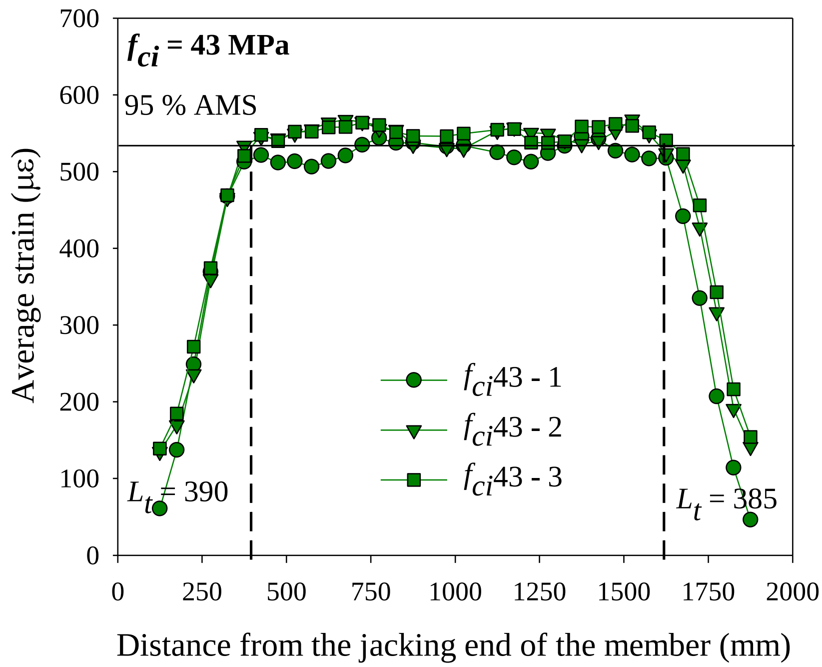

Figure 5.9 Average strain on the concrete surface for f_{ci} = 43 MPa

The values of $L_{t,\,measured}$ at both the jacking end (JE) and releasing end (RE) were indicated in the figures. From the plots, it was observed that the values of $L_{t,\,measured}$ at both JE and RE were similar as the gradual releasing method was adapted in this study (Benítez and Gálvez, 2011). The average L_t for f_{ci} = 23, 28, 36, and 43 MPa strength concretes were 582, 565, 463, and 386 mm, respectively, with coefficients of variations of about 2 to 10%, which is reasonable. As the compressive strength of concrete increases, the bond strength increases due to increased stiffness and results in a reduction of L_t. When the f_{ci} increased from 23 to 43 MPa, L_t decreased by about 35%. Further, the relationship between the f_{ci} and L_t was discussed in the following Section 5.51.

5.5.1 Development of empirical equation based on experimental results

Figure 5.10 indicates the variation of $L_{t,\,measured}$ with the compressive strength of concrete at transfer. Then the measured values of L_t were normalised to f_{pe} and d_s to model the L_t as a function of only f_{ci}. This was based on the assumptions that the L_t varies linearly with respect to f_{pe} and d_s alone. As the L_t decreased with increasing f_{ci}, to capture the effect of f_{ci}, a scatter plot between the inverse of f_{ci} and the normalised $L_{t,\,measured}$ to f_{pe} and d_s was developed (see Figure 5.11). From the plot, it was observed that the trend of L_t as a function of $1/f_{ci}$ was bilinear. For a lower f_{ci} (23 and 28 MPa), the L_t did not decrease significantly with increase in f_{ci}. However, in concrete with strength higher than 28 MPa, a significant reduction (say, up to 32%) in the L_t was observed. Also, it was observed that the scatter in the values of L_t was less with the increasing strength of concrete. Therefore, a bilinear model was proposed as shown in Eqs. (5.1) and (5.2).

$$L_t = f_{pe} d_s \left(0.028 + \frac{0.24}{f_{ci}} \right) \qquad f_{ci} < 28 \text{ MPa} \qquad \text{Eq. (5.1)}$$

$$L_t = f_{pe} d_s \left(0.0036 + \frac{0.94}{f_{ci}} \right) \qquad 28 < f_{ci} < 43 \text{ MPa} \qquad \text{Eq. (5.2)}$$

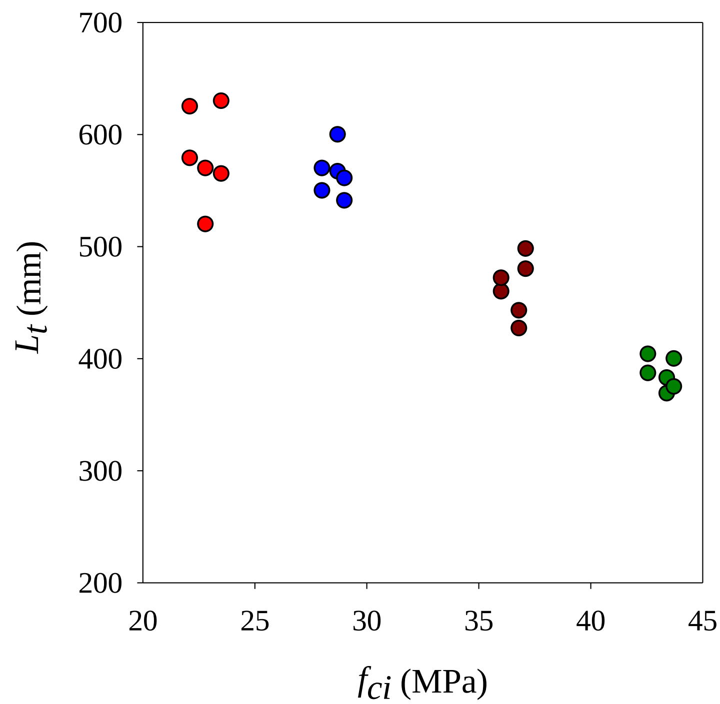

Figure 5.10 Variation of L_t with the compressive strength of concrete at transfer

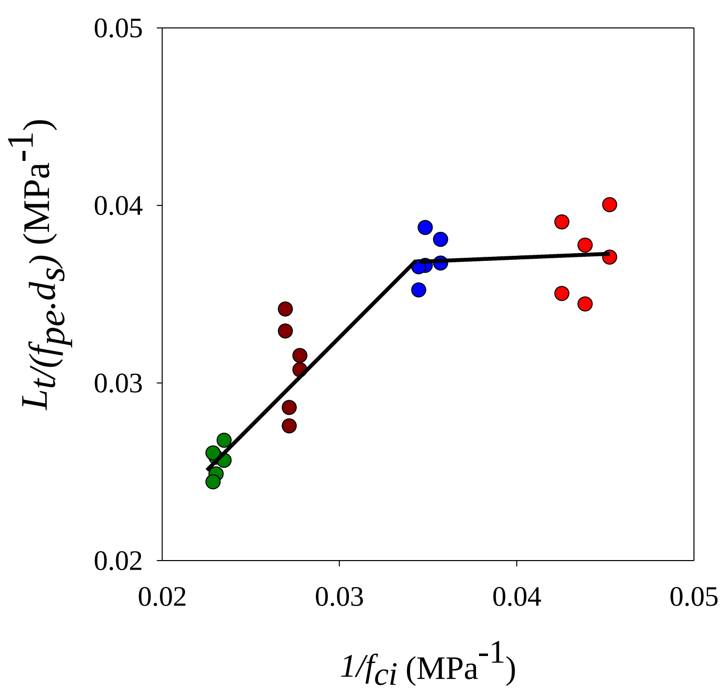

Figure 5.11 The proposed bilinear model for L_t as a function of f_{ci}

Figure 5.12 shows the correlation between the L_t estimated using the proposed model Eqs. (5.1) and (5.2) and $L_{t,\,measured}$. Many data points lie between the two dashed-lines (one standard deviation away from the average line) indicating the reasonable prediction. Also, the mean absolute percent error (MAPE) of the model is found to be 3%, - indicating a reasonable prediction accuracy.

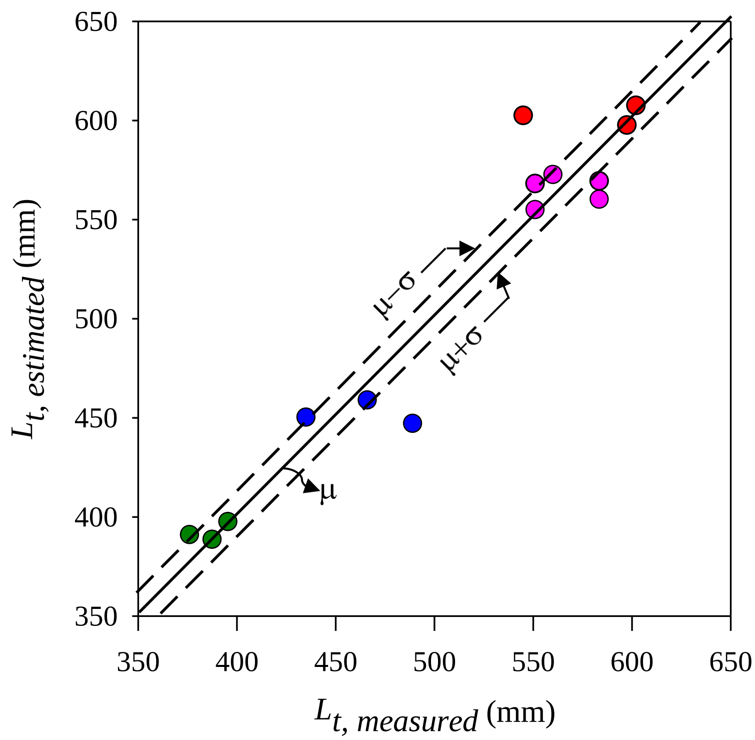

Figure 5.12 Correlation between the $L_{t,\,estimated}$ and $L_{t,\,measured}$

5.5.2 Comparision of the L_t obtained from the proposed model and various codes

Figure 5.13 shows the comparison of L_t obtained from the proposed model and various code (considering f_{ci}). The straight lines indicate that the L_t, obtained using AASHTO, AS, ACI, CSA, and IS codes (i.e., not a function of f_{ci}). However, the L_t based on EN 2 (2004), *fib* MC (2010), and the proposed model show a downward trend as the concrete strength increases. It was evident that consideration of the f_{ci} in the design L_t equation represents the rational behaviour of the PTC systems from the experimental results obtained in this study.

Therefore, the f_{ci} should be considered in the design L_t equations specified by standard for a realistic estimation of L_t. In practice, the PTC members will use concrete with f_{ci} more than 20 MPa. Considering this, Figure 5.13 indicates that all the codes, except IS 1343 (2012) and the proposed model overestimate the L_t.

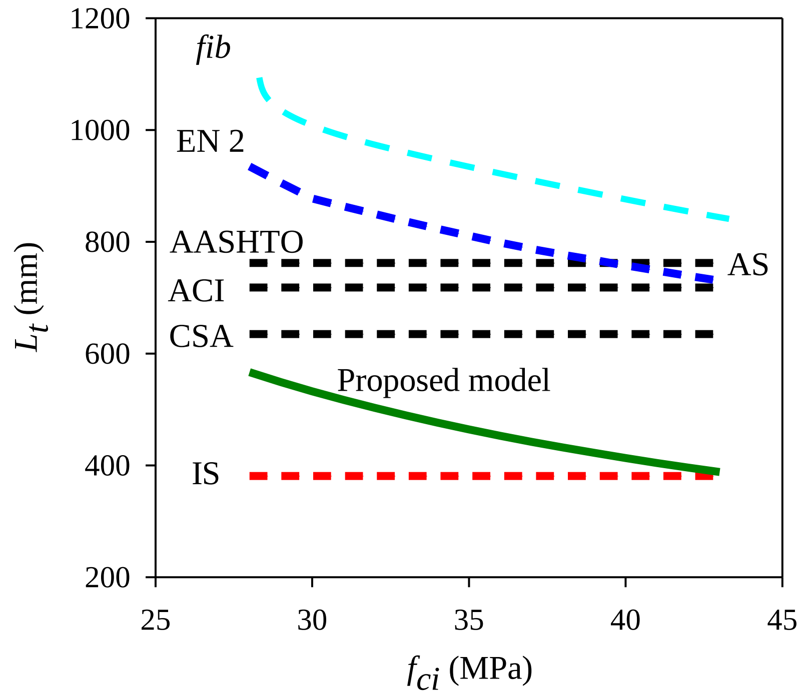

Figure 5.13 Comparison of L_t models as function of f_{ci}

Table 5.3 provides the ratio of $L_{t,\, code}$ to $L_{t,\, estimated}$ ($L_{t,\, R}$ herein) for the selected codes. Except IS 1343 (2012), the $L_{t,\, R}$ for other codes was greater than 1 and represented the conservative L_t designs. The $L_{t,\, R}$ based on IS 1343 were 0.65, 0.67, 0.82, and 0.99 for f_{ci} of 23, 28, 36, and 43 MPa, respectively. For lower concrete strength, i.e., when the f_{ci} = 23 MPa, the actual L_t of the member was almost double the design L_t based on IS 1343 (2012). $L_{t,\, R}$ increases with increase in f_{ci}. $L_{t,\, R}$ becomes almost 1 for high strength concrete with f_{ci} = 43 MPa. This indicates that the codal design equation can be used only for the high strength concrete. However, in practice at the construction site, concrete strength could be lower and could result in the longer L_t. Therefore, for a standard, it is important to overestimate the required L_t by considering the vulnerable conditions. However, the overestimation of L_t beyond a certain level is also not a conservative approach for the design of stirrups for bursting stress near the ends and this is explained in the following section. Hence, a rational approach in estimating the L_t is required based on f_{ci}.

Table 5.3 The ratio of $L_{t,\,code}/L_{t,\,estimated}$

Codes	$L_{t,\,code}$ (mm)				$L_{t\,R} = \frac{L_{t,\,code}}{L_{t,\,estimated}}$			
	f_c23	f_c28	f_c36	f_c43	f_c23	f_c28	f_c36	f_c43
AASHTO (2012) & ACI (2009)	760	760	760	760	1.31	1.35	1.65	1.99
ACI 318 (2014)	720	720	720	720	1.23	1.27	1.55	1.87
CSA A23 (2004)	635	635	635	635	1.09	1.12	1.37	1.66
IS 1343 (2012)	380	380	380	380	0.65	0.67	0.82	0.99
BS 8110 (1997)	635	575	510	465	1.09	1.02	1.10	1.21
EN 2 (2004)	1275	1090	930	850	2.19	1.93	2.01	2.22
fib MC (2010)	1550	1285	1100	980	2.66	2.28	2.37	2.56

Note: The values are rounded off to nearest 5 mm.

Figure 5.14 shows the comparison of the proposed model as a function of f_{ci} with the experimentally obtained L_t by various research work. It indicates that the obtained L_t using the proposed model is lower than many researchers' work (Oh et al., 2000; Martí-Vargas et al., 2012a; Deatherage et al., 1994; Russell and Burns, 1997). The difference in the result could be due to different materials and prestress releasing method adapted in their study. However, the results indicated that the f_{ci} significantly influence the L_t. Hence, f_{ci} has to be included in the design equation to represent the realistic L_t and avoid under or overestimation of L_t, which could lead to the poor shear performance of the member.

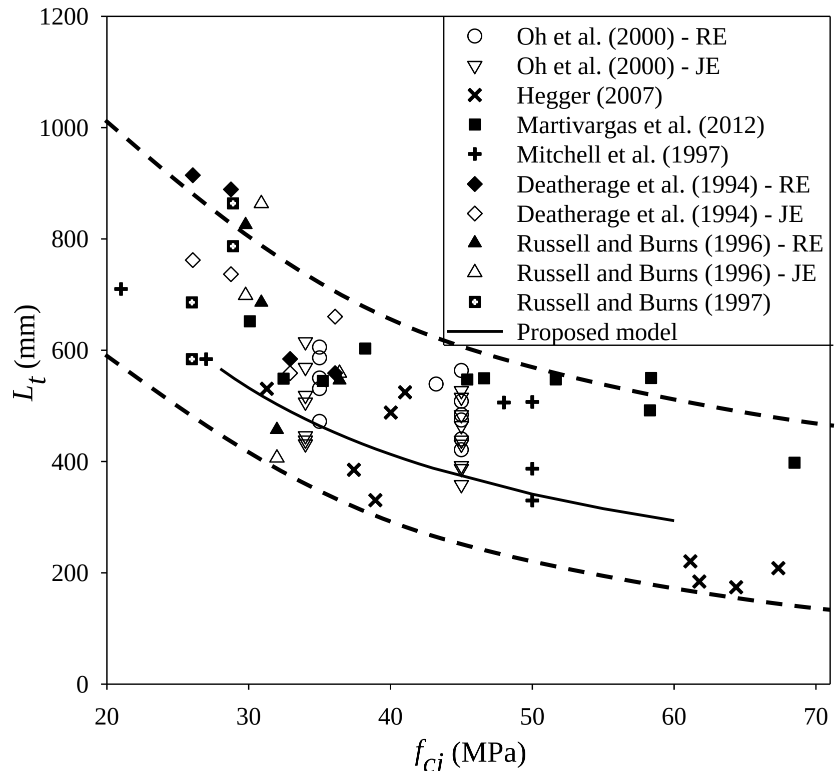

Figure 5.14 L_t as a function of f_{ci} from literature and proposed model

5.6 EFFECT OF TIME ON THE MEASUREMENT OF L_t

As explained in the literature section, L_t varies with time due to creep and shrinkage. However, in the literature, no conclusive results were reported. This study attempts to capture the effect of time on L_t at different ages for different $f_{ci.}$ Figure 5.15 - Figure 5.17 show the variations of strain (along the length of the specimen) at different ages of concrete for f_{ci} = 23 MPa.

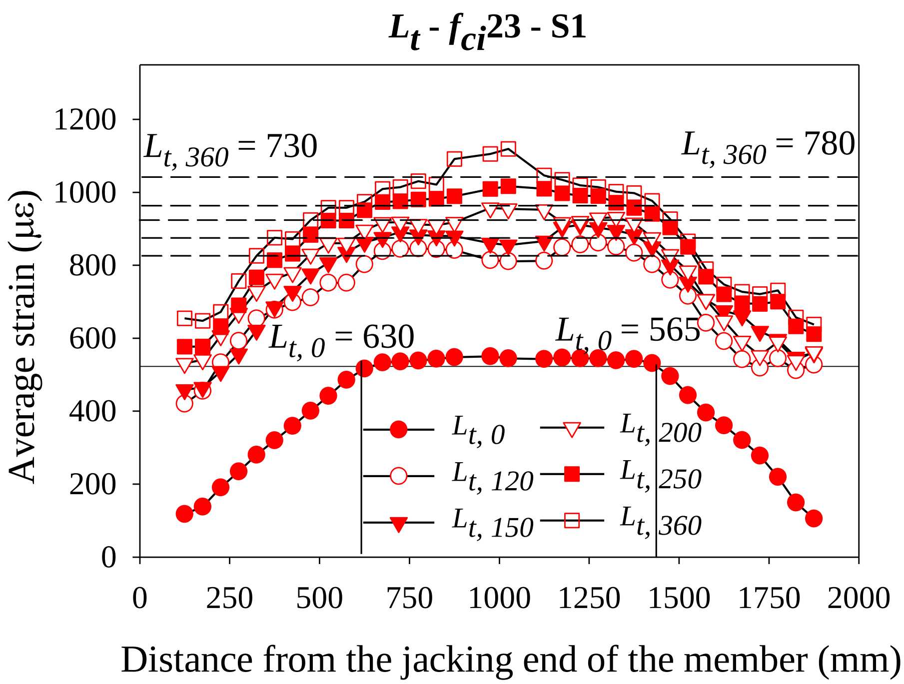

Figure 5.15 Effect of time on L_t of f_{ci}23 – Specimen 1 (until 360 days)

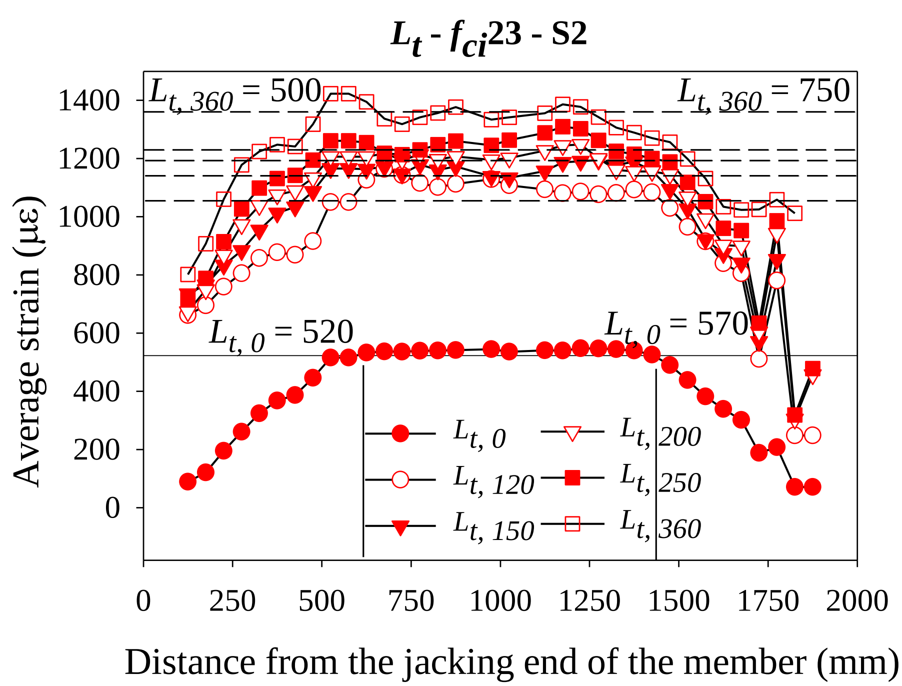

Figure 5.16 Effect of time on L_t of f_{ci}23 – Specimen 2 (until 360 days)

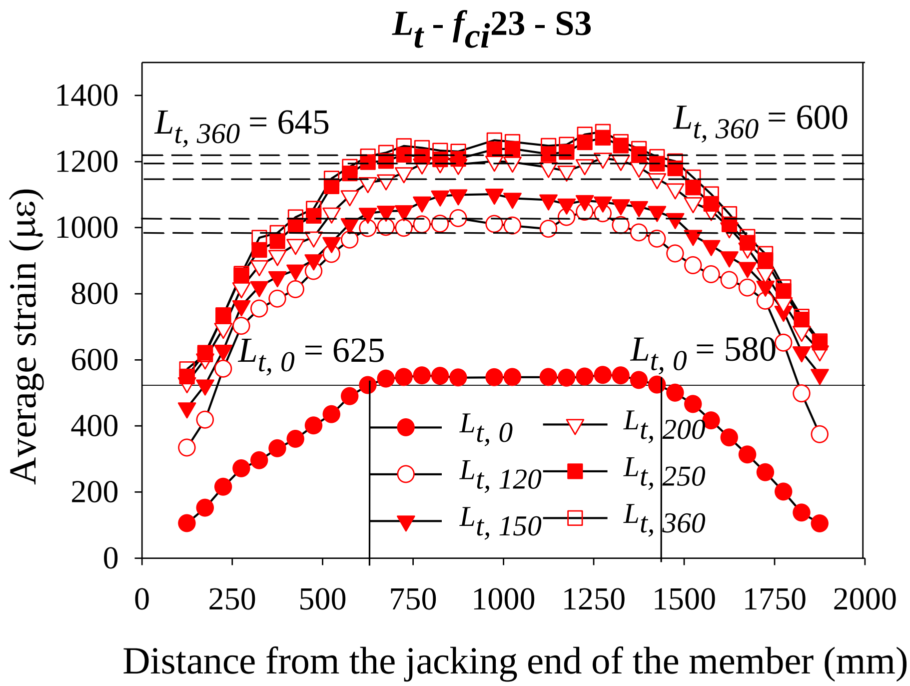

Figure 5.17 Effect of time on L_t of f_{ci}23 – Specimen 3 (until 360 days)

The L_t was measured at transfer, 120, 150, 200, 250, and 360 days for the f_{ci}23 specimens. The average $L_{t, measured}$ of each specimen at 0 and 360 days after the stress transfer denoted as $L_{t, 0}$ and $L_{t, 360}$, respectively. The horizontal dashed lines indicate the 95 % $\mathcal{E}_{c, max}$ at 120, 150, 200, 250, and 360 days of exposure.

At the time of stress transfer, the $\mathcal{E}_{c, max}$ for all the specimens were about 500 με. By 360 days of exposure, this $\mathcal{E}_{c, max}$ increased to about 1200 με for f_{ci}23-S1 and f_{ci}23-S3. Erroneous results were obtained for f_{ci}23-S2 at about 1750 mm from the jacking end of the member. Also, the maximum strain obtained on the surface of f_{ci}23-S2 was higher than that of f_{ci}23-S1 and f_{ci}23-S3. This difference indicates that the specimen has higher prestress loss than the other two specimens. Based on the 95% AMS, the average $L_{t, 360}$ was 750, 625, 620 mm, respectively for f_{ci}-S1, S2, S3. Unlike f_{ci}23-S1 and f_{ci}23-S3, the $L_{t, measured}$ at releasing end was longer than the jacking end due to erroneous results obtained. In addition to this, at the jacking end, the values of $L_{t, 360}$ was shorter than that of $L_{t, 0}$ which was not the expected behaviour. However, similar observations were reported in the literature, which say the

$L_{t, measured}$ could increase or decrease with time and the pattern varied with specimen to specimen (Swamy and Anand, 1975; Lane, 1998; Mitchell et al., 1993; Ramiriz and Russell, 2008; Pozolo and Andrawes, 2011). Also, some researchers had reported that the L_t varied significantly at both ends of the same specimens as in the case of f_{ci}23-S2 of this work, where the value of L_t at the jacking end was 33% shorter than that at the releasing end of the member (Swamy and Anand, 1975; Lane, 1998; Mitchell et al., 1993; Ramiriz and Russell, 2008; Pozolo and Andrawes, 2011).

Figure 5.18 - Figure 5.20 illustrate the average strain profile at different ages of concrete for f_{ci}36 specimens. The strain profiles are obtained at 150, 200, 250, and 300 days after the transfer of prestress. At transfer, the average strain on the concrete surface was about 550 με. The strain value on the concrete surface increased with time and at 150 days, the value of average strain was about 1000 με and further, with increasing time at 300 days, the average strain on the concrete surface increased to about 1220 με.

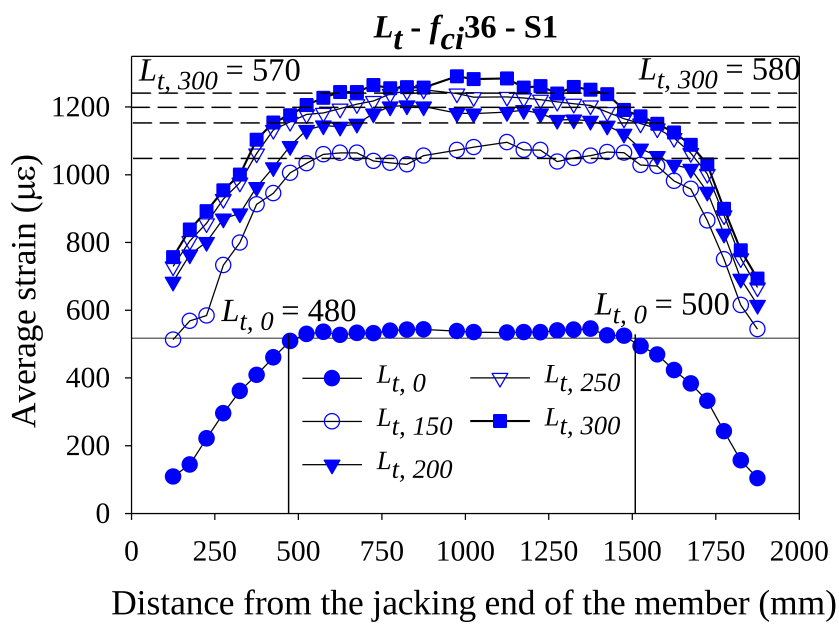

Figure 5.18 Effect of time on L_t of f_{ci}36 – Specimen 1 (until 300 days)

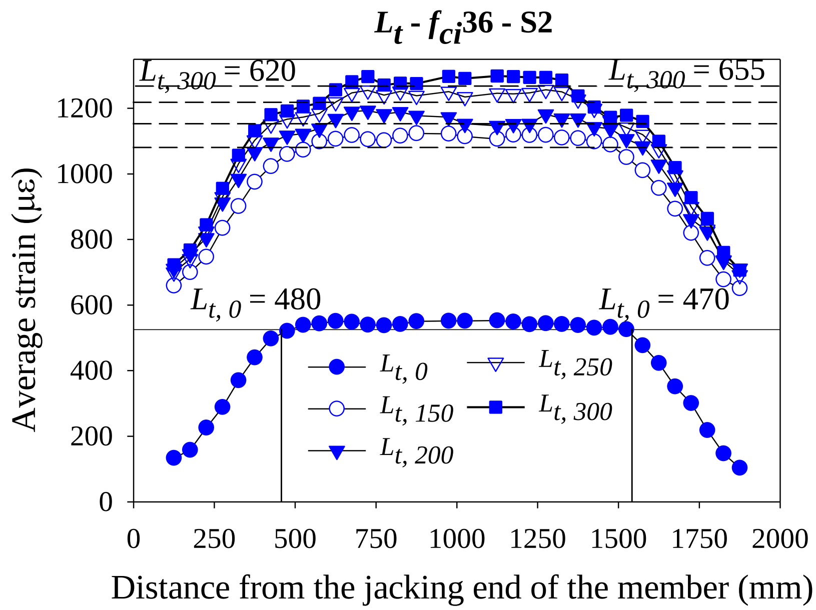

Figure 5.19 Effect of time on L_t of f_{ci}36 – Specimen 2 (until 300 days)

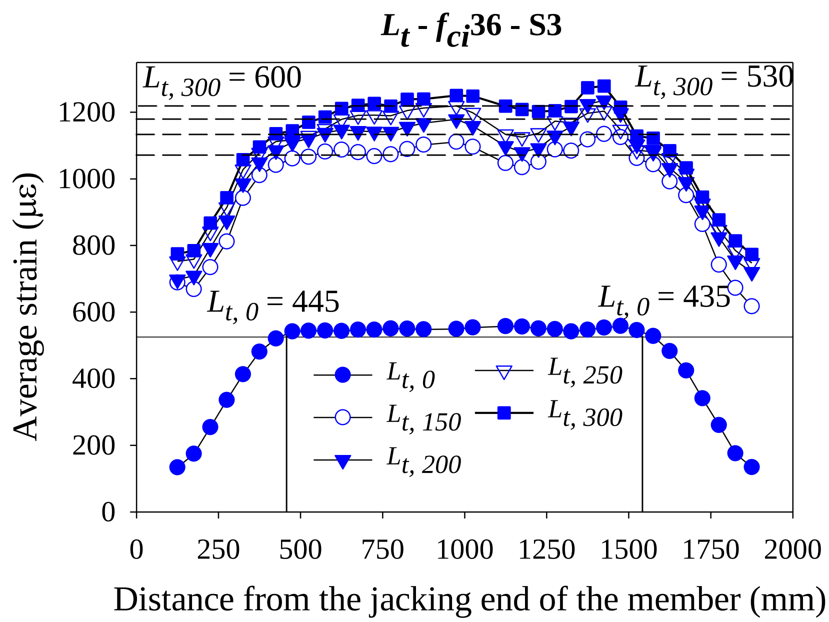

Figure 5.20 Effect of time on L_t of f_{ci}36 – Specimen 3 (until 300 days)

Figure 5.21 - Figure 5.23 indicate the average strain profile at transfer and 7 days of the PTC members for f_{ci}28 specimens. At transfer, the average strain on the concrete surface was about 550 με. At 7 days, with increasing compressive strength of concrete, the values of average strain increased by about 600 με. The average value of $L_{t,0}$ at transfer was 545, 583, 550 mm for f_{ci}28-S1, S2, and S3, respectively. The average value of $L_{t,\ 7}$ was 580, 640, and 580 mm for f_{ci}28-S1, S2, and S3, respectively. The maximum of 9% increment in the L_t values was observed at 7 days.

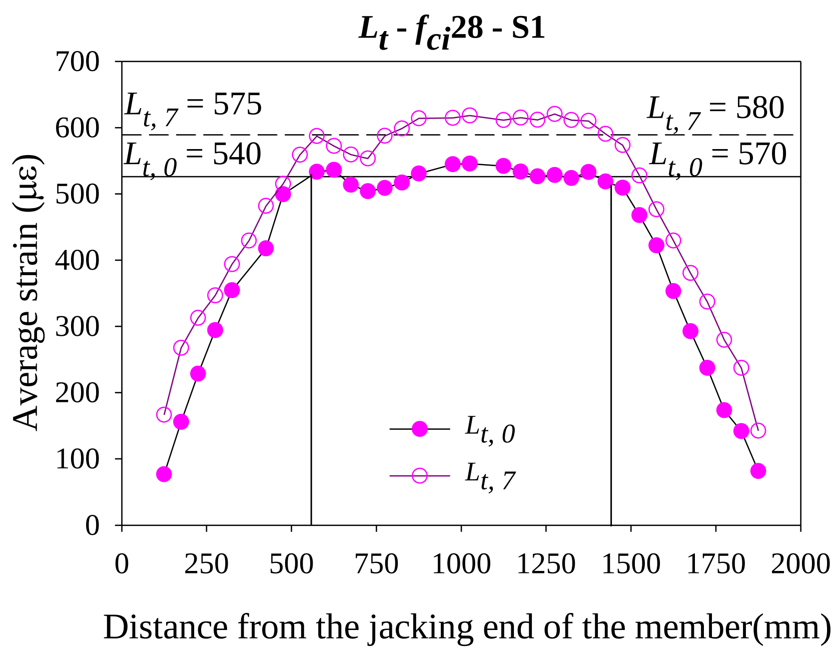

Figure 5.21 Effect of time on L_t of f_{ci}28 – Specimen 1 (at transfer and 7 days)

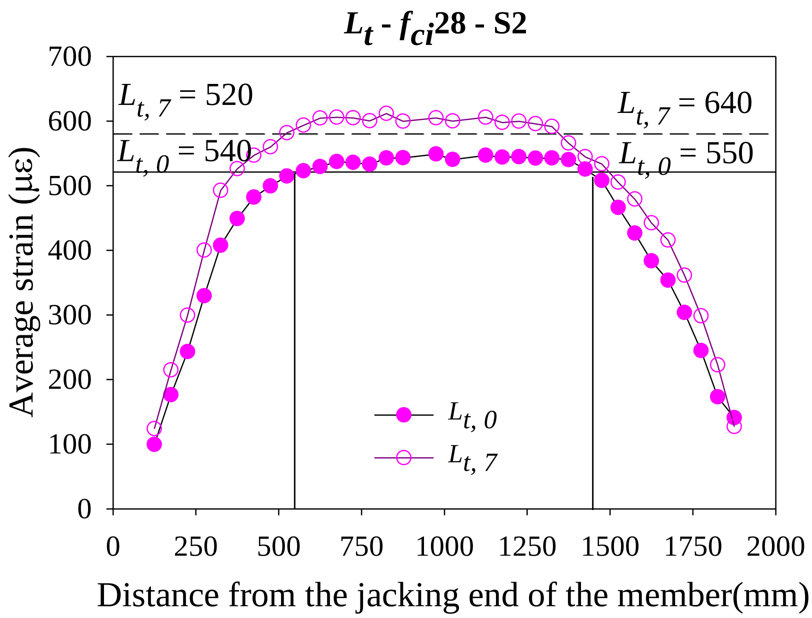

Figure 5.22 Effect of time on L_t of f_{ci}28 – Specimen 2 (at transfer and 7 days)

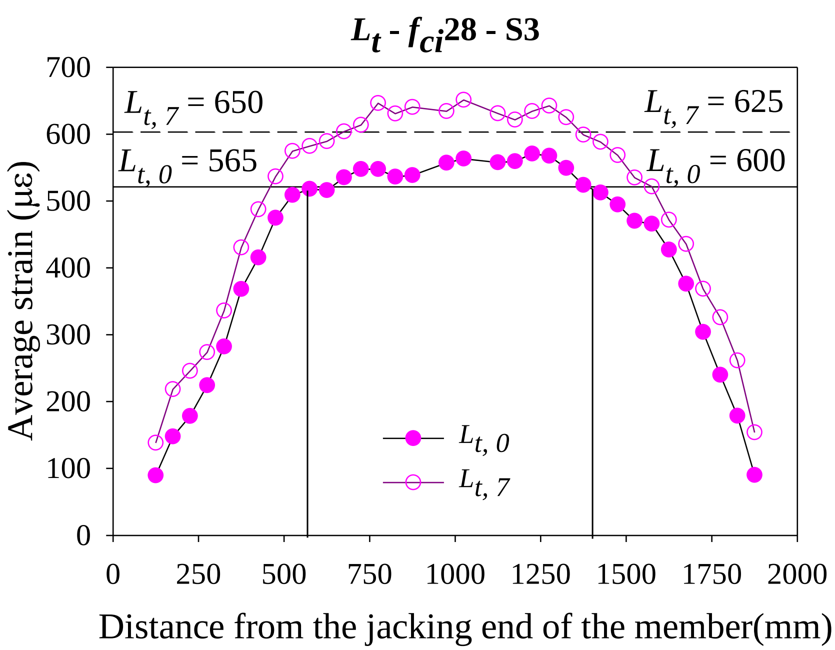

Figure 5.23 Effect of time on L_t of f_{ci}28 – Specimen 3 (at transfer and 7 days)

Figure 5.24 - Figure 5.26 shows the average strain profile at transfer and 28 days of the PTC members for f_{ci}43 specimens. At transfer, the average strain on the concrete surface was about 550 με. At 28 days, with increasing compressive strength of concrete, the values of average strain increased by about 750 με. The average value of $L_{t,0}$ at transfer was 380, 400, 390 mm for f_{ci}43-S1, S2, and S3, respectively. The average value of $L_{t,28}$ was 440, 445, and 485 mm for f_{ci}28-S1, S2, and S3, respectively. The maximum of about 25 % increment in the L_t values was observed at 28 days.

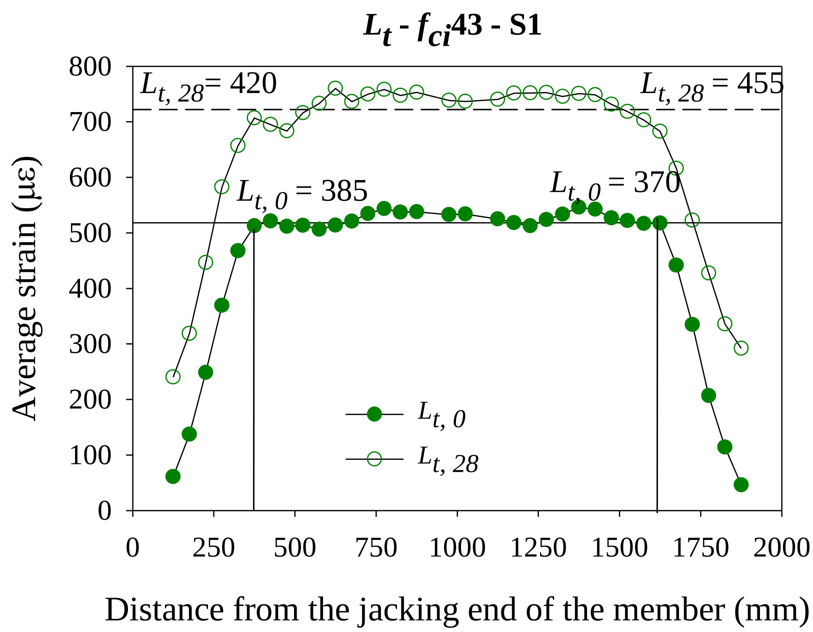

Figure 5.24 Effect of time on L_t of f_{ci}43– Specimen 1 (at transfer and 28 days)

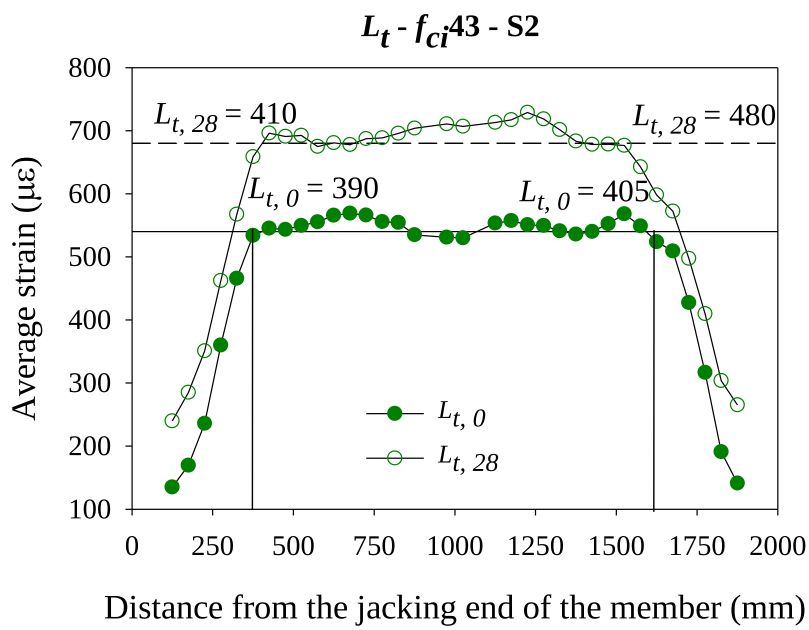

Figure 5.25 Effect of time on L_t of f_{ci}43– Specimen 2 (at transfer and 28 days)

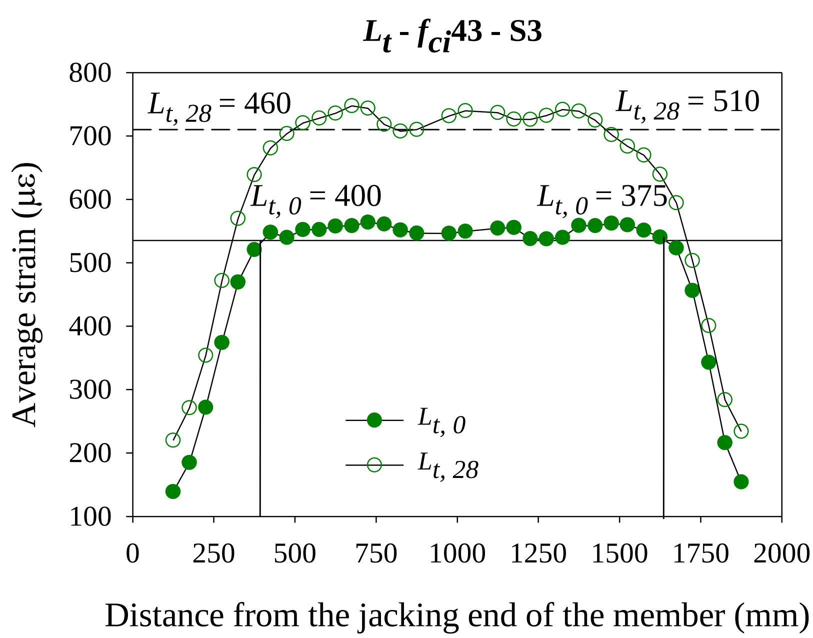

Figure 5.26 Effect of time on L_t of f_{ci}43– Specimen 3 (at transfer and 28 days)

Figure 5.27 shows the variation of L_t with time. The variation of L_t is significant at 7 and 28 days. However, after 120 days, the increase in L_t is found not significant. From the plot, it is seen that no uniform pattern was observed. The value of $L_{t,\ measured}$ was increasing with time for specimen (f_{ci}36-3); whereas, for other specimens (f_{ci}28-1, f_{ci}28-2, f_{ci}28-3, f_{ci}36-1, and f_{ci}36-3) both increase and decrease in trends were observed in the $L_{t,\ measured}$. At 120 days, the maximum increase of about 6% was observed for f_{ci}23-S1 and a negligible decrease of about 1% was observed for f_{ci}23-2 and f_{ci}23-3. At 150 days, the values of $L_{t,\ measured}$ was increased to maximum of about 12% for f_{ci}36 specimens; whereas, f_{ci}23 specimens experienced about 6% increment and 4% decrement in the L_t values. At 250 days, the value of L_t did not increase significantly for f_{ci}23 specimens whereas, f_{ci}36 specimens experienced increment of 15 to 30% compared to the $L_{t,\ 0}$. The f_{ci}23 specimens exposed to 360 days resulted in 15 to 25% variation except for f_{ci}23-3, which did not show any variation.

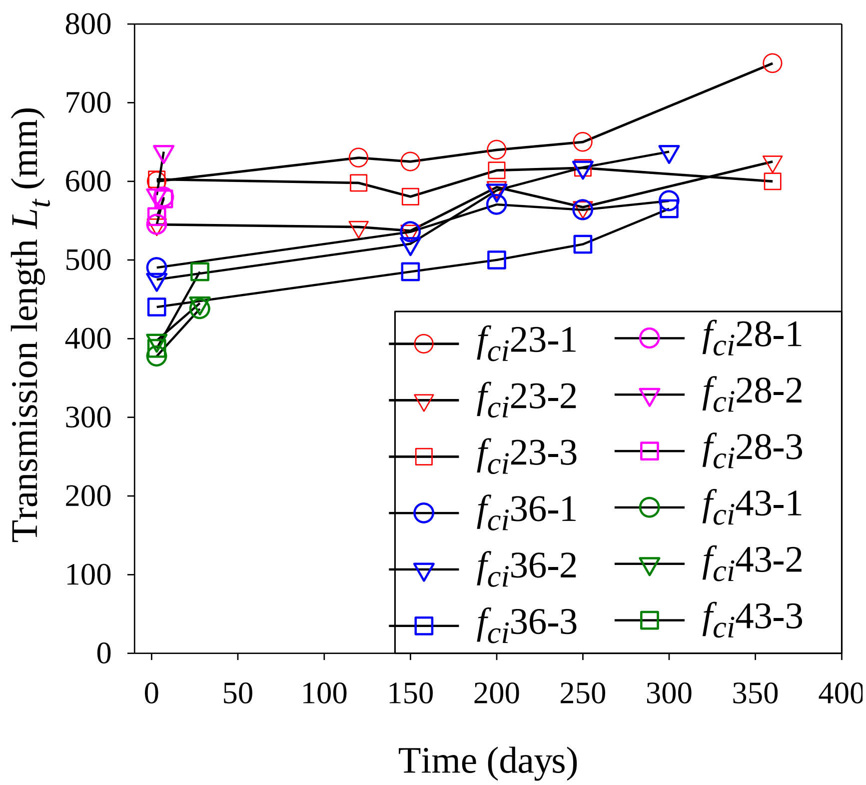

Figure 5.27 Variation of L_t as a function of time

Low relaxation strands meeting ASTM A416 (2017) were used in this study. Hence, the observed change in the L_t could be mainly due to the creep and shrinkage of concrete. It is evident that the results are significantly different between specimens and no pattern was observed. From this study, it is difficult to conclude the effect of time on the L_t. Further testing on similar specimens is required to comment more on these numbers and the rate of change of L_t. The initial time from 7 to 28 days plays significant role on L_t as the concrete hardens to gain its design strength. In general, it can be concluded that the rate of change of L_t after 150 days is not significant.

5.7 INFLUENCE OF L_t ON SHEAR CAPACITY OF THE PTC SYSTEMS – A CASE STUDY

The L_t of prestressed strands plays a crucial role in achieving the desired shear capacity ($V_{n,\,max}$) within the shear-critical region, especially when the elements do not have shear stirrups. To ease the placement of concrete (casting), it is common not to use stirrups in the pretensioned hollow-core slabs (HCS) and rely on the prestressed strands to achieve the desired shear resistance. The shear design can be conservative if the $L_{t,\,measured}$ is adequate. However, if the $L_{t,\,measured}$ is inadequate, then the available prestress at the shear critical region would be less to resist the shear stresses. To understand the effect of L_t on the shear resistance of HCS members, a case study was performed on the influence of L_t on the distance from the end of the member to the point, where $V_{n,\,max}$ is achieved. For this case study, a typical HCS design given in PCI (1999) was considered (PCI, 1999). As shown in Figure 5.28, the depth and width of this HCS was 254 and 1220 mm, respectively. There were six strands at 38 mm from the bottom of the slab. For this case study, two commonly used concrete grades were chosen M35 and M55 whose f_{ci} were 23 and 36 MPa and named here as Concrete A and Concrete B, respectively. Three commonly used codes in India for PTC building structure, ACI, *fib*, and IS were considered. The shear capacity calculated using the $L_{t\,code}$ based on ACI, *fib*, and IS codes were compared with that using the $L_{t,\,measured}$ from the experiments.

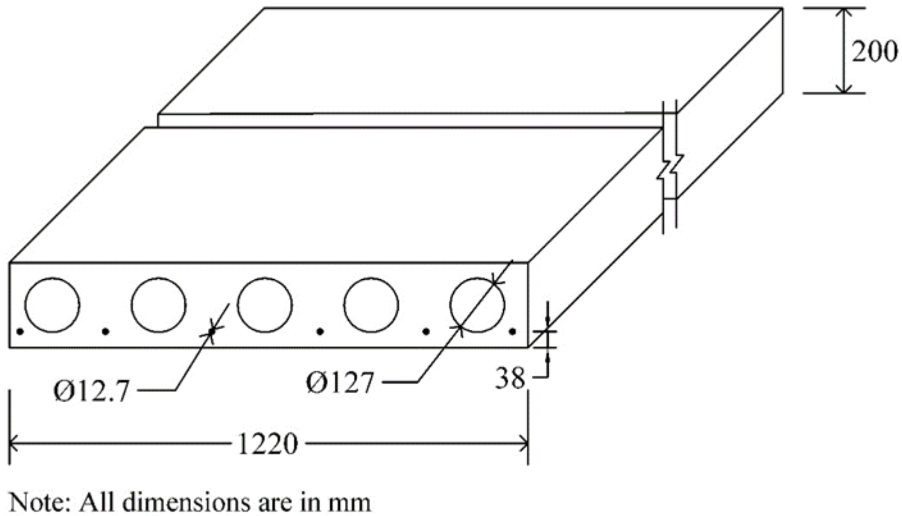

Figure 5.28 The cross section of hollow-core slab used in this case study

For the selected HCS, the nominal shear resistance (denoted as V_n) determined using the $L_{t,\ measured}$ and the $L_{t,\ code}$ calculated as per the *fib*, ACI, and IS codes Figure 5.29 - Figure 5.31. Figure 5.29 indicates that the *fib* MC (2010) estimates the $V_{n,\ max}$ of HCS to be 69 and 82 kN for Concretes A and B, respectively. As shown in Figure 5.30 the ACI 314 (2014) code estimated the $V_{n,\ max}$ of the HCS to be 151 and 173 kN using Concretes A and B, respectively, which is almost double than the estimates by *fib* MC (2010). Figure 5.31 indicates that the IS 1343 (2012) estimated the intermediate $V_{n,\ max}$ of about 118 and 137 kN for Concretes A and B, respectively.

Figure 5.32 indicates the distance from the end of the member to reach the $V_{n,\ max}$. Based on the $L_{t,\ measured}$ for Concretes A and B, the distance (from the end of the member) to achieve $V_{n,\ max}$ was about 0.6 and 0.5 m, respectively. However, for both the Concretes A and B, ACI 318 (2014) estimated this distance to be about 0.7 m and the IS 1343 (2012) estimated this distance to be about 0.4 m. There is no difference for Concretes A and B based on ACI and IS formulations, as they do not consider f_{ci} to calculate the $L_{t,\ code}$. The *fib* MC (2010) estimated a distance of 0.9 m to achieve $V_{n,\ max}$ for Concrete B with f_{ci} = 36 MPa. For Concrete A with f_{ci} = 23 MPa, this was about 1.3 m, which was 44% longer than the estimate for Concrete B.

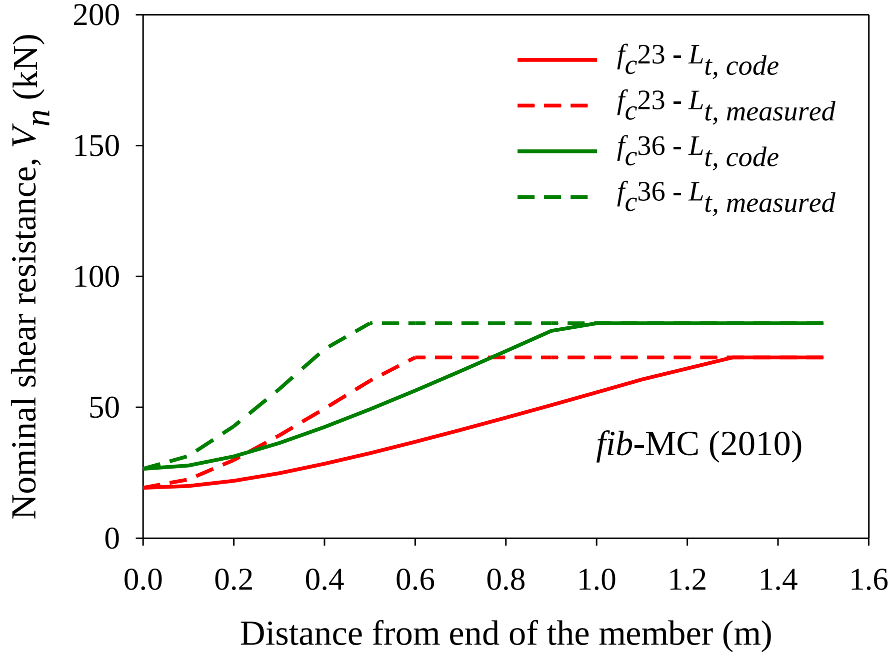

Figure 5.29 Shear resistance determined using *fib* MC (2010)

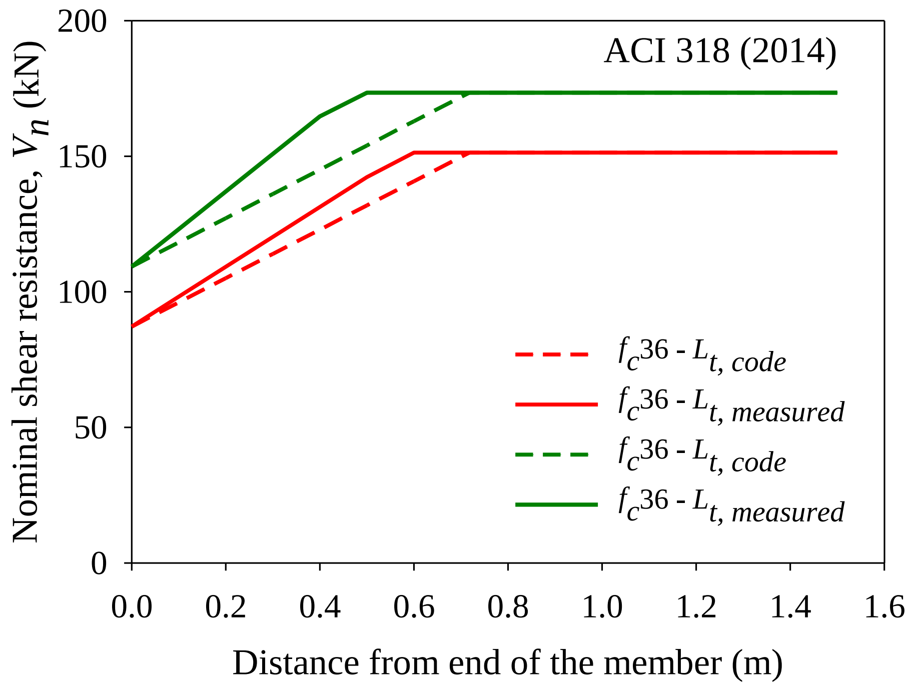

Figure 5.30 Shear resistance determined using ACI 318 (2014)

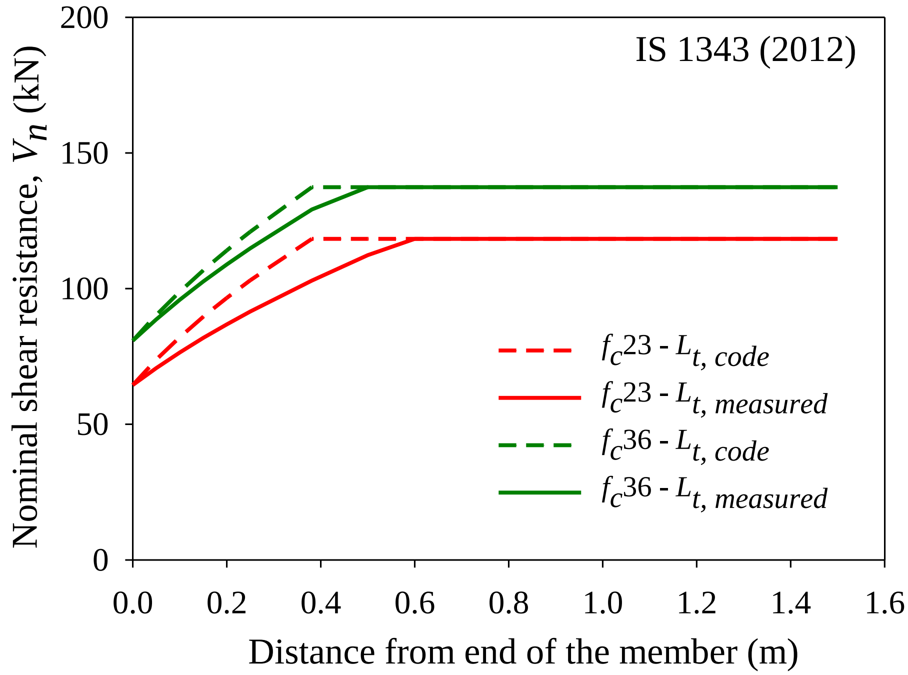

Figure 5.31 Shear resistance determined using IS 1343 (2012)

Using equations which incorporate f_{pe} and/or f_{ci} will ensure that sufficiently long estimate of L_t is used for the design purposes and sufficient shear resistance is achieved within the shear critical regions – as adapted by *fib* MC and ACI codes (but, not by IS code).

As mentioned earlier, the IS 1343 (2012) estimates L_t as the 30(d_s), which leads to a condition where $V_{n,\ max}$ is achieved at a shorter distance than $L_{t,\ measured}$. For Concretes A and B, these were 0.2 and 0.1 m, respectively, shorter than $L_{t,\ measured}$. This could lead to a less conservative design. Therefore, it is proposed that the IS 1343 (2012) uses the Eqs. (5.1) and (5.2) with f_{pe}, d_s, and f_{ci}, for estimating $L_{t,\ code}$ and arrive at conservative shear designs. Such sophisticated design approaches become very important, especially when the quality control measures at the site are not stringent enough.

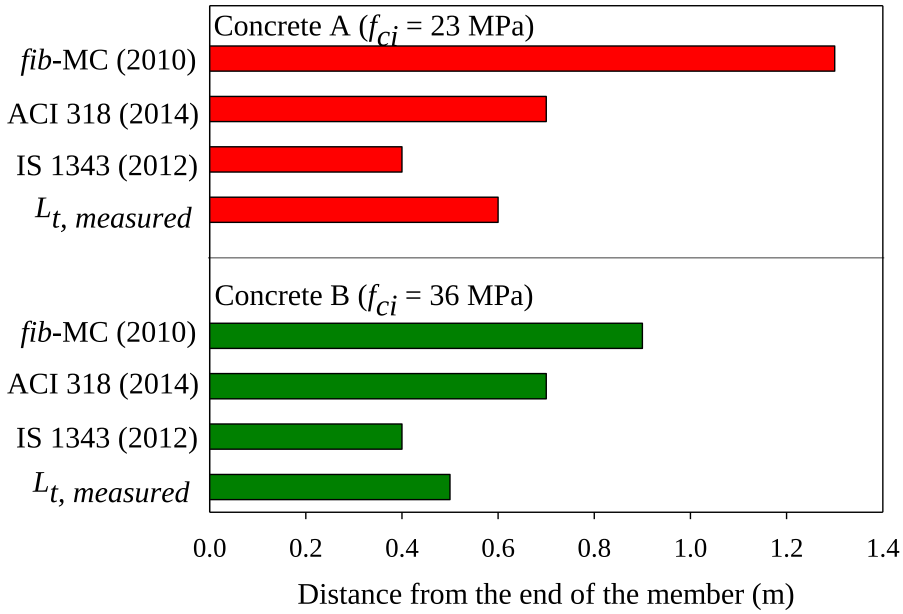

Figure 5.32 Distance from the end of the member to reach $V_{n, max}$

5.8 EFFECT OF OVERESTIMATION ON THE BURSTING STRESS IN THE TRANSMISSION ZONE – A CASE STUDY

In the transmission zone, transverse tensile stresses can develop due to the vertical component of bearing force and the Hoyer effect of the strand. These stresses are maximum at the end face of the member. These tensile stresses are dependent on the prestress level, rate of prestress transfer along the length, etc., which influence the L_t. As a case study, the effect of overestimation of L_t on the transverse tensile stress at the end of the member was calculated considering a simple I girder. Figure 5.33 shows the geometry details of the I girder considered for the case study. If L_t is overestimated, then the maximum tensile stress is underestimated and vice versa. The estimation of transmission length and maximum tensile stress in the transmission zone influences the amount and spacing shear reinforcements.

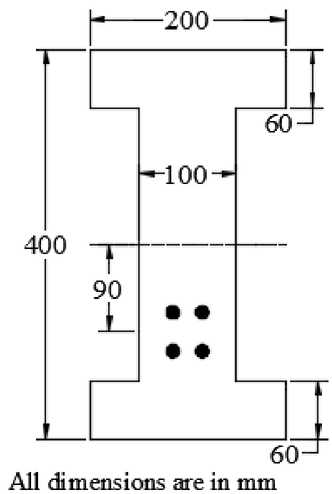

Figure 5.33 Cross section of a simple I girder (Source: Raju (2011))

As explained in the literature, the tensile stress induced due to the transfer of prestress varies along the transmission length. Figure 5.34 shows the tensile stress distribution due to the prestress transfer for different transmission length. It indicates that the short L_t results in high tensile stress distribution.

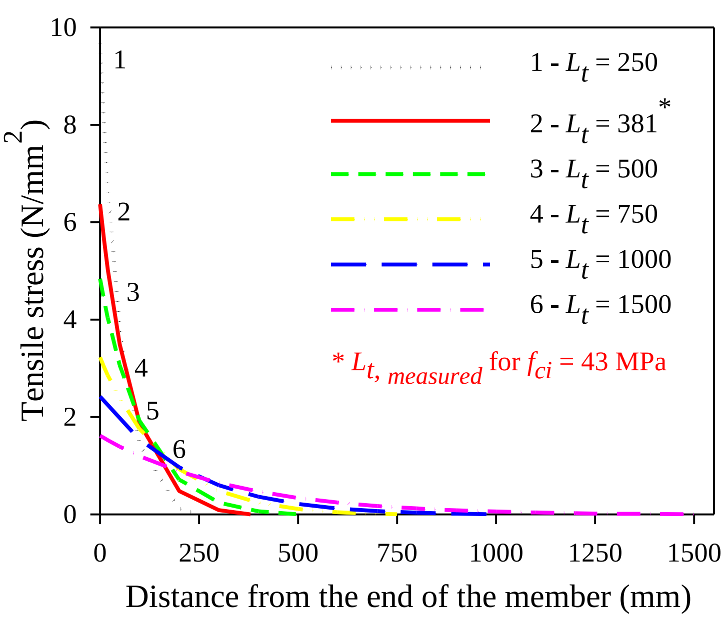

Figure 5.34 Tensile stress distribution in the transmission zone

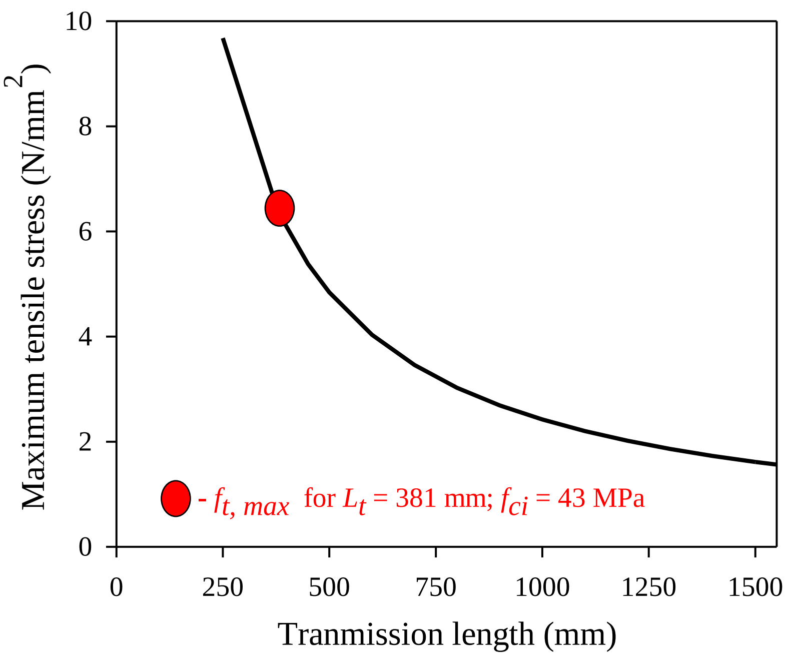

Figure 5.35 Maximum tensile stress as a function of transmission length

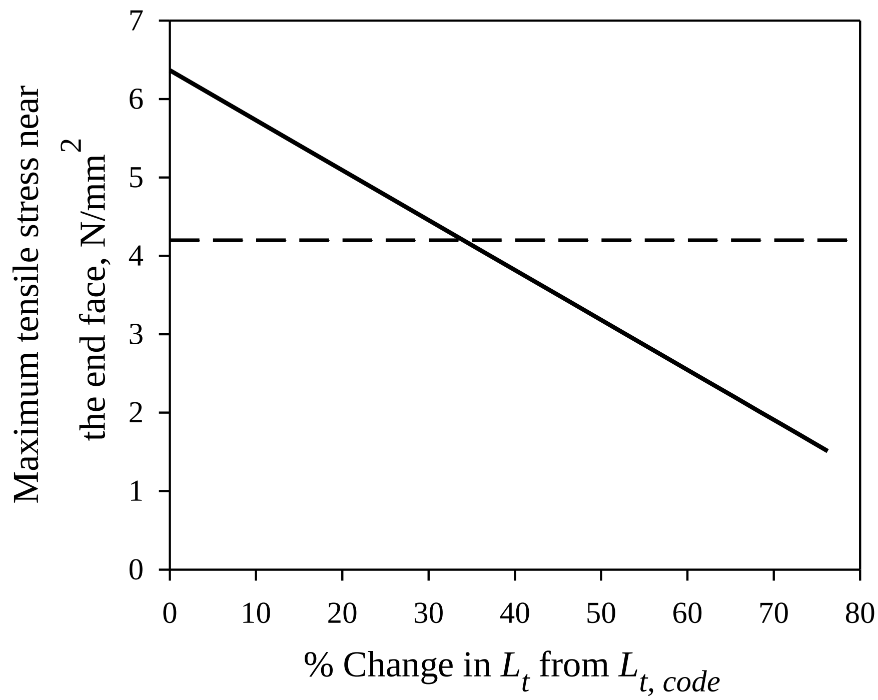

Figure 5.36 Maximum tensile stress in the transmission zone

Figure 5.35 shows the variation of maximum tensile stress with the transmission length of the member. To understand this plot better, the maximum tensile stress as a function of the percent change in L_t (i.e., the difference between the actual L_t and design L_t) for the concrete properties of f_{ci} = 42 MPa and f_t = 4.2 MPa is shown in Figure 5.36. Based on the experimental results, the required L_t was overestimated by about 40, 50, 60, and 70 % by CSA, ACI, AASHTO, EN, and *fib* design codes. However, the result indicated that if the L_t is overestimated by more than 30% of the actual L_t, then the induced tensile stresses could exceed the tensile strength of concrete and result in bursting cracks in the absence of stirrups. This scenario could become worse, if the strength of concrete is lower than 42 MPa. This is critical, especially in narrow web pretensioned beams/girders, where the strands would be closely placed and congested (Tuan et al., 2004). Therefore, the overestimation of L_t beyond 30% of the values from tests should be avoided while designing the PTC members. Generally, overestimation of values taken for granted as safe. However, it is not the case in the PTC systems. A shorter estimation of L_t is necessary to prevent unexpected high stresses near the end of the members (Floyd et al., 2015). Hence, care should be taken to ensure adequate L_t in the design to avoid such issues.

5.9 SUMMARY

This chapter discussed the significance of f_{ci} on L_t using various codal and literature equations. It was observed that for a particular f_{ci}, design L_t has varied from 380 to 1500 mm. Also, empirical equations from the literature were compared and found that significant variations in L_t. Then, this chapter detailed the experimental investigation on the effect of compressive strength of concrete at transfer and time on the transmission length. The human error on the DEMEC measurement is presented to obtain reliable data. Based on the experimental result, a bilinear model is proposed to determine the L_t. The calculated L_t based on the standard design equations over/underestimate the required L_t. Also, case studies demonstrating the effect of underestimation and overestimation of L_t on the shear capacity and tensile stresses induced due to the transfer of prestress in the transmission zones were presented. The findings of this chapter would be presented in Chapter 7

6 RESULTS AND DISCUSSION – BOND STRENGTH (τ_b)

6.1 INTRODUCTION

This chapter details the results of the experimental investigations performed to meet Objective 2. This objective aims to develop a test procedure to determine the bond strength of PTC specimens and investigate the effect of compressive strength of concrete, prestress level, and embedment length of the strand on the determination of bond strength. Initially, the challenges associated with the measurement of bond slip are explained. Then, to overcome the challenges associated with the conventional methods in determining the bond strength, a method based on the yield point/region on the bond stress-slip curve is proposed. Also, the significance of the proposed method over the conventional method is presented. Finally, the failure mechanism at the S-C interface is explained.

6.2 LIMITATIONS ON DETERMINING BOND STRENGTH AS A FUNCTION OF ABSOLUTE SLIP AT FREE/LIVE ENDS

Bond strength is computed by assuming a uniform τ distribution over the embedment length (l_e) of the strand in concrete, as given in Eq. (6.1)

$$\tau = \frac{P}{\pi p l_e} \qquad \text{Eq. (6.1)}$$

Perimeter (p) is calculated as the sum of the arc lengths of six outer wires (representing the area in contact with the concrete). The thick/blue curve in Figure 6.1 indicates this perimeter. The diameter of the outer wires (d_o) is 4.2 mm. For the 12.7 mm diameter strand used in this study, the arc length of outer wire is 8.8 mm; p is 52.8 mm and the embedment length (l_e) of the strand in concrete is 450 mm for short specimen and 950 mm for long specimens.

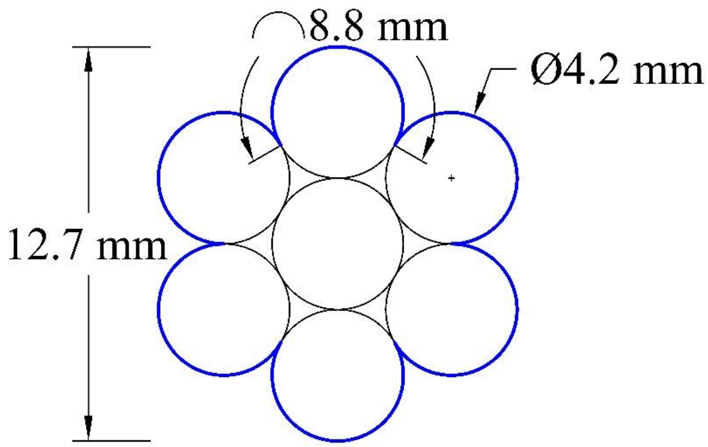

Figure 6.1 Cross section of 7-wire strand

Typically, the measurement of slip at the free end is preferred due to its ease to place the LVDT. This is because placing the LVDT at the live end is difficult due to the non-availability of space as the strand is gripped only for loading. Therefore, in this study specimens were designed in such a way that it could accommodate the placement of LVDT at the LE. Accordingly, 350 and 150 mm lengths of strand were kept outside the concrete surface at the LE and FE, respectively to place the LVDTs.

The ASTM A1081 (2012), IS 2770 (1967), and RC 6 (1983) recommend to determine the τ_b of PTC systems as the τ corresponding to the pre-defined slip of 2.5 mm at the free end. This approach has the following limitations. In the pull-out testing, the strand at the live end can start slipping much earlier than the strand at the free end. This is because the strain has to develop along the length of the specimen to cause slipping at the free end. The difference in the instantaneous slips at live and free ends depends on the length of the embedded strand. This indicates that the bond stress at a particular time instant is maximum near the live end and reduces towards the free end. The difference in bond stress at live and free ends increases with increasing l_e of the member. This indicates that the measurement at the free end is not reliable for the determination of tb, especially for PTC members, whose l_e varies depending on the L_t of the specimens. Hence, the measurement of slip at the live end is more suitable and representative than at the free end. However, the slip at the live end is also dependent on the length of the specimen. The longer the length, the larger will be the load to cause similar slip at the live end.

Columns 4 and 5 in Table 6.1 show the $\tau_{2.5}$ determined using the 2.5 mm slip at live and free ends, respectively, for short strand specimens. Table 6.2 shows similar data for long specimens. For short specimens with taut strands, the estimated $\tau_{2.5}$ based on live end slip is about 20% less than that of free end slip. For long specimens with stressed strands, this difference is about 50%. These differences are significant and not acceptable for quality control practices in the field. Based on the aforementioned scenario, defining τ_b as τ corresponding to a pre-defined slip at either live or free end seems inappropriate. There is a need to determine τ_b as a parameter independent of the l_e and f_{ps}.

6.3 DETERMINATION OF BOND STRENGTH USING YIELD STRESS METHOD

To overcome the challenges associated with the 2.5 mm slip method, this thesis determines τ_b based on bond stress at the yield point where the slope of τ-s changes significantly. The bond stress at the yield point is known as bond yield stress (τ_{yield}) and the load at the yield point is called yield load (P_{yield}). τ-s plot has two regions – an initial steep portion where, τ increases with small increase in s and yields into a region where an increase in τ_b is less with a significant increase in the slip. The friction mechanism between the strand and concrete contributes to the initial steep portion and after yield where the slope changes indicates the loss of friction. Then, the mechanical interlock mechanism contributes to the bond and gives further resistance to slip, which increases the bond stress after yield.

The yield points on the τ-s curves were categorized into two cases as follows (see Figure 6.2 and Figure 6.3).

- Case 1: A point on the curve indicating a sudden change in slope.

- Case 2: A region on the curve with a gradual and significant change in slope.

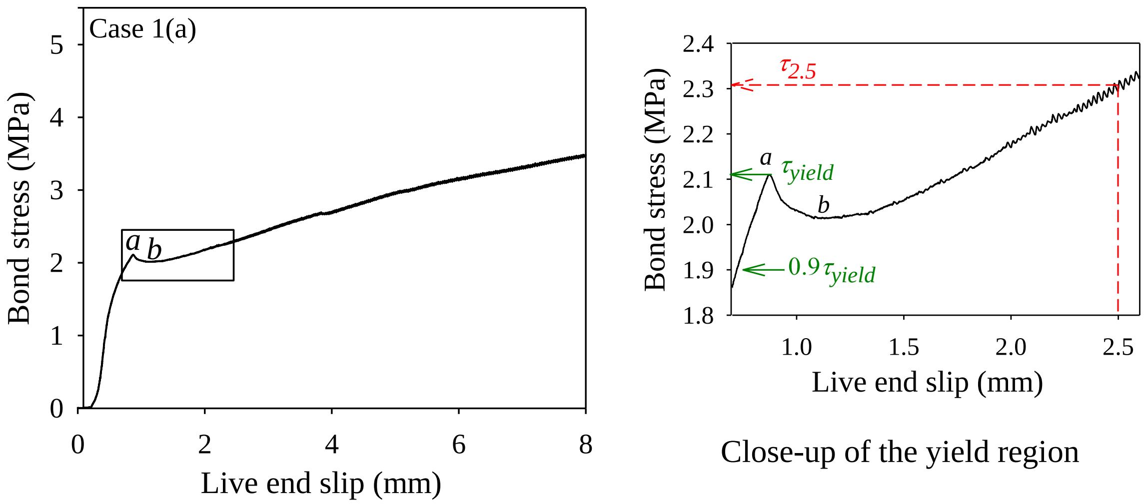

(a) Case 1(a): Short taut strands in low strength concrete and close-up of the yield region

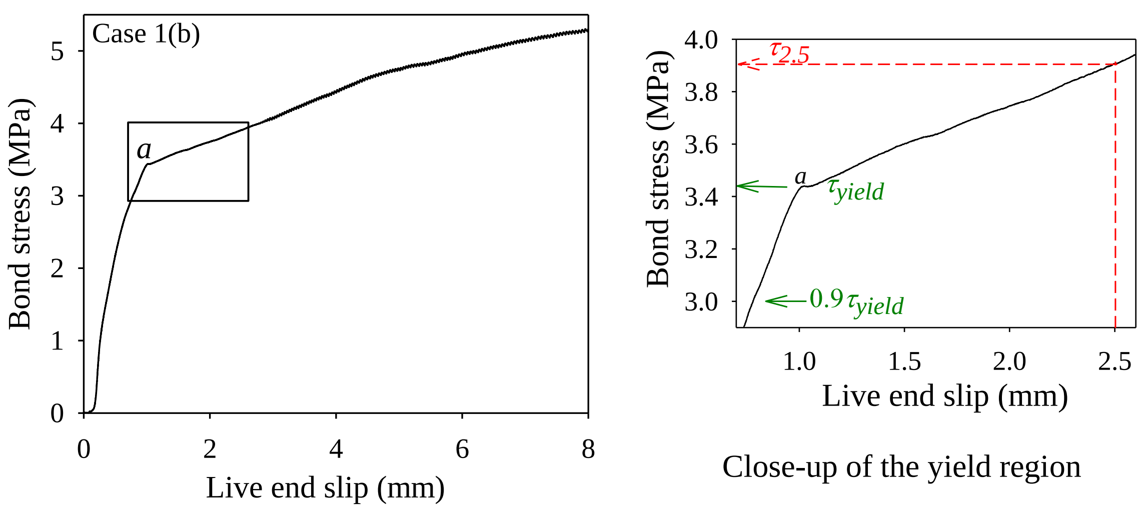

(b) Case 1(b): Short taut strands in high strength concrete and close-up of the yield region

Figure 6.2 Determination of τ_b using the bond yield stress method – Case 1

Case 1 was observed in the specimens with the short taut strands in concrete. Further, based on the shape of the yield region observed, Case 1 was divided into two categories – Cases 1(a) and 1(b). The close-up views near the yield point for these cases are shown on the right side of Figure 6.2 (a) and (b). In Case 1(a), the bond stress increases till the Point '*a*' and yield occurs at that point (with a loss in frictional resistance). After yield, the bond stress reduces (towards Point '*b*' in the close-up view of the Figure 6.2 (a)). This indicates that once the friction is lost, the applied load would compress the concrete keys formed due to the helical shape of the strand at the S-C interface. Then, the mechanical interlock governs the strand-concrete interaction at the interface. This action results in an increase in the bond stress after Point '*b*' (i.e., curve moves upwards). Case 1(a) with significant drop at Point '*a*' was observed in the short taut strand specimens embedded in low strength concrete (f_c = 43 MPa).

On the other hand, no significant drop at Point '*a*' was observed in Case 1(b). Figure 6.2 (b) indicates that after yield at point '*a*', bond stress is not decreased significantly. This could happen in concretes with high stiffness, where once the friction is lost, the concrete keys may not experience significant compression. Further, the mechanical interlock contributes to give resistance to slip and the curve starts moving upward right after Point 'a'. Typically, an increase in compressive strength leads to an increase in the stiffness. As a result, Case 1(b) was observed in the short taut strand specimens are embedded in high strength concrete (f_c = 62 MPa).

Case 2 was typically observed in long specimens with both taut and stressed strands embedded in high strength concrete (f_c = 62 MPa). Here, in Case 2, the length of the member was twice that in Case 1. As the length of the member increases, more load is needed to pull the strand. Also, gradual yielding occurs, as shown in Figure 6.3. After yield, the bond stress does not increase significantly. As the yield is gradual, the yield point was determined as a point, where the parallel line of each region meet, and stress corresponding to that point can be considered as τ_{yield}. To be conservative, this thesis defines τ_b of PTC systems as 90% of τ_{yield} (i.e., $\tau_b = 0.9\,\tau_{yield}$), herein.

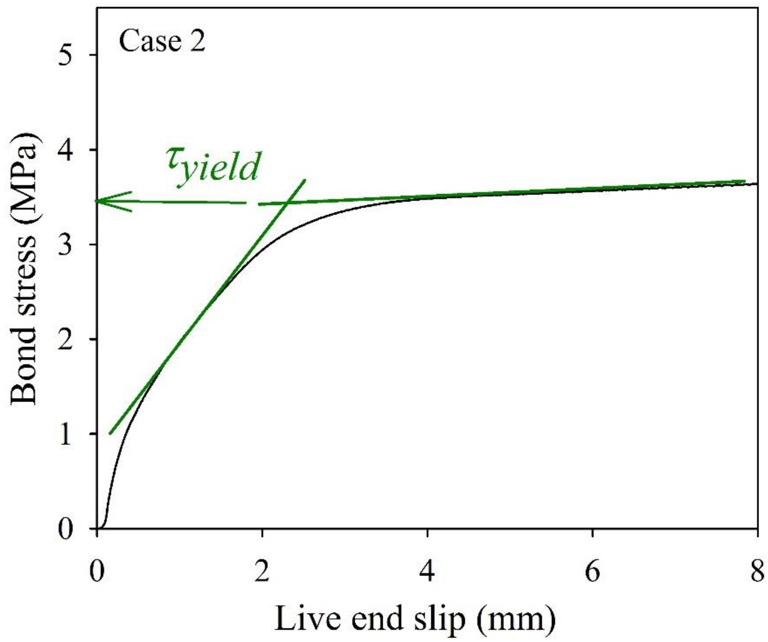

Figure 6.3 Determination of τ_b using the bond yield stress method – Case 2

6.4 OBSERVED BOND STRESS-SLIP BEHAVIOUR

6.4.1 Bond stress-slip (τ-s) behaviour at live end PTC systems

The τ-s behaviour was obtained by capturing the applied load and the total slip measured by LVDTs (s_m). The s_m represents the net measurement due to the elastic deformation of the strand portion outside the concrete (Δl_{nc}), and the true slip of the strand (s). Figure 6.4 shows the schematic diagrams of these movements at the live end of PTC test specimens during the pull-out test. Figure 6.4 (a) indicates the specimen configuration with preload (P_0). The length of the strand portion, which is not in contact with the concrete is denoted as l_{nc}. This includes the portion of the strand from the inner end of the bond-breaker to the LVDT clamp. Figure 6.4 (b) shows the movement of the strand during the test under load. As soon as the load is applied, the l_{nc} portion of the strand gets stretched due to the elastic nature and the strand starts slipping. The true slip, s, was calculated by subtracting the Δl_{nc} from s_m; and τ-s curves were plotted.

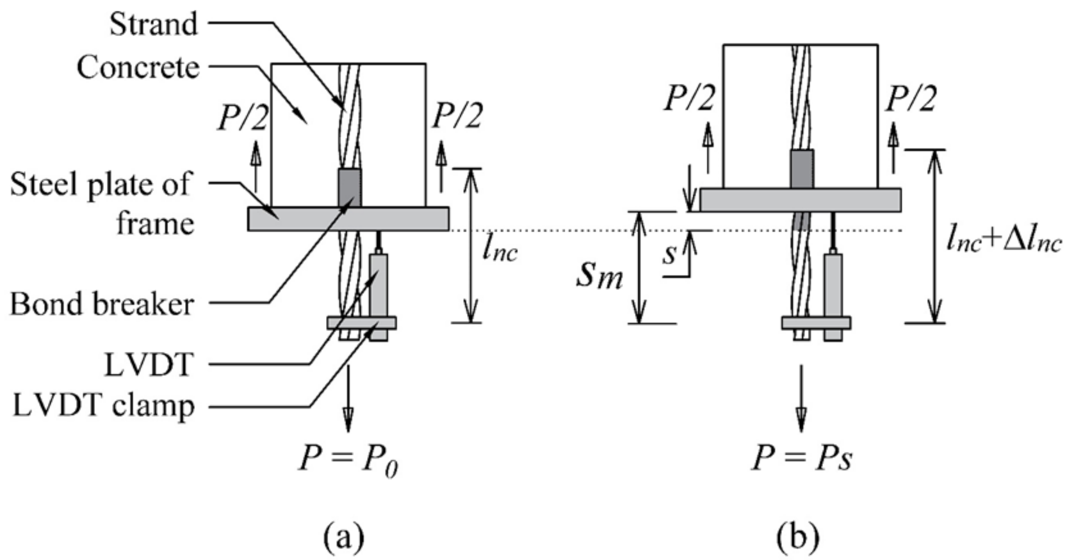

Figure 6.4 Movements at the live end in PTC systems (a) At preload and (b) During the pull-out test

6.4.2 Measured bond stress-slip relationship

As explained earlier, the measured slip is not the true slip of the strands as it includes the deformation of the strand. Therefore, to obtain the true slip of the strand, the effect of the strand deformation has to be eliminated. Figure 6.5 - Figure 6.8 show the representative bond stress-slip behaviour of taut and stressed strands using the measured and true slip. The true slip is obtained by subtracting the deformation due to elongation of the 200 mm long l_{nc} region. The figures show a significant change/shift in the τ-s plots due to the strand deformations. From Figure 6.5 and Figure 6.6 with Case 1 type curves, the yield point was obtained with a sharp point about 2 and 1 mm slip based on the measured and true slip, respectively. Similarly, Figure 6.7 and Figure 6.8 with Case 2 type curves, the yield occurred around about 6 and 4 mm based on the measured and true slip, respectively. It indicates that a significant difference between the measured and corrected true slip values. Therefore, the determination of bond strength using 2.5 mm slip could give erroneous results. Hence, the strand deformation from the measured slip was eliminated to obtain the true τ-s for all the specimens. Figure 6.9 to Figure 6.14 show the corrected τ-s plots.

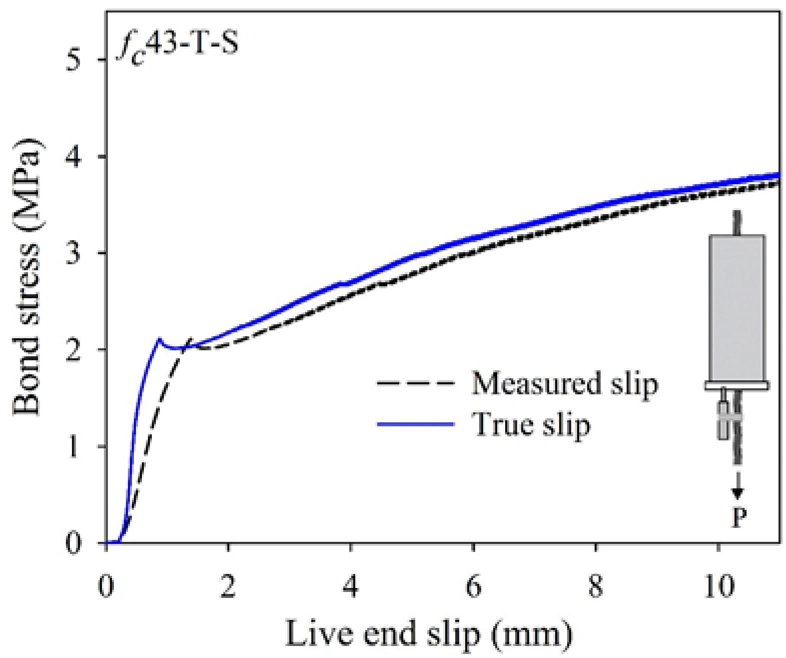

Figure 6.5 Representative bond stress-slip behaviour of taut strands with l_e = 450 mm in f_c = 43 MPa

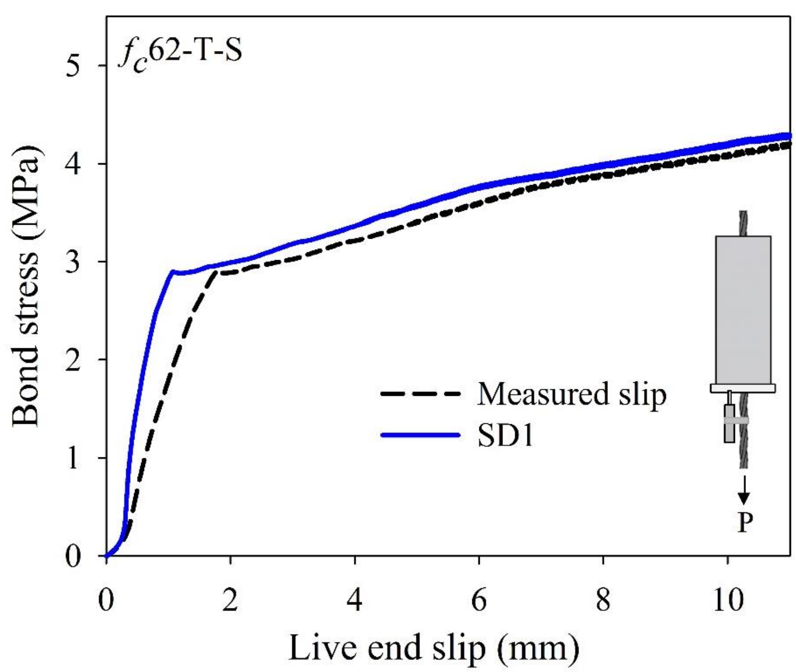

Figure 6.6 Representative bond stress-slip behaviour of taut strands with l_e = 450 mm in f_c = 62 MPa

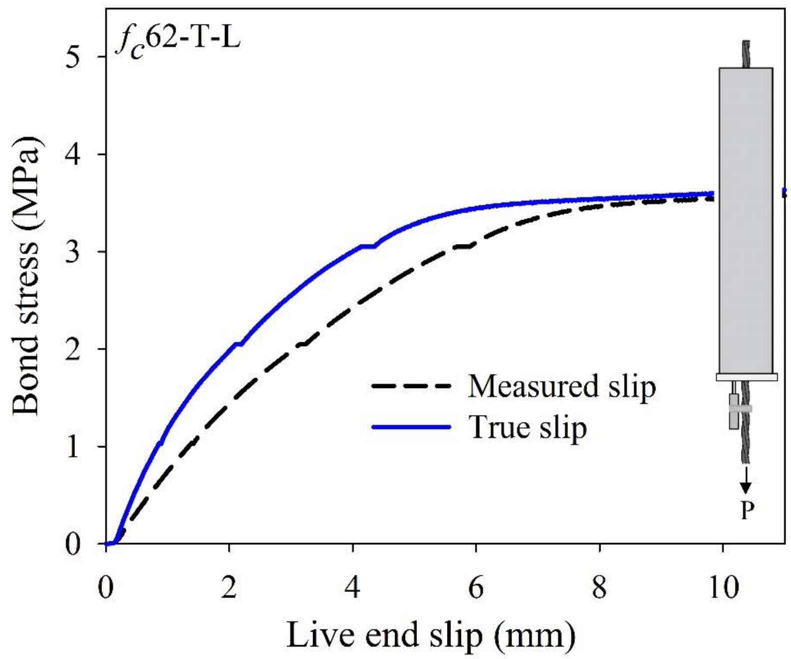

Figure 6.7 Representative bond stress-slip behaviour of taut strands with l_e = 950 mm in f_c = 62 MPa

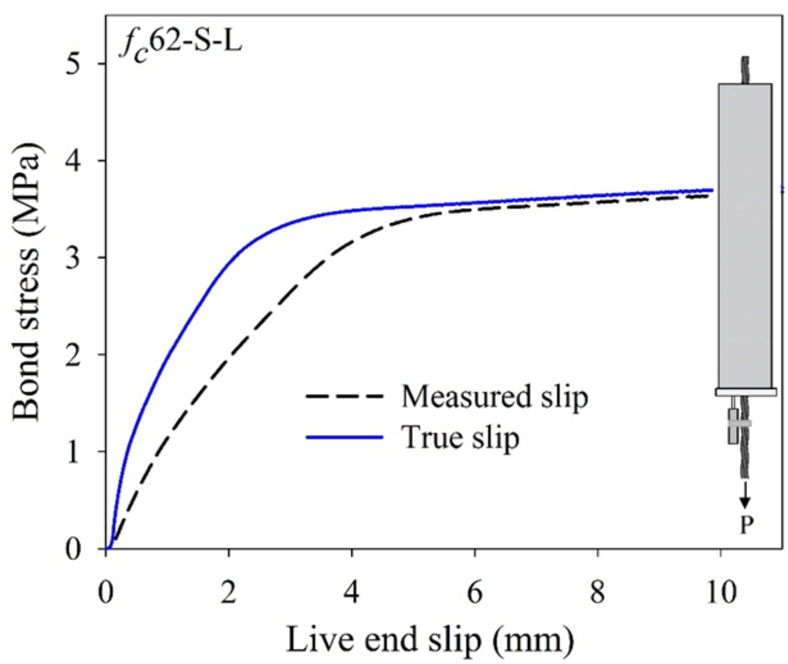

Figure 6.8 Representative bond stress-slip behaviour of stressed strands with l_e = 950 mm in f_c = 62 MPa

6.4.3 Bond stress - slip behaviour of taut and stressed strands embedded in concrete

Figure 6.9 and Figure 6.11 represent the τ-s behaviour for taut strands with l_e = 450 mm in f_c = 43 and 62 MPa, respectively. Specimen identification is provided at the top left of each figure. Note that 'f_c43-T-S' indicates specimen with 43 MPa concrete, Taut strand, and a Short embedment length (say, l_e = 450 mm); 'f_c62-S-L' indicates specimen with 62 MPa concrete, Stressed strand, and a Long embedment length (say, l_e = 950 mm); and so on. The zoomed portions near the yield point were shown in Figure 6.10 and Figure 6.12 indicating the change on τ–s plot. From the plots, it is observed that the average bond yield stress was about 2 and 3.2 MPa for f_c = 43 and 62 MPa, respectively. The yield of short taut strands was obtained before the strand experiences the 2.5 mm slip. Therefore, the value of τ_{yield} was lesser than the $\tau_{2.5}$. A lot of scatter was observed on the τ–s plot of the short taut strands in both f_c = 43 and 62 MPa. Table 6.1 presents the determined τ_b of taut strands with l_e = 450 mm.

Figure 6.13 and Figure 6.14 exhibit the τ-s behaviour of long taut and stressed strands with l_e = 950 mm in 62 MPa strength concrete, respectively. τ was increased about 3.5 MPa for both taut and stressed strands with l_e = 950 mm and the slope of τ–s changes gradually. The average maximum load experienced by the taut and stressed specimens were about 190 kN. As the breaking strength of 12.7 mm strands is ~190 kN, strands got ruptured once it reached its breaking strength. It was observed that the τ-s behaviour of stressed strands was stiffer and more consistent than that of the taut strands due to the high prestress. As a result, the average τ at 2.5 mm slip of stressed strands was higher than that of the taut strands. As l_e increases, the resistance to slip also increases. As a consequence, the yield was delayed and attained after reaching the 2.5 mm slip. Therefore, the τ_{yield} was higher than the $\tau_{2.5}$ for both taut and stressed strands with l_e = 950 mm. Table 6.2 presents the determined τ_b of pull-out specimens with l_e = 950 mm.

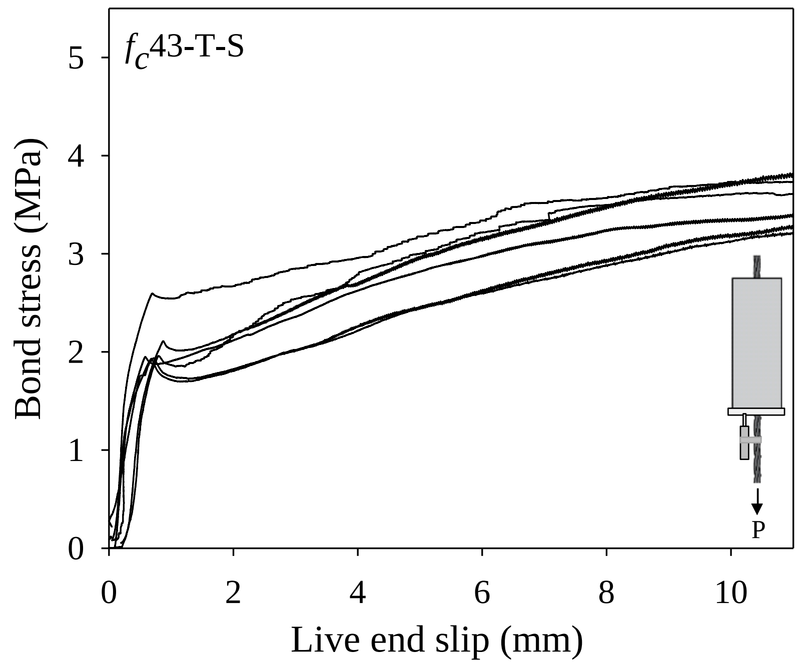

Figure 6.9 Bond stress-slip behaviour of f_c43-T-S

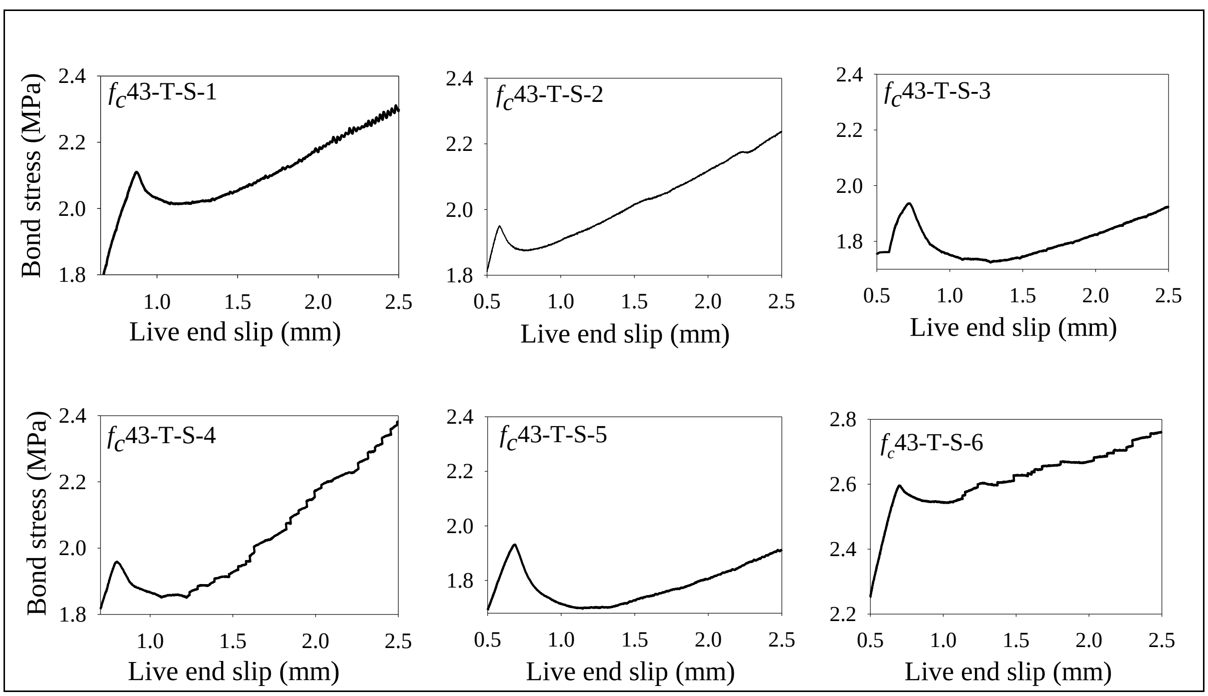

Figure 6.10 Zoomed portions at yield point for f_c43-T-S specimens

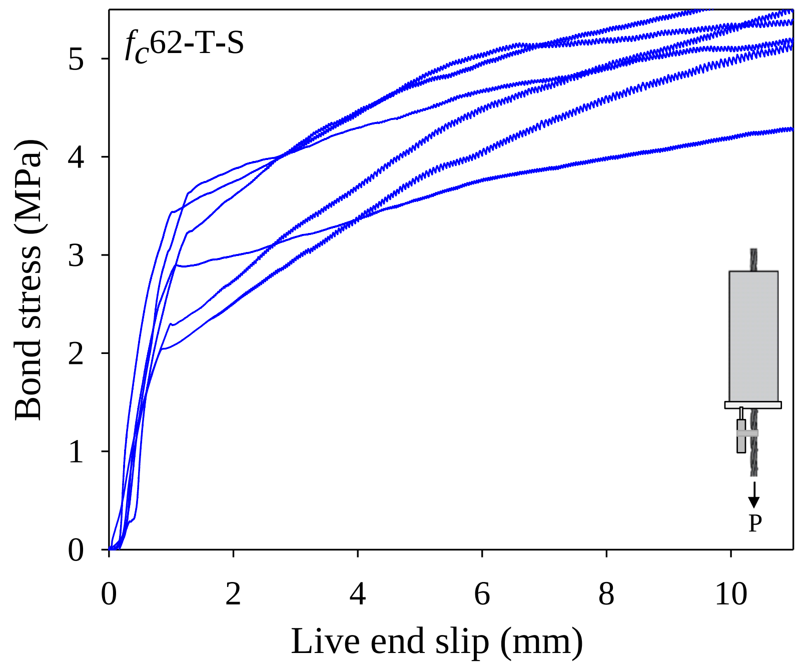

Figure 6.11 Bond stress-slip behaviour of f_c62-T-S

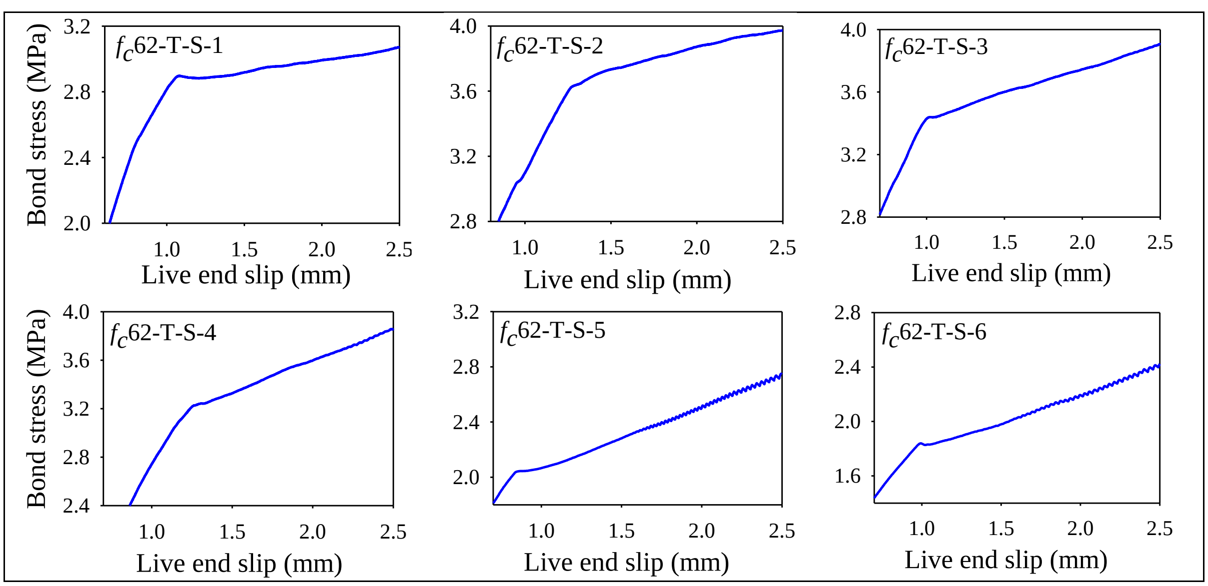

Figure 6.12 Zoomed portions at yield point for specimens f_c62-T-S

Table 6.1 Bond strength of taut strands (l_e = 450 mm) in f_c = 43 and 62 MPa concrete

Specimen ID	Compressive strength of concrete at testing (f_c) in MPa	Maximum bond load (P_{max}) in kN	Bond strength (τ_b) MPa			
			$\tau_{2.5}$		After subtracting the elongation from LE slip	
			Live End	Free End	$\tau_{2.5}$	0.9 τ_{yield}
f_c43-T-S-1	44.1	101	2.17	2.58	2.30	1.81
f_c43-T-S-2	43.8	93	2.11	2.39	2.24	1.72
f_c43-T-S-3	43.7	95	1.83	2.06	1.92	1.72
f_c43-T-S-4	42.9	94	2.15	2.57	2.38	1.75
f_c43-T-S-5	44.5	95	1.80	2.04	1.91	1.73
f_c43-T-S-6	42.3	89	2.13	2.86	2.67	1.85
f_c62-T-S-1	63.1	119	2.96	3.31	3.07	2.61
f_c62-T-S-2	61.8	132	3.74	4.28	3.97	3.28
f_c62-T-S-3	60.2	150	3.63	4.39	3.94	3.05
f_c62-T-S-4	60.4	131	3.42	4.48	3.85	2.93
f_c62-T-S-5	61.6	145	2.46	3.20	2.75	2.16
f_c62-T-S-6	62.2	144	2.67	3.65	3.02	2.06

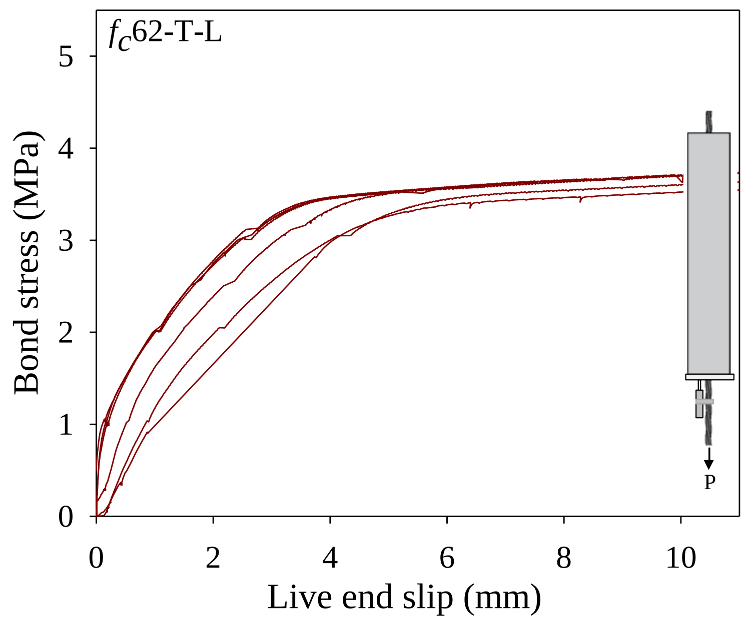

Figure 6.13 Bond stress-slip behaviour of long taut strands with l_e = 950 mm in f_c = 62 MPa concrete

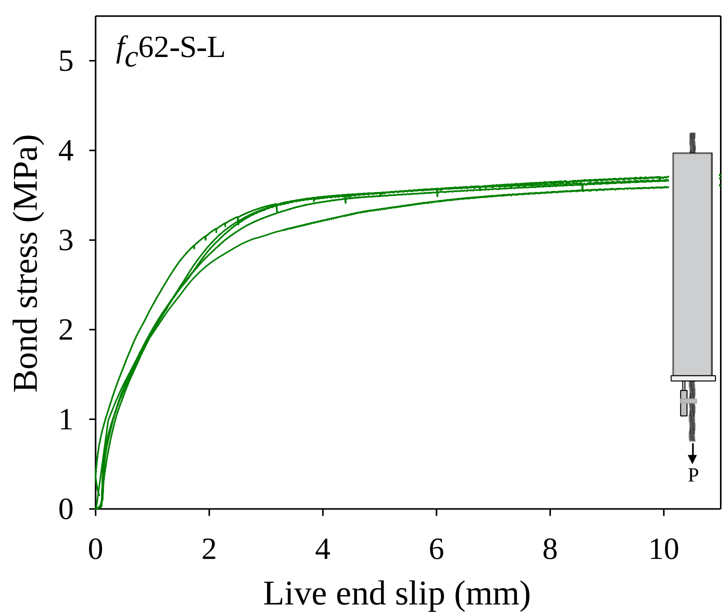

Figure 6.14 Bond stress-slip behaviour of stressed strand with l_e = 950 mm in f_c = 62 MPa concrete

Table 6.2 Experimentally obtained τ_b of taut and stressed strands with l_e = 950 mm in f_c = 62 MPa concrete

Specimen ID	Compressive strength of concrete at testing (f_c) in MPa	Maximum bond load (P_{max}) in kN	Bond strength (τ_b) MPa			
			$\tau_{2.5}$		After subtracting the elongation from LE slip	
			LE	FE	$\tau_{2.5}$	0.9 τ_{yield}
f_c62-T-L-1	63.4	194	2.26	3.86	3.02	3.11
f_c62-T-L-2	64.7	179	2.29	--	2.42	3.07
f_c62-T-L-3	61.2	191	2.28	--	3.09	3.08
f_c62-T-L-4	63.9	189	2.02	--	2.65	3.10
f_c62-T-L-5	62.5	191	1.72	--	2.26	3.09
f_c62-T-L-6	63.1	190	1.75	--	2.20	2.97
f_c62-S-L-1	65.8	192	2.31	3.50	2.96	2.95
f_c62-S-L-2	63.5	194	2.51	3.66	3.12	3.10
f_c62-S-L-3	62.6	191	2.31	3.77	3.21	3.06
f_c62-S-L-4	62.8	190	2.31	3.64	3.10	3.04
f_c62-S-L-5	62.3	189	2.32	3.66	3.18	3.04

6.4.4 Difference between $\tau_{2.5}$ and 0.9 τ_{yield}

Statistical hypothesis tests were conducted to check if the difference between the 0.9 τ_{yield} and $\tau_{2.5}$ are statistically significant. The Q-Q Normality tests were conducted on the obtained data sets for the taut and stressed strands. For those data sets passing the normality test, the Students' *t*-test were conducted to check if the data sets are statistically different. For those data set, which did not pass the normality test, the Mann-Whitney rank sum test was performed to check the statistical difference between the data sets.

The $\tau_{2.5}$ and 0.9 τ_{yield} were dot plotted to understand the significance of the results and shown in Figure 6.15 and Figure 6.16, respectively. It was found that the average value of $\tau_{2.5}$ for the taut strands in 43 and 62 MPa strength concrete with l_e = 450 mm was 2.2 (CoV = 13%) and 3.43 MPa (CoV = 16%), respectively. When the f_c increased from 43 to 62 MPa, the value of $\tau_{2.5}$ increased by about 50%. The average value of $\tau_{2.5}$ for taut and stressed strands in 62 MPa strength concrete with l_e = 950 mm was 2.61 (CoV = 15%) and 3.18 MPa (CoV = 3%), respectively. When the stress level increased from 0.1 to 0.7 f_{pu}, the τ_b increased by about 15%. As the slope of the τ-s for stressed strands was stiffer than that for the taut strands in concrete, the average value of $\tau_{2.5}$ of the stressed strands was higher than that of the taut strands with l_e = 950 mm. It was also observed that the effect of l_e was predominant on determining the τ_b using the 2.5 mm slip method. The results indicated that when the l_e of strand increased from 450 to 950 mm, the value of $\tau_{2.5}$ decreased significantly by about 25%. The slip method provides τ_b as a function of l_e. Therefore, the slip method becomes critical for PTC systems as the l_e of the member depends on the L_t of the specimen. The l_e of the strand could vary with specimen to specimen using different materials for PTC members. For some cases, the l_e could be more or less than 1000 mm. In such cases, the determined τ_b should be independent of the l_e of the member and should be represented as a material parameter. Therefore, the determination of τ_b using 2.5 mm slip method cannot be valid as it varies with different l_e of the PTC systems.

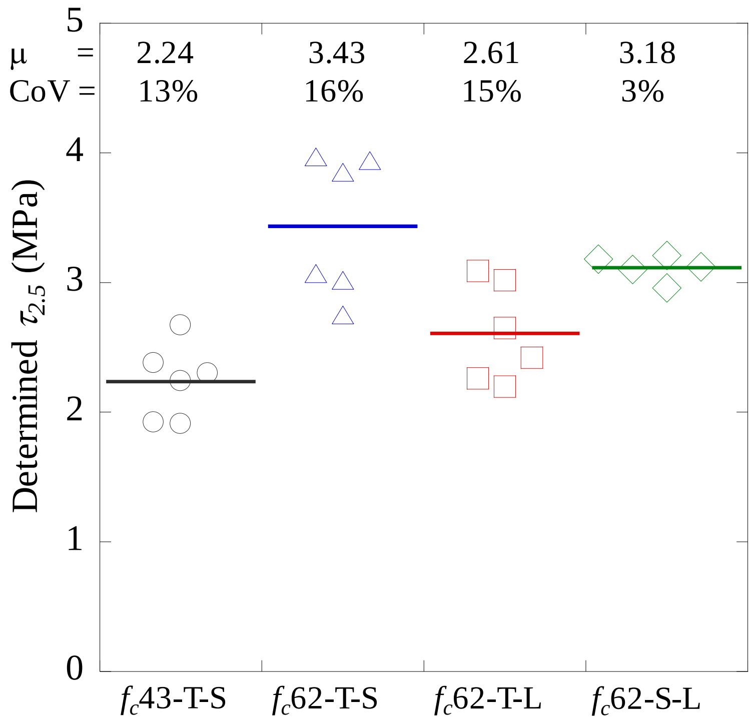

Figure 6.15 Determined $\tau_{2.5}$

Figure 6.16 elucidates the determined 0.9τ_{yield} of the taut and stressed strands in concrete with l_e = 450 and 950 mm. The average 0.9τ_{yield} of the taut strands in 43 and 62 MPa strength concrete with l_e = 950 mm was 1.83 (CoV = 13%) and 2.68 MPa (CoV = 18%), respectively. As the yield attained before the strands experiencing the 2.5 mm slip, the τ_{yield} was lower than the $\tau_{2.5}$ for these cases. When the f_c increased from 43 to 62 MPa, the 0.9 τ_{yield} increased by about 40% due to the improved confinement at the S-C interface. Based on *t*-test, the value of P for f_c = 43 and 62 MPa was 0.030 and 0.031, respectively (less than 0.005). Therefore, it confirmed that the 0.9 τ_{yield} method has a significant difference on the τ_b compared with the 2.5 mm slip method for the taut short strands embedded in f_c = 43 and 62 MPa.

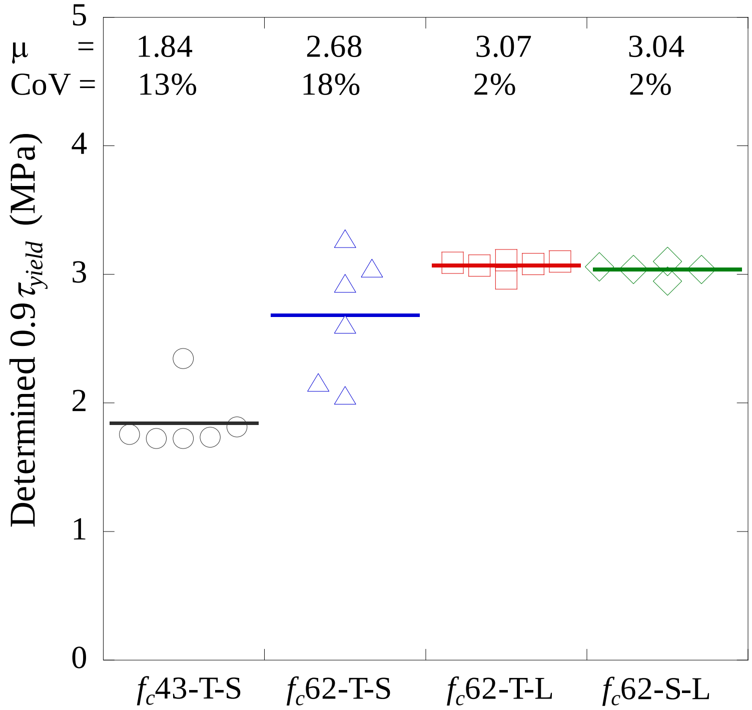

Figure 6.16 Determined 0.9 τ_{yield}

In the case of long specimens (l_e = 950 mm) with the taut and stressed strands in f_c = 62 MPa, the determined 0.9 τ_{yield} was almost the same, 3 MPa (CoV = 2%). Based on the yield method the determined τ_b of the taut strands increased by about 13% and almost the same for the stressed strands compared to the determined τ_b based on slip method. The values of P for the taut and stressed strands was 0.026 and 0.165, respectively. It indicates that the 0.9 τ_{yield} has significant difference on the τ_b of the taut strands and not on that of the stressed strands. From the results, it is evident that the yield method could eliminate the effect of stress on the determined τ_b. The τ_b of taut strands (with l_e = 450 mm) using slip method was 20% lesser than that using yield method. The effect of l_e was minimized using the yield method.

Figure 6.17 shows the determined τ_b as a function of the f_c. The solid and hollow markers indicate the $\tau_{2.5}$ and 0.9 τ_{yield}. It signifies a lot of variation on the determined $\tau_{2.5}$ of the taut strands in concrete. The cluster of solid markers of specimens f_c62-T-S, f_c62-T-L, and f_c62-S-L, indicate that the value of 0.9 τ_{yield} is same for the specimens with different l_e and f_{ps}.

However, the 0.9 τ_{yield} of taut strands with l_e = 450 mm has a lot of scatter than that of taut strands with l_e = 950 mm.

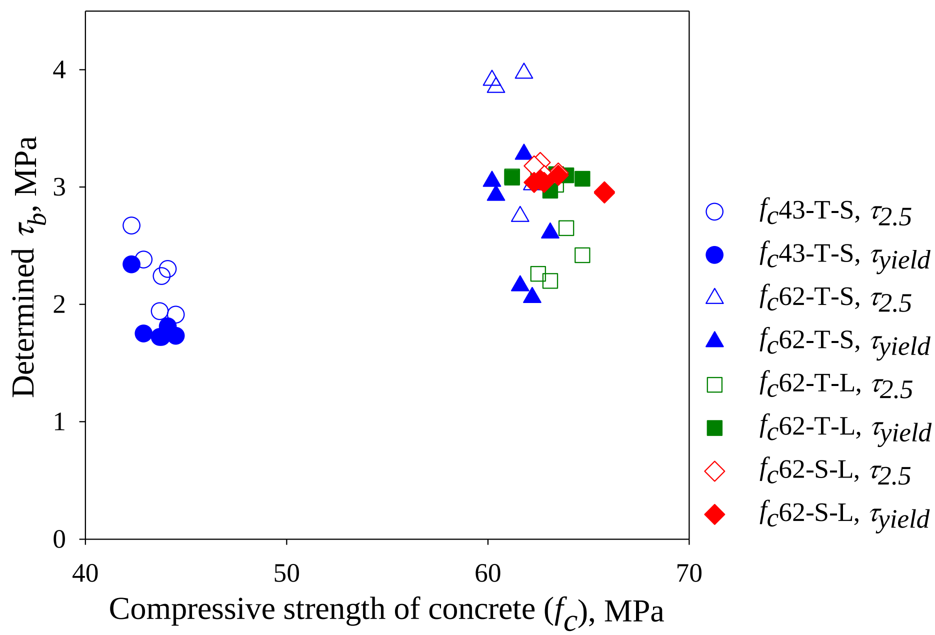

Figure 6.17 Determined τ_b as a function of compressive strength of concrete

The limitation of the slip method can be overcome by using the 0.9 τ_{yield} method, which represents the behaviour of the S-C bond by eliminating the effect of l_e. This method indicates that the stress at yield would remain the same irrespective of the l_e of the strands. The slip at the τ_{yield} was longer than that at the $\tau_{2.5}$ for the long specimens of about 3 mm. However, the slip of τ_{yield} would attain before the 2.5 mm slip of the strand at the FE, which is typically considered in many standards. Hence, the slip range would also be well within the range specified by the codes.

Figure 6.18 displays the difference in the τ_b between the taut and stressed strands ($\Delta\tau_b$). The $\Delta\tau_b$ was calculated by subtracting the mean τ_b of stressed strands from the τ_b of taut strands using yield method. The figure indicates that the $\Delta\tau_b$ for taut strands with l_e = 950 mm is close to zero with less scatter compared to that for taut strands with l_e = 450 mm. From this observation, it can be concluded that the 0.9 τ_{yield} of the stressed and taut strand specimens with l_e = 950 mm did not vary significantly. Thus, the τ_b of the stressed strands can be obtained by using the taut strands with l_e = 950 mm in concrete.

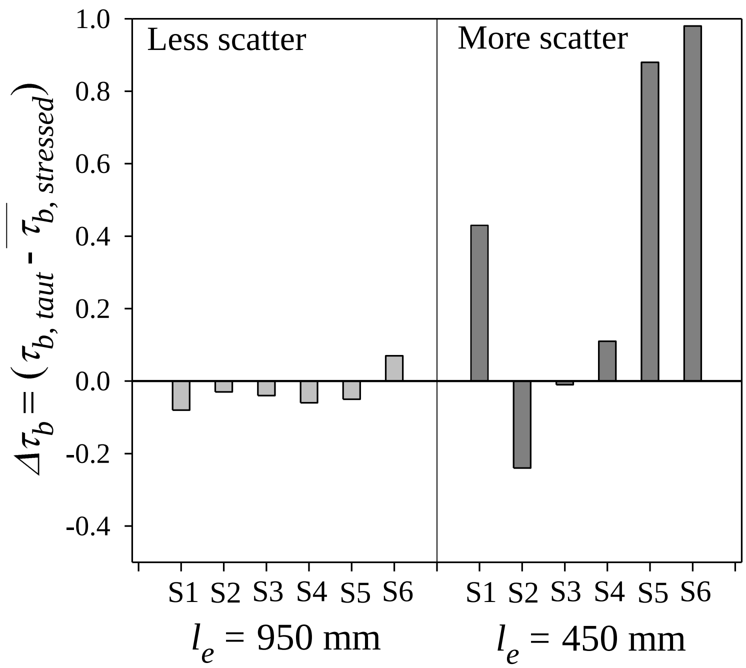

Figure 6.18 The difference in the τ_b between the taut and stressed strands

Based on the experimental results and above discussions, using the 0.9 τ_{yield}, the taut strands with l_e = 950 mm embedded in concrete strength not less than about 60 MPa could be used to determine the τ_b in the PTC systems. Also, both the taut and stressed strands with l_e = 950 mm ruptures at the maximum load of about 190 kN exhibiting similar behaviour after the yield. It should be noted that the bond failures of all the specimens were by the pull-out of the strand. The mode of failure observed in the taut and stressed strands is explained in the following section. A similar type of pull-out failure was observed for taut and stressed specimens with l_e = 950 mm followed by the strand rupture.

6.4.5 Modes of failure

From the experimental investigations, it is observed that all the taut strand specimens with short l_e = 450 mm failed by the pull-out of the strand than by splitting of the concrete which is expected for high strength concrete. This is due to the mechanical interlock mechanism which provides bearing action against concrete keys due to the helical shape of the strand. The pull-out specimen was cut open to observe the failure at the S-C interface. Figure 6.19 indicates the S-C bond failure at the interface due to strand slippage.

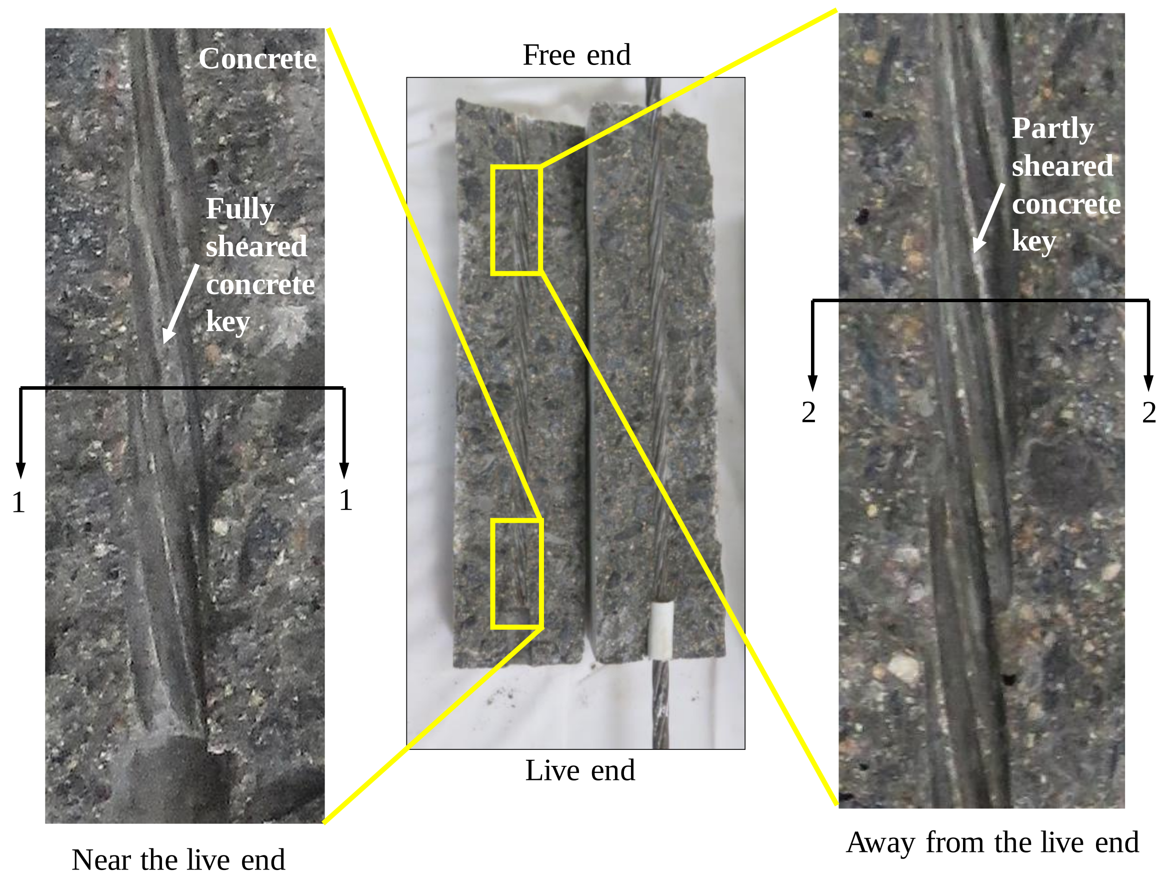

Figure 6.19 The S-C bond failure at the interface (with close-up views)

The bottom left side of the specimen is zoomed out to display the interface damage near the live end. The damage of the concrete keys was maximum near the live end. The damage of concrete keys is a progressive failure and gets reduced as it progresses along the length away from the live end. Figure 6.20 illustrates the damage of concrete keys at the interface. Figure 6.20 (a) shows the perfect concrete keys between the outer wires at the S-C interface before strand starts slipping. Then, once the strand starts slipping, the tip of the concrete keys get damaged and partly sheared (see Figure 6.20 (b)) at the S-C interface away from the live end as in Section 2-2 of Figure 6.19. As the stress concentration is high near the live end of the member, concrete keys at live end were fully sheared due to increasing load as shown in Figure 6.20 (c), which is the case of Section 1-1 of Figure 6.19. Once the concrete keys were sheared off during the testing, a smooth path like through pipe was formed for the strand to slip freely. Thus, the specimens failed by pull-out of strand from concrete. The damage of concrete keys and pull-out failure are the common failure mode of the short taut strands in concrete.

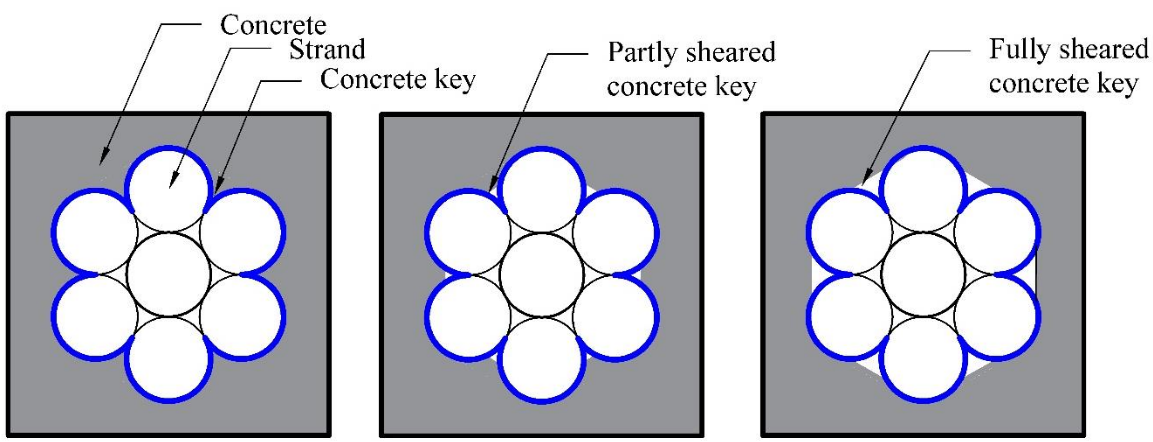

(a) Intact concrete keys

(b) Partly sheared concrete keys (as in Section 2-2 in Figure 6.19)

(c) Fully sheared concrete keys (as in Section 1-1 in Figure 6.19)

Figure 6.20 Damage of concrete keys at the interface

A similar type of pull-out failure was observed with the long taut and stressed strands (l_e = 950 mm) followed by strand rupture. Since the l_e is long, the bond resistance to slip is high. Consequently, the load required to bond failure is increased and reached the breaking strength of strands about 190 kN, where the strand ruptures. Figure 6.21 (a) shows the failure patterns observed in short, where the failure is only by pull-out not by strand rupture. On the other hand, Figure 6.21 (b) shows the strand rupture of long strands. The failure mode of long taut and stressed strands is the same by strand rupture. The failure mechanism for stressed and taut strands is explained in the following section.

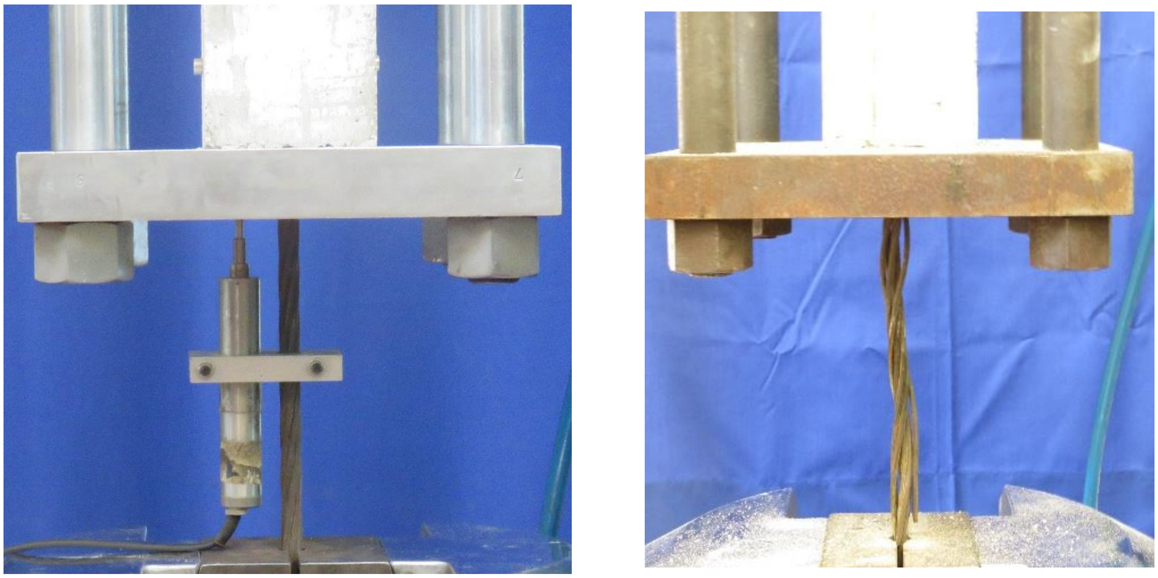

(a) In short specimens, strands get pulled-out and strands do not rupture

(b) In long specimens, strands get pulled-out and eventually gets ruptured

Figure 6.21 Failure patterns in short and long specimens

6.5 Failure mechanism of the S-C bond

The τ-s behaviour of the taut and stressed strand is different at the S-C interface due to the applied initial prestress and Hoyer effect. To illustrate this mechanism, changes at the interface near the live end of the specimen during the pull-out test is shown in Figure 6.22. During pull-out test, at $P_s < P_{yield}$, strand at the interface elongates and gets debonded with the surrounded concrete. It is assumed that the strand deforms elastically till P_{yield}. The Hoyer effect is insignificant in the taut strand specimens where, the applied initial stress is minimal (about 0.1 f_{pu}) just to keep the strand straight. The dashed lines in Figure 6.22 (a) indicate the outer surface of the taut strand in contact with concrete. The shaded region in the figure shows the debonded region (gap between the strand and concrete).

On contrary, in the stressed strand specimens, the Hoyer effect would be significant, which precompresses the surrounding concrete at the transfer of applied f_{ps} (about $0.7f_{pu}$). As a result, while strand elongates under the load, the concrete gets decompressed due to elasticity, which prevents the debonding of strand from the surrounding concrete (Figure 6.22 (b)). The white region between the two solid helical lines indicates the decompressed concrete in contact with the strand.

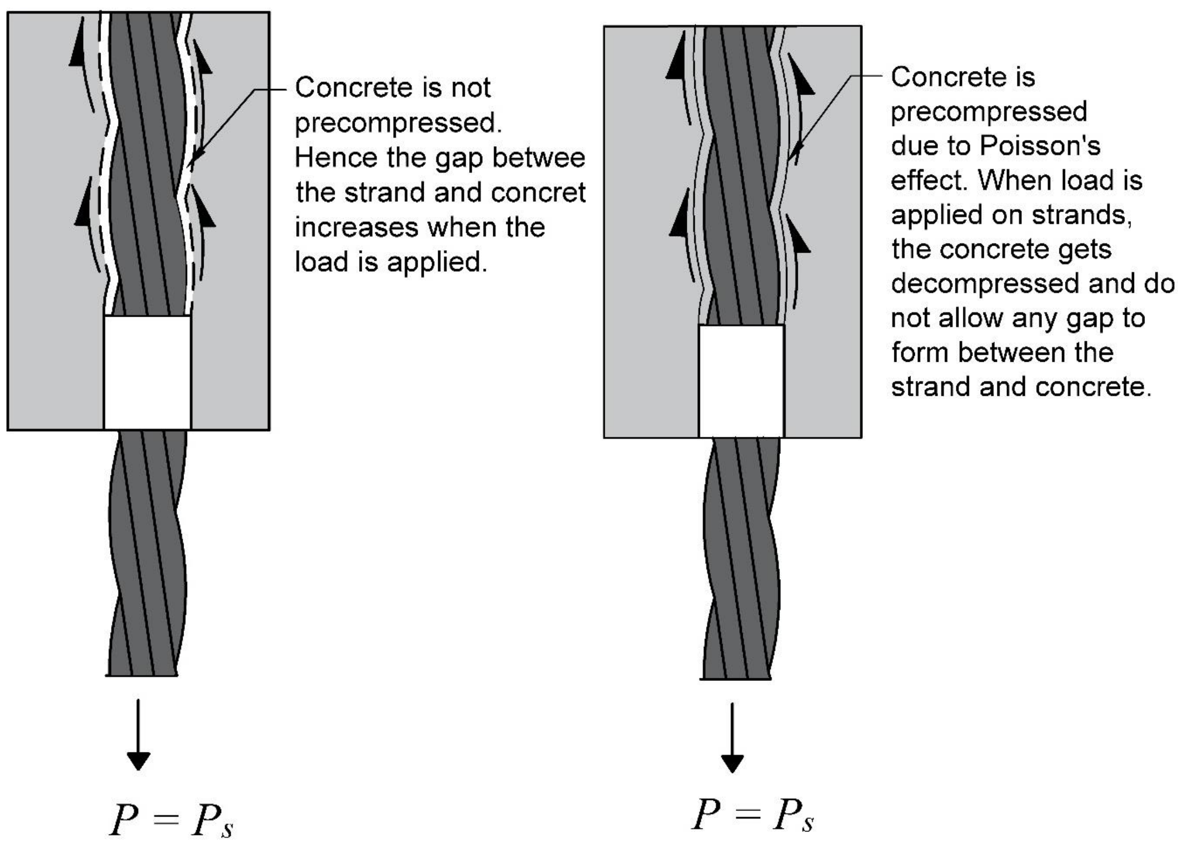

where, $P_s < P_{yield}$

(a) Taut strand in concrete (b) Stressed strand in concrete

Figure 6.22 Changes at the S-C interface during the pull-out test (until τ_{yield})

In the case of the stressed strands, the expansion of the concrete due to decompression, gives more stiffness and resistance to the slip of the strand, whereas, in the taut strand specimen, the concrete would not experience such expansion and leaves a gap between the strand and concrete when the strand deforms. Hence, there is no restrain for the strand movement, and the strand starts slipping once the load is applied. The significance of this mechanism is clearly seen in Figure 6.13 and Figure 6.14, which display the bond stress – slip behaviour of stressed and taut strands in concrete. The τ-s behaviour indicates that for a particular load, the stressed strand specimens would experience less slip than the taut strand specimens. This implies that the Hoyer and Poisson's effect at transfer and loading plays a critical role on the bond stress at the S-C bond of the PTC systems.

Once the strand starts slipping, the shear and bearing forces would be induced on the concrete keys (typically the cement paste with fine aggregates) between the outer wires of the strand. Figure 6.23 displays the mechanism of bond failure at S-C interface. A close-up of the region ABCD is shown and indicates the forces acting on the concrete keys under loading. When the load is applied, the strand tends to slip. This activates the friction and mechanical interlock mechanisms and induces the shear force (F_s) and bearing force (F_b) on the interface between the concrete key and outer wires. $I_{K\text{-}W1}$ and $I_{K\text{-}W2}$ represent the interfaces between the concrete key and outer wires shown.

The following assumptions are made in developing the bond failure mechanism: (i) the curved region (dashed line) of outer wire is considered as straight line for simplification and the triangle formed by the points K1, K2, and K3 forms the concrete key and (ii) there is no relative movement between the outer wires – indicating no resistance offered by the $I_{K\text{-}W2}$ interface. Also, note that in PTC elements, the strands exhibit complete pull-out failure due to shearing of the concrete keys. At the S-C interface, when the strand starts slipping, the surrounding concrete resist the movement of the strand and induces the normal force (N) and frictional force (μN) on the outer surface of the concrete key (K1-K2). Shear force and bearing forces from the strand on the $I_{K\text{-}W}$ act at an angle 'θ'. Therefore, to be in equilibrium, the sum of the forces acting in the vertical and horizontal direction is zero as given Eqs. 6.2 and 6.3.

$$\Sigma F_x = 0; \quad N - F_b\cos\theta + F_s\sin\theta = 0$$ Eq. (6.2)

$$\Sigma F_y = 0; \quad \mu N - F_b\sin\theta - F_s\cos\theta = 0$$ Eq. (6.3)

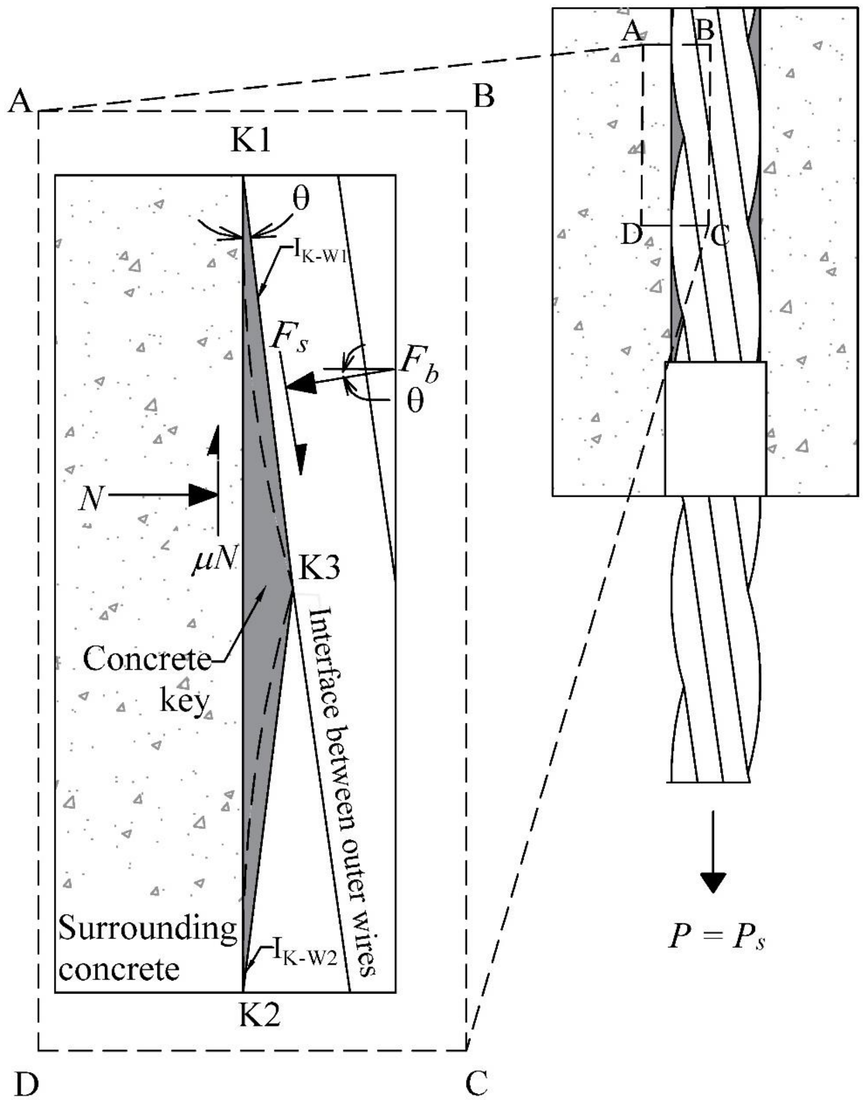

Figure 6.23 Mechanisms of bond failure at S-C interface

As the test progresses, with the increase in applied load, the shear force at the interface increases; when the $F_s \; sin\theta + F_b \, cos\theta > \mu N$, the concrete key region (K1-K2-K3) gets sheared and forms a path for the strands to slide. Then, the debonding region continues to propagate along the length of the member. Consequently, this failure facilitates the free movement of the strands and the concrete keys along the interface K1-K2 surface (complete pull-out failure). Once the concrete keys get sheared, the mechanical interlock mechanism becomes insignificant and the strand slips freely (i.e., without much additional load). This can be seen from Figure 6.13 and Figure 6.14, where the slope of the bond stress changes gradually and approaches zero with the increasing slip of the strand. Thus, the bond failure of the PTC members depends on the failure of the concrete keys between the wires, which is a function of the compressive strength and shear strength of concrete. This indicates (as discussed earlier) that the prestress plays a role on the slope of the initial region of the τ-s plot (say, up to yield point); but not on the yield point or bond strength. After yield, the sheared concrete keys allow the free movement of strand - indicated by the region with negligible slope on the τ-s plot. Therefore, the load required to fail the concrete keys is same irrespective of the slip of the strand. Hence, the yield and post peak behaviour are the same for both taut and stressed strands in concrete.

6.6 Summary of Objective 2

In sum, this chapter explained the challenges involved in determining the bond stress using the conventional method. Also, it has addressed the strand deformation during the pull-out test and eliminated the strand deformation from the measured slip to obtain the true slip of the PTC members. Then, to overcome the challenges associated with the conventional method, 90% bond yield stress method is proposed to determine the bond strength between the strand and concrete. Using 90% bond yield stress method, effect of compressive strength, prestress level, and embedment length of the strand on the bond strength of the PTC members were assessed. Finally, the modes of failure and failure mechanism of bond are detailed. The conclusion from this chapter are provided in the following Chapter 7.

7 CONCLUSIONS AND RECOMMENDATIONS

7.1 SUMMARY OF THE STUDY

The transmission lengths for pretensioned concrete (PTC) members for different compressive strength of concrete at transfer (f_{ci} = 23, 28, 36, and 43 MPa) were estimated using the codal formulations and compared with the experimentally obtained L_t of twelve specimens. Based on the experimental data, a bilinear model was proposed to standards for a rational estimation of L_t. Also, case studies were conducted in order to understand the significance of underestimation or overestimation of L_t on the structural performance of the PTC members. The limitations on determining the bond strength were discussed. Pull-out test was performed using the taut and stressed strands in concrete (f_c = 43 and 62 MPa) to determine the bond strength of the PTC members. A 90% bond yield stress method was proposed to determine the bond strength as an S-C interface parameter that is independent of l_e and f_{ps}. Based on the experimental study the following conclusions were drawn:

7.2 CONCLUSIONS

The specific conclusions from each objective are presented in the following subsections.

7.2.1 Objective 1 – To determine and model the effect of compressive strength at transfer (f_{ci}) on the transmission length (L_t) of pretensioned concrete systems.

1. DEMEC readings are highly sensitive and it could vary with persons. Hence, care should be taken to avoid or minimise the error in the reading. The commonly used DEMEC discs are not suitable for the L_t measurements – provides lower strain than expected. Hence, DEMEC inserts are suggested for proper L_t measurements which is the best suitable for long-term measurements also.
2. The compressive strength of concrete at transfer has significant influence on L_t. When f_{ci} increased from 23 to 43 MPa, the possible range in practice, the values of L_t decreased by about 34%. Therefore, the f_{ci} has to be included in the design equations for a rational estimation of L_t. From the experimental work, a bilinear model was proposed to determine the L_t as a function of f_{ci}.

3. The initial time from 7 to 28 days plays significant role on L_t as the concrete hardens to gain its design strength. However, after 150 days no trend was observed on the L_t measurement. More controlled study has to be carried out to obtain the accurate L_t with time. In general, it can be concluded that the rate of change of L_t after 150 days is not significant.
4. For the range of concrete compressive strength at transfer used in the PTC systems, the $L_{t,\,code}$ based on AASHTO, ACI, AS, CSA, EN, *fib* MC overestimated the L_t based on the proposed model. However, the L_t based on IS 1343 (2012) underestimated the required L_t. Therefore, the design L_t equation in IS 1343 (2012) has to be revised to meet the actual L_t required to transfer the effective stress from strand to concrete. Also, it is recommended to revise the L_t as a function of f_{ci} in the design equations of other codes which do not consider f_{ci} but overestimates the L_t.
5. From the case studies, it was observed that the underestimation and overestimation of L_t are not advisable for the design of shear and transmission zone reinforcement required for the bursting stresses, respectively. Hence, the proposed model that considers the compressive strength of concrete at transfer to estimate L_t precisely is expected to provide a more rational design of the shear and transmission zone reinforcement.

7.2.2 Objective 2 – To develop a simplified procedure and determine the bond strength of strand in concrete as a function independent of the embedment length and prestress level.

1. The τ corresponding to 2.5 mm at the free end cannot be used to determine the τ_b as it is not reliable for the long PTC members. Also, the measured slip obtained by the LVDT at the live end does not represent the true slip of the strand as it measures the elongation of the strand along with the slip of the strand. This necessitates the need to eliminate the elongation of strand from the measured slip to get the true τ-s behaviour.

2. Using the 2.5 mm slip method, the determined τ_b increased by about 50% when the f_c increased from about 40 to 60 MPa. Also, when the applied prestress increased from 0.1 f_{pu} to 0.7 f_{pu}, the τ_b increased by about 15% and when the l_e of strands increased from 450 to 950 mm, τ_b decreased significantly by 25%. Therefore, the 2.5 mm slip method is not suitable for determining the bond strength of the PTC systems as τ_b becomes function of l_e which is critical.

3. Using the bond yield stress method, when the f_c increased from 40 to 60 MPa, the τ_b increased by about 40% due to increased confinement at the S-C interface. Hence, f_c is an important parameter to be considered in the design formulation to determine the bond strength of PTC members.

4. The determined τ_b of both taut and stressed strands were almost the same, say about 3 MPa using the proposed method based on bond yield stress. Also, the determined τ_b did not vary with different l_e as the yield stress represents the behaviour of the S-C interface independent of the applied prestress and embedment length. The difference in the τ_b between the taut with 950 mm and stressed strands is insignificant, close to zero.

5. Based on the proposed method, the complexity in determining the τ_b of the stressed strands can be reduced. For a proper controlled study, taut strands with l_e = 950 mm could be used to determine the τ_b of the stressed strands.

6. The S-C interface of stressed and taut strands was different till yield point due to transferred stress from strand to concrete. After yield, the concrete keys formed at the S-C interface gets sheared off under loading and creates a path for strands to move freely. Thus, the failure of bond depends on the strength of concrete keys which is the function of the compressive strength of concrete. Therefore, irrespective of stress, the τ–s behaviour after yield is the same for both long and stressed strands in concrete. Then, the failure mechanism of taut and stressed strands in concrete is mainly by pull-out of strands (short taut strands) and strand rupture (long taut and stressed strands).

7.3 RECOMMENDATIONS FOR FUTURE WORK

1. The effect of time on L_t can be studied with proper controlled condition to capture the shrinkage and creep effects.
2. Effect of member size and geometry on L_t and τ_b can be studied and those parameters should be defined as a function of material properties irrespective of member size and geometry. Further, a full-scale member testing can be done to determine the transmission length.
3. Bond stress-slip relationship is obtained by measuring the slip at live and free ends of the member. The strain on the concrete surface along the length of the specimen under pull-out testing needs to be studied to get deeper understanding of bond
4. mechanisms. The digital image correlation technique could be used for this.
5. Further, this study can be extended to study the bond behaviour of strands embedded in concrete using supplementary cementitious materials. Also, testing more specimens with different stress levels would be helpful to obtain the correlation between the applied prestress and bond strength of PTC members.
6. Many PTC members are subjected to aggressive environment in reality which are expected to deteriorate by corrosion and degrade the structural performance of the members. Hence, it is important to study the bond behaviour of strands embedded in concrete subjected to different corrosion level and service life estimation is required to ensure its structural performance and safety.
7. Numerical models can be developed to conduct parametric studies on L_t and τ_b.

REFERENCES

AASHTO (2012). LFRD bridge design specifications, interim revisions 6th ed., American Association of State Highway and Transportation, Washington, DC

Abdelatif, A. O., Owen, J. S., and Hussein, M. F. M. (2015). Modelling the prestress transfer in pretensioned concrete elements. Finite Elements in Analysis and Design, 94: 47–63. *DOI:10.1016/j.finel.2014.09.007*

Abrishami, H. H., and Mitchell, D. (1993). Bond characteristics of pretensioned strand. ACI Materials Journal, 90 (3): 228–235.

ACI 318 (1963). Building code requirements for structural concrete (ACI 318-1963) and Commentary (ACI 318R-1963). American Concrete Institute, Detroit, MI, USA.

ACI 318 (2011). Building code requirements for structural concrete (ACI 318-2011) and Commentary (ACI 318R-2011). American Concrete Institute, Farmington Hills, MI, USA.

ACI 318 (2014). Building code requirements for structural concrete (ACI 318-2014) and Commentary (ACI 318R-2014). American Concrete Institute, Detroit, MI, USA.

Akhnoukh, A. L. (2008) Development of high performance precast prestressed bridge girders. Ph.D. thesis, University of Nebraska-Lincoln, Lincoln, NE, USA.

Alsiwat, J. M. and Saatcioglu, M. (1992**).** Reinforcement anchorage slip under monotonic loading. Journal of Structural Engineering, 118(9): 2421-2438.

AS 3600 (2009). Concrete Structures, Standards Australia limited, Australian Standard, Sydney, NSW, Australia.

ASTM A1081 (2012). Standard test method for evaluating bond of seven-wire steel prestressing strand, American Society of Testing and Materials International, Conshohocken, PA, USA.

ASTM A416 (2018). Standard specifications for low-relaxation, seven-wire steel strand for prestressed concrete. American Society of Testing and Materials International, Conshohocken, PA, USA.

ASTM C192 (2016). Standard practice for making and curing concrete test specimens in the laboratory. American Society of Testing and Materials International, Conshohocken, PA, USA.

ASTM C204 (2016). Standard test methods for fineness of hydraulic cement by air permeability apparatus. American Society of Testing and Materials International, Conshohocken, PA, USA.

Baláz, G. L. (1992). Transfer control of prestressing strands. PCI Journal, 37: 60-71.

Barnes, R. W., Grove, J. W., and Burns, N. H. (2003). Experimental assessment of factors affecting transfer length. ACI Structural Journal, 100(6): 740– 748.

Belhadj, A. and Bahai, H. (2001). Friction-slip: an efficient energy dissipating mechanism for suddenly released prestressing bars, Engineering Structures, 23: 934-944.

Benítez, J. M. and Gálvez, J. C. (2011). Bond modelling of prestressed concrete during the prestressing force release, Materials and Structures, 44: 263-278.

Brearley, L. M., and Johnston, D. W. (1990). Pull-out bond tests of epoxy-coated prestressing strand. Journal of Structural Engineering, 116(8): 2236–2252.

Bruce, R. N., Russell, H. G., Roller, J. J., and Martin, B. T. (1994). Feasibility evaluation of utilizing high-strength concrete in design and construction of highway bridge structures. Baton Rouge, LA.

BS 8110-1 (1997). Structural use of concrete - Part 1: Code of practice for design and construction, British Standards, London, UK.

Buckner, C. D. (1995). A review of strand development length for pretensioned. PCI Journal, 40(2): 84–105.

Caro, L. A., Martí-Vargas, J. R., and Serna, P. (2013a). Prestress losses evaluation in prestressed concrete prismatic specimens. Engineering Structures: 48: 704–715. *https://doi.org/10.1016/j.engstruct.2012.11.038.*

Caro, L. A., Martí-Vargas, J. R., and Serna, P. (2013b). Time-dependent evolution of strand transfer length in pretensioned prestressed concrete members. Mechanics of Time-Dependent Materials, 17 (4): 501–527. *https://doi.org/10.1007/s11043-012-9200-2.*

Cousins, T. E., Johnston, D. W., and Zia, P. (1986). Bond of epoxy-coated prestressing strand. Federal Highway Administration, Publication No. FHW A/NC/87-005, Washington, D.C.

Cousins, T. E., Johnston, D. W., and Zia, P. (1990). Development length of epoxy-coated prestressing strand. ACI Materials Journal, 87(4): 309–318.

CP 110-1 (1972). Code of practice for the structural use of concrete. Design, materials and workmanship, UK.

CSA A23.3 (2004). Design of concrete structures, Canadian Standards Association Mississauga, Canada.

Dang, C. N. (2015). Measurement of transfer and development lengths of 0.7 in. strands on pretensioned concrete elements. Ph.D. dissertation. University of Arkansas, Fayetteville, AK, USA.

Dang, C. N., Floyd, R. W., Hale, W. M. and Martí-Vargas, J. R. (2016a). Measured transfer lengths of 0.7 in. (17.8 mm) strands for pretensioned beams. ACI structural Journal, 113(3): 525-535.

Dang, C. N., Floyd, R. W., Murray, C.D., Hale, W. M., and Martí-Vargas, J.R. (2015). Bond stress-slip model for 0.6 in. (15.2 mm) diameter strand. ACI Structural Journal, 112 (5): 625-634.

Dang, C. N., Floyd, R. W., Prinz, G. S., and Hale, W. M. (2016b). Determination of bond stress distribution coefficient by maximum likelihood method. Journal of Structural Engineering, 142(5): 1-10.

Dang, C. N., Murray, C. D., Floyd, R. W., Hale, W. M., and Martí-Vargas, J. R. (2014b). Correlation of strand surface quality to transfer length. ACI Structural Journal, 111(5): 1245-1252.

Dang, C. N., Murray, C. D., Floyd, R. W., Hale, W. M., and Martí-Vargas, J. R. (2014a). Analysis of bond stress distribution for prestressing strand by strand test for strand bond. Engineering Structures, 71: 152-159.

Deatherage, J. H., Burdette, E. G., and Chew, C. K. (1994). Development length and lateral spacing requirements of prestressing strand for prestressed concrete bridge girders. PCI Journal, 39(1): 70–83.

den Uijl, J. A. (1998). Bond Modelling of prestressing strand. ACI special publication 180: 145-169.

Deng, Y., Morcous, G, and Ma Z. J. (2015). Strand bond stress – slip relationship for prestressed concrete members at prestress release. Materials and Structures, 49 (3): 889-903. DOI: 10.1617/s11527-015-0546-1.

Dorsten, V., Hunt, F. F., and Preston, H. K. (1984). Epoxy coated seven-wire strand for prestressed concrete. PCI Journal, 29(4): 100–109.

Elliott, K. S. (2014). Transmission length and shear capacity in prestressed concrete hollow core slabs. Magazine of Concrete Research, 66(12): 585-602.

EN 2 (2004) Design of concrete structures - Part 1-2: General rules for buildings, European standard Brussels, Belgium.

Floyd, R. W., Hale, W. M., and Howland, M. B. (2015). Measured transfer length of 0.6 in. prestressing strands cast in lightweight self-consolidating concrete. PCI Journal, 60(3): 84–98.

Girgis, A. F. M. and Tuan, C. Y. (2005). Bond strength and transfer length of pretensioned bridge girders cast with self-consolidated concrete. PCI Journal, 56 (6): 72-87.

Gustavson, R. (2004). Experimental studies of the bond response of three-wire strands and some influencing parameters. Materials and Structures, 37: 96-106.

Hanson, N. W. and Kaar, P. H. (1959). Transmission length of pretensioned prestressed beams. Journal of the American Concrete Institute, 55(51): 783–802.

Harajli, M. H., Hout, M., and Jalkh (1995). Local bond stress-slip relationship of reinforcing bars embedded in plain and fiber concrete. ACI Materials Journal, 92(4): 343-354.

Hegger, J. and Bertran, G. (2008) Anchorage behaviour of pretensioned strands in steel fiber reinforced UHPC, Ultra High Performance Concrete (UHPC). Proceedings of the second International symposium on ultra high performance concrete. Kassel, Germany: 537-544.

Hegger, J., Will, N., and Bülte, S. (2007). Bond strength and shear capacity of prestressed beams made of SCC. Self-Consolidating concrete for precast prestressed applications, SP-247, American Concrete Institute, Fajardo, P. R: 123-138.

Hoyer, E. and Friedrirch (1939). Beitrag zur frage der haftspannung in eisinbeton bautellin. Beton und Eiren, 50: 717–736.

International Federation for Structural Concrete (*fib*) (2000). Bond of reinforcement in concrete-State of the art report *fib* Bulletin No. 10, Lausanne, Switzerland.

International Federation for Structural Concrete (*fib*) (2010). Model code for concrete structures, *fib* Bulletin No. 55, Lausanne, Switzerland.

IRC 112 (2011). Code of practice for concrete road bridges, Indian Road Congress, New Delhi, India.

IS 10262 (2009). Concrete Mix Proportioning – Guidelines, Bureau of Indian Standards (BIS), New Delhi, India.

IS 1199 (1959). Methods of sampling and analysis of concrete. Bureau of Indian Standards (BIS), New Delhi, India.

IS 1199 (1959). Methods of sampling and analysis of concrete, Bureau of Indian Standards (BIS), New Delhi, India.

IS 1343 (2012). Prestressed concrete - code of practice, Bureau of Indian Standards (BIS), New Delhi, India.

IS 269 (2015). Ordinary portland cement - specification, Bureau of Indian Standards (BIS), New Delhi, India.

IS 2770 (1967) - Part 1. Methods of testing bond in reinforced concrete, Part 1 Pull-out test. Bureau of Indian Standards (BIS), New Delhi, India.

IS 383 (2016). Coarse and fine aggregate for concrete – Specification, Bureau of Indian Standards (BIS), New Delhi, India.

IS 4031 (1998) – Part 4. Methods of physical tests for hydraulic cement. Part 4 Determination of consistency of standard cement past, Bureau of Indian Standards (BIS), New Delhi, India.

IS 4031 (2008) - Part 1-15. Methods of physical tests for hydraulic cement, Bureau of Indian Standards (BIS), New Delhi, India.

Issa, M. A., Sen, R., and Amer, A. (1993). Comparative Study of Transfer ength in Fiberglass and Steel Pretensioned Concrete Members. PCI Journal, 38(6): 52–63.

Janney, J. R. (1954). Nature of bond in pre-tensioned prestressed concrete. Journal of the American Concrete Institute, 25(9): 717–736.

Kaar, P. H., Lafraugh, R. W., and Mass, M. A. (1963). Influence of concrete strength on strand transfer length. In Ninth Annual Convention of the Prestressed Concrete Institute: 47–67.

Kasan, J. and Harries, K. A. (2011). Redevelopment of prestressing force in severed prestressing strand. ASCE journal of bridge engineering, 16(3): 431-437.

Khayat, K. H. (1998). Use of Viscosity-Modifying admixture to reduce top-bar effect of anchored bars cast with fluid concrete. ACI Materials Journal 95(2): 158-167

Kim, J. K., Yang, J. M., and Yim, H. J. (2016). Experimental evaluation of transfer length in pretensioned concrete beams using 2400 MPa prestressed strands. Journal of Structural Engineering, 142(11: 04016088-1-04016088-10/

Kose, M. M. and Burkett, W. R. (2005). Formulations of new development length equation for 0.6 in. prestressing strand. PCI Journal, September-October: 96-105.

Krishna Murthy, D. (1971). A method of determining the tensile stresses in the end zones of pre-tensioned beams. The Indian concrete journal, 45(7): 286-697.

Lane, S. (1998). A new development length equation for pretensioned strands in bridge beams and piles. Mclean, VA.

Larson, K. H., Peterman, R. J., and Esmaeily, A. (2007). Bond Characteristics of Self-consolidating Concrete for Prestressed Bridge Girders. PCI Journal, 52(4): 44–57.

Logan, D. R. (1997). Acceptance Criteria for Bond Quality of Strand for Pretensioned Prestressed Concrete Applications. PCI Journal, 42(2): 52–90.

Mahmoud, Z. I., Rizkalla, S. H., and Zaghloul, E. R. (1999). Transfer and development lengths of carbon fiber reinforced polymers prestressing reinforcement. ACI Structural Journal, 96 (4): 594-602.

Marshall, W. T. and Krishna Murthy, D. (1969). Transmission length of prestressing tendons from concrete cube strengths at transfer. The Indian Concrete Journal, 43(7): 244-253

Martin, B. L. D. and Scott, N. L. (1976). Development of prestressing strand in pretensioned members. In Proceedings of ACI Journal, 73(8): 453–456

Martí-Vargas, J. R., Serna, P., Navarro-Gregori, J., and Bonet, J.L. (2012b). Effects of concrete composition on transmission length of prestressing strands. Constr. Build. Mater., 27: 350-356

Martí-Vargas, J. R., Serna-Ros, P., Navarro-Gregori, J. and Pallarés, L. (2012a). Bond of 13 mm prestressing steel strands in pretensioned concrete members. Engineering Structures, 41: 403-412

Martí-Vargas, J. R. and Hale, W. M. (2013). Predicting Strand Transfer Length in Pretensioned Concrete: Eurocode versus North American Practice. Journal of Bridge Engineering, 18 (December): 1270–1280. doi: 10.1061/(ASCE)BE.1943-5592.0000456.

Martí-Vargas, J. R., Serna-Ros, P., Fernandez-Prada, M. A., and Miguel-Sosa, P. F. (2006). Test method for determination of the transmission and anchorage lengths in prestressed reinforcement. Magazine of Concrete Research, 58(1): 21–29.

Mayfield, B., Davies, G., and Kong, F. K. (1970). Some tests on the transmission length and ultimate strength of pre-tensioned concrete beams incorporating deform strand. Magazine of Concrete Research, 22(73): 219–226.

Mirza, S. M. and Houde, J. (1979). Study of bond stress-slip relationships in reinforced concrete. ACI Journal, Symposium paper, 76: 19-46.

Mitchell, D., Cook, W. D., and Khan, A. A. (1993). Influence of high strength concrete on transfer and development length of pretensioning Strand. PCI Journal, 38(3): 52–66.

Mohandoss, P. and Pillai, R. G. (2017). Effect of prestress on the bond strength of pretensioned concrete systems. International conference on Advances in construction materials and systems, 71st RILEM WEEK and ICACMS, Chennai, India, 4: 153-160.

Mohandoss, P., Pillai, R. G., and Sengupta, A. K. (2015). Comparison of prediction models for transmission length and shear capacity of pre-tensioned concrete systems, 4th Asian conference on Ecstasy in Concrete (ACECON), Kolkata, India: 183-193.

Mohandoss, P., Pillai, R. G., and Sengupta, A. K. (2018). Transmission length of pretensioned concrete systems - comparison of codes and test data, Magazine of concrete research. DOI: 10.1680/jmacr.17.00553.

Moon, D.Y., Zi, G., Kim, J., Lee, S, and Kim, G. (2010). On strain change of prestressing strand during detensioning procedures, Engineering Structures, 32: 2570-2578

Murphy, R., Zhao, W., Peterman, R., and Beck, B. T. (2012). Determining the transfer length in prestressed concrete railroad ties produced in the united states. Report no. 25-1121-0001-453, Mid-America transportation center. University of Nebraska-Lincoln, NE, USA.

Naito, C., Cetisli, F., and Tate,T. (2015). A method for quality assurance of seven-wire strand bond in portland cement concrete. PCI Journal: 69-84.

Nawy, E. G. (2003). Prestressed concrete a fundamental approach 4th edition, Pearson Education, Inc. New Jersery, US.

Oh, B. H. and Kim, E. S. (2000). Realistic evaluation of transfer lengths in pretensioned , prestressed concrete members. ACI Structural Journal, 97(6): 821–830.

Over, R. S. and AU, T. (1965). Prestress transfer bond of pretensioned strands in concrete, Journal of the ACI Journal, Proceedings, 62(11): 1451-1460.

Park, H., Din, Z. U., and Cho, J. (2013). Methodological aspects in measurement of strand transfer length in pretensioned concrete. ACI Structural Journal, 109(5): 625–634.

Pellegrino, C., Zanini, M. A., Faleschini, F., and Corain, L. (2015). Predicting bond formulations for prestressed concrete elements. Engineering Structures, 97: 105-117.

Peterman, R. J. (2007). The effects of as-cast depth and concrete fluidity on strand bond. PCI Journal, 52(3): 72–101.

Pillai, S. U. and Menon, D. (2009). Reinforced concrete design. McGraw Hill Education Private Limited, 3rd edition, New Delhi, India.

Pozolo, A. M. and Andrawes, B. (2011). Transfer length in prestressed self-consolidating concrete box and I-girders. ACI Structural Journal, 108(3): 341–349.

Raju, K. N. (2011). Prestressed concrete, fourth edition, Tata McGraw Hill , New Delhi, India.

Ramirez, J. and Russell, B. (2008). Transfer, development, and splice length for strand/reinforcement in High-Strength concrete. NCHRP (National Cooperative Highway Research Program) report 603. Washington, CS: Transportation Research Board

Ramirez-Garcia, A. T., Dang, C. N., Hale, W. M., and Martí-Vargas, J. R. (2017). A higher-order equation for modelling strand in pretensioned concrete beams. Engineering structures, 131: 345-361.

Ramirez-Garcia, A. T., Floyd, R. W., Hale, W. M., and Martí-Vargas, J. R. (2016). Effect of concrete compressive strength on transfer length. Structures, 5: 131-140.

RILEM TC (1983). RILEM recommendations for the testing and use of construction materials, RC 6 bond test for reinforcement steel. 2. Pull-out test, E & FN SPON, 1994: 218-220

Roller, J. J., Martin, B. T., Russell, H. G., and Bruce, R. N. (1993). Performance of Prestressed High Strength Concrete Bridge Girders. PCI Journal, 38(3): 34–45.

Rose, D. R., and Russell, B. W. (1997). Investigation of Standardized Tests to Measure the Bond Performance. PCI Journal, 44(4), 56–80.

Russell, B. W. and Burns, N. H. (1996). Measured transfer length of 0.5 and 0.6 in. strands in pretensioned concrete. PCI Journal, 41: 44-65.

Russell, B. W. and Burns, N. H. (1997). Measurement of transfer lengths on pretensioned concrete elements. Journal of Structural Engineering, 12(3): 541– 549.

Russell, B. W. and Paulsgrove, G. A. (1999). Assessing repeatability and reproductivity of the moustafa test, the PTI bond test and NASP bond test, Final Report 99-04. Norman, Ok: University of Oklahoma, Fears Structural Engineering Laboratory.

Shahawy, M. A., Issa, M., and Batchelor, B. (1992). Strand transfer lengths in full scale AASHTO prestressed concrete girders. PCI Journal, 37(3): 84–86.

Shin, H., Lee, S., and Yoo, D. (2018). Bond Behavior of pretensioned strand embedded in ultra-high-performance fiber-reinforced concrete. International Journal of Concrete Structures and Materials. DOI 10.1186/s40069-018-0249-4. ISSN 1976-0485/ eISSN 2234-1315

Song, X, Wu, Y., Gu, X., and Chen, C. (2015**).** Bond behaviour of reinforcing steel bars in early age concrete. Construction and Building Materials, 94: 209-217.

Song, W., Ma, Z. J., Vadivelu, J., and Burdette, E. G. (2014). Transfer length and splitting force calculation for pretensioned concrete girders with high-capacity strands. Journal of Bridge Engineering, 19(7): 1–8. DOI: 10.1061/(ASCE)BE.1943-5592.0000566.

Sulaiman, M. F., Ma, C. K., Apandi, N. M., Chin, S., Awang, A. Z., Mansur, S. A. and Omar W. (2017). A review on bond and anchorage of confined high-strength concrete. Structures, DOI: 10.1016/j.istruc.2017.04.004.

Swamy, R. N. and Anand, K. L. (1975). Losses in transmission length and prestress in high alumina cement concrete. Proc. Instn Civ. Engrs, 59(2): 293–307.

Tabatabai, H. and Dickson, T. (1993). The history of the prestressing strand development length equation PCI Journal, 38(6): 64-75.

Tuan, Y. C., Yehia, A. S., Jongpitaksseel, N., and Tadros, K. M. (2004). End zone reinforcement for pretensioned concrete girders. PCI Journal, 49(3): 68-82.

Vázquez-Herrero, C., Martínez-Lage, I., and Martínez-Abella, F. (2013). Transfer length in pretensioned prestressed concrete structures composed of high performance lightweight and normal-weight concrete. Engineering Structures, 56: 983–992. doi: 10.1016/j.engstruct.2013.06.020

Yalciner, H., Eren, O., and Sensoy, S. (2012). An experimental study on the bond strength between reinforcement bars and concrete as a function of concrete cover, strength and corrosion level. Cement and Concrete Research, 42(5): 643-655.

Zhao, J., Cai, G., and Yang, J. (2016). Bond-slip behavior and embedment length of reinforcement in high volume fly ash concrete. Materials and Structures, 49(6): 2065-2082.

Zia, P. and Mostafa, T. (1997). Development length of prestressing strands. PCI Journal, 22(5): 54–65.

APPENDIX A - TEST PROCEDURE TO DETERMINE THE TRANSMISSION LENGTH OF PRETENSIONED CONCRETE MEMBERS

INTRODUCTION

There is no standard method available to determine the transmission length of the pretensioned concrete (PTC) members. This method suggested here is based on the background knowledge of literature. Some modifications are done to obtain quality transmission length data. The detailed description of the specimen preparation and procedure to obtain the transmission length are discussed in the following sections.

SCOPE

- This method targets to determine the bond strength of pretensioned concrete systems by means of a pull-out test.

REFERENCED DOCUMENTS

- ASTM C192 (2016). Standard practice for making and curing concrete test specimens in the laboratory. American Society of Testing and Materials International, Conshohocken, PA, USA.
- ASTM C204 (2016). Standard test methods for fineness of hydraulic cement by air permeability apparatus. American Society of Testing and Materials International, Conshohocken, PA, USA.
- ASTM A416 (2018). Standard specifications for Low-relaxation, seven-wire steel strand for prestressed concrete. American Society of Testing and Materials International, Conshohocken, PA, USA.
- IS 1343 (2012): Prestressed concrete - code of practice. Bureau of Indian Standards, New Delhi, India.
- IS 102362 (2009). Concrete Mix Proportioning – Guidelines, Bureau of Indian Standards (BIS), New Delhi, India.

SIGNIFICANCE AND USE

- The transmission length of PTC members is crucial for its shear performance. Hence, a more rational estimate of the L_t is required for its more refined structural designs; especially, for the end zone reinforcements of the PTC members. Design/site engineers or precast manufactures could use this method as a quality check test to achieve the intended shear performance of the PTC members. If the PTC member did not meet the design L_t or the difference between the measured and design L_t is significant, the member can be rejected for failing to meet the design requirements.

MATERIALS

The following materials are required for the preparation of L_t specimens

1. Strand - The low relaxation seven wire strand of 12.7 mm diameter properties conforming to IS 6000 (1983).
2. Cement - The Ordinary Portland Cement (OPC) 53S sleeper grade conforming to IS 4031(1988-1999).
3. Aggregates - The crushed granite and natural sand can be used as coarse and fine aggregates conforming to IS 383 (2016).
4. Superplasticizer - Master Glenium 8233, a polycarboxylate (PCE) based superplasticizer.

APPARATUS /TOOLS

1. Concrete mixer – A 120 kg capacity mixer is used to obtain the uniformly mixed concrete.
2. Prestressing bed – A 6 m long hollow steel frame is used a prestressing bed to prestress the strands.
3. Hydraulic jack – A 300 bar capacity hydraulic jack is used to apply the initial prestress.

4. Load cell – A 500 kN capacity ring load cell is used to monitor the load applied while stressing.
5. Load cell indicator – It displays the load measured by the load cell.
6. LVDT / dial gauge – A LVDT of 50 mm travel length or a dial gauge to measure the displacement of 50 mm is used to measure the slip during transferring of prestress from strand to concrete.
7. PVC specimen mould – A PVC mould is fabricated and used to cast the pretensioned concrete specimens.
8. Acrylic strips – Acrylic strips of 2 m long with 50 mm c/c to hole to place the inserts are used.
9. DEMEC inserts - A custom made brass inserts are fabricated and embedded on the concrete surface to obtain the change in distance due to prestress transfer.
10. DEMEC gauge – A demec gauge of 150 mm gauge length is used to obtain the strain on the concrete surface due to prestress transfer.
11. Spanners – Small spanners of 12 mm size are used to fix, demould the moulds and fix the inserts and large spanners of 36 mm size are used tighten the nuts of SAS to transfer the stress gradually from strand to concrete.
12. Hammers – It is used to lock the wedge and barrel after stressing the strands.
13. Tamping rods – A circular tamping rods are used to compact the concrete uniformly to obtain good quality concrete.
14. Nuts and bolts – Nuts and bolts are used to fix the moulds and welded to the steel plate of SAS.
15. Wedges and barrels – A three sets of wedge and barrels are required to lock the stress.
16. Steel chair – an arrangement placed to activate the stress.
17. Shim plate – a thin steel plates helps to place the wedges and barrels and loadcell in its position.

18. Stress adjusting systems – a three sets of nut bolts are welded to the steel plate to facilitate the stress adjustment to transfer the stress gradually from the strand to concrete.
19. Ring holder – A ring holder made of using thick steel washer and rod, helps to lock the wedge and barrel at the jacking end.
20. Spatula – It is used to pour the concrete into the mould.
21. Pan – A pan used to save the concrete material.
22. Wet sack and Plastic covers – It is used to moist cure the specimens and prevent the moisture loss during curing.
23. Adhesive – An acrylic based adhesive is used to fix the acrylic plates on the inside faces of the specimen mould.
24. Spirit level – It is used to check the level of the SAS.
25. Chop saw machine – It is used to cut the strands after transferring the prestress.

SPECIMEN PREPARATION AND PROCEDURE

1. Insert the strands in the through – holes of the end brackets.
2. Place the shim plates and load cell next to the end bracket at the jacking end.
3. Place wedge and barrel loosely (not to be locked while stressing the strand) outside the loadcell.
4. Place the ring holder next to wedge and barrel placed at the jacking end.
5. Place the steel chair resting against the end bracket at the jacking end.
6. Place the hydraulic jack next to steel chair.
7. Place the wedge and barrel at the end of hydraulic jack.
8. Place the stress adjusting system at the releasing end after adjusting the levels of the three nuts using spirit level; leave a about 3 to 4 cm for releasing the stress purpose.

9. Apply an initial stress of about 0.75 f_{pu} using the hydraulic jack with the help of pressure gauge attached with the it.
10. Lock the wedge and barrel placed outside of the loadcell with the help of ring holder and rubber hammer.
11. Monitor the load applied using the load cell indicator.
12. Fix the specimen mould on the prestressing bed around the strand.
13. Fix the brass inserts in the acrylic plate and affix them to the inside faces of the PVC moulds using adhesive.
14. Prepare the concrete using the concrete mixer.
15. Pour the concrete in the PVC prism and cube mould (six companion cube specimens) in one layer.
16. Compact the concrete using tamping rod (25 numbers of tamping for every 100 mm length of prism).
17. Demould the prism and cube specimens after 24 hours.
18. Remove the acrylic strips attached on the mould by detaching the head portion of the inserts.
19. After removing the strips, place the head portions of the inserts by tightening it using spanner.
20. Moist cure the specimens using wet sack and plastic covers for three days.
21. Test the compressive strength of concrete after three days.
22. Measure the distance (two readings) between the demec inserts embedded on the concrete surface using DEMEC gauges, before transferring the stress from the strand to the concrete.
23. Transfer the prestress gradually from the strand to concrete using SAS system by closing the distance between the nuts and plates of the SAS.

24. Measure the distance (two readings) between the brass inserts embedded on the concrete surface using DEMEC gauges, before transferring the stress from the strand to the concrete.
25. Cut the strands just outside of the specimens using a chop saw machine.

CALCULATIONS

1. Calculate the strain on the concrete surface (ε_c) due to prestress transfer.
2. Calculate the smoothened strain on the concrete surface (ε'_c) over the three consecutives points (x-1, x, x+1) using the following equation as 150 mm gauge length overlaps the across the inserts.

$$(\varepsilon'_c)_x = \frac{(\varepsilon_c)_{x-1} + (\varepsilon_c)_x + (\varepsilon_c)_{x+1}}{3}$$

3. Plot the average strain profile along the length of the specimen using the smoothen data.
4. Find the 95% of the average maximum strain (AMS) on the profile.
5. Compute the L_t as the distance from the end of the member to reach the 95% of AMS on the strain profile.

APPENDIX B - TEST PROCEDURE TO DETERMINE THE BOND STRENGTH OF STRANDS IN CONCRETE

PROPOSED STANDARD TEST METHOD FOR DETERMINING THE BOND STRENGTH OF STRANDS IN CONCRETE

SCOPE

- This method targets to determine the bond strength of pretensioned concrete systems by means of a pull-out test.

REFERENCED DOCUMENTS

- ASTM A1081 (2012): Standard test method for evaluating bond of seven-wire steel prestressing strand, American Society of Testing and Materials International, West Conshohocken, PA, USA.
- ASTM C192 (2016). Standard practice for making and curing concrete test specimens in the laboratory. American Society of Testing and Materials international, West Conshohocken, PA, USA.
- ASTM C204 (2016). Standard test methods for fineness of hydraulic cement by air permeability apparatus. American Society of Testing and Materials international, Conshohocken, PA, USA.
- ASTM A416 (2018). Standard specifications for Low-relaxation, seven-wire steel strand for prestressed concrete. American Society of Testing and Materials International, Conshohocken, PA, USA
- IS 1343 (2012): Prestressed concrete - code of practice. Bureau of Indian Standards, New Delhi, India.
- IS 102362 (2009). Concrete Mix Proportioning – Guidelines, Bureau of Indian Standards (BIS), New Delhi, India
- IS 2770 (1967) - Part 1: Methods of testing bond in reinforced concrete, Part 1 Pull-out test. Bureau of Indian Standards, New Delhi, India.

- RILEM TC (1983). RILEM recommendations for the testing and use of construction materials, RC 6 bond test for reinforcement steel. 2. Pull-out test, E & FN SPON, 1994: 218-220.

SIGNIFICANCE AND USE

- The bond strength of strands embedded in concrete plays a vital role for any structural systems. However, determination of the bond strength in the PTC systems are crucial and involves complexity as the strands are stressed. This method helps to determine the bond strength of strands in concrete by reducing its complexities involved with the stressed specimens.

APPARATUS/TOOLS

- The test equipment and tools required for bond testing are as follows

1. Concrete mixer: A concrete mixer is used to obtain the uniformly mixed concrete
2. Prestressing bed: A 6 m long hollow steel frame can be used as a prestressing bed to prestress the strand
3. Hydraulic jack: A 300 bar capacity hydraulic jack is used to apply the initial prestress
4. Load cell: A 500 kN capacity ring load cell is used to monitor the load applied while stressing.
5. Load cell indicator: It is used to display the load measured by the load cell.
6. LVDT / dial gauge: A LVDT of 50 mm travel length or a dial gauge could measure the displacement of 50 mm is used to measure the slip during transferring of prestress from strand to concrete.
7. PVC specimen mould: A PVC mould is fabricated and used to cast the pretensioned concrete specimens.
8. Spanners: Small spanners of 12 mm size are used to fix, demould the moulds and fix the inserts and large spanners of 36 mm size are used to tight the nuts of SAS to transfer the stress gradually from strand to concrete.

9. Hammers: It is used to lock the wedge and barrel after stressing the strands.
10. Tamping rods: A circular tamping rods are used to compact the concrete uniformly to obtain good quality concrete.
11. Nuts and bolts: Nuts and bolts are used to fix the mould and welded to the streel plates of SAS.
12. Wedges and barrels: A three sets of wedge and barrel are required to lock the stress.
13. Steel chair: A steel chair type of arrangement can be placed to activate the stress
14. Shim plate: A thin steel plates helps to place the wedges and barrels and loadcell in its position.
15. Stress adjusting systems: A three sets of nut bolts are welded to the steel plate to facilitate the stress adjustment to transfer the stress gradually from the strand to concrete.
16. Circular ring holder: A ring holder made of using thick steel washer and rod, helps to lock the wedge and barrel at the jacking end.
17. Spatula: It can used to pour the concrete into the mould.
18. Pan: A pan can be used to save the concrete material and transport the concrete from the mixer to prestressing bed
19. Wet sacks and plastic cover: It can be used to moist cure the specimens and prevent the moisture loss during curing.
20. Data acquisition system: A data acquisition system can be used to record the applied load and slip of the strand during testing.
21. Spirit level: A spirit level can be used to check the level of the SAS.
22. Universal testing machine: A universal testing machine can be used to perform a pull-out test
23. Pullout test frame: A pull-out frame is fabricated as shown in Figure 4.14
24. LVDT holders: Two LVDT holders are used to position the LVDTs

25. Ruler and Vernier caliper: These are used to measure the dimensions of the test specimens

26. Shim plates with a centre hole: Shim plates with a center hole can be used to place at the end face of the mould to get a uniform surface for pull-out testing.

MATERIALS

- The materials required and preparation of specimens are same as the L_t specimens. A few extra steps has to be taken for the preparation of pullout specimens that are explained in the following section.

PROCEDURE FOR CASTING TEST SPECIMEN

1. Fix the specimen mould on the prestressing bed.
2. Insert the strands in the through – holes of the end brackets.
3. Place the bond breaker around the strand at the pulling end of the specimen.
4. Place the shim plates and load cell next to the end bracket at the jacking end.
5. Place the wedge and barrel loosely (not to be locked while stressing the strand) outside the loadcell.
6. Place the ring holder next to wedge and barrel placed at the jacking end.
7. Place the steel chair resting against the end bracket at the jacking end.
8. Place the hydraulic jack next to steel chair.
9. Place the wedge and barrel at the end of hydraulic jack.
10. Place the stress adjusting system at the releasing end after adjusting the levels of the three nuts using spirit level; leave a about 3 to 4 cm for releasing the stress purpose.
11. Apply an initial stress of about 0.1 f_{pu} and 0.75 f_{pu} (for taut and stressed strands, respectively) using the hydraulic jack with the help of pressure gauge attached with it.

12. Lock the wedge and barrel placed outside of the loadcell using ring holder and rubber hammer.
13. Monitor the load applied using the load cell indicator.
14. Prepare the concrete using the concrete mixer
15. Place the concrete in the PVC prism and cube mould (six companion cube specimens) in one layer.
16. Compact the concrete using tamping rod (25 numbers of tamping for every 100 mm length of prism).
17. Demould the prism and cube specimens after 24 hours.
18. Moist cure the specimens using wet sack and plastic covers for one day and three days for taut and stresses strand specimens, respectively.
19. Test the compressive strength of concrete and transfer the stress when the concrete is attained 60% of its target strength. Typically, for taut strand specimens, the stress would be transferred after one day whereas, for stressed strands specimens, the stress would be transferred after three days.
20. Cut the strands just outside of the specimens leaving 350 mm and 150 mm length using a chop saw machine.
21. Moist cure the specimens for 28 days to attained target compressive strength.
22. White wash the surface of the specimens using plaster of paris before testing to find observe fine cracks developing on the concrete surface during pullout test.
23. Care should be taken to have a proper leveled surface at the ends of the member (live and free end).

TEST PROCEDURE

1. Arrange and set the DAQ system to monitor the applied load, displacement of the actuator, and slip of the strand from the concrete.
2. Mount the pullout frame on the UTM and grip the holding rod of the frame at the upper wedge of the machine.

3. Measure the geometry details of the specimen using the ruler and Vernier caliper.
4. Place the pullout specimens on the frame by inserting the strand (350 mm long portion from the concrete surface) through the center hole of the machine.
5. Grip the strand at the bottom wedge of the machine.
6. Place a thin acrylic plate on the concrete surface at the free end of the member to place the LVDT.
7. Place the LVDTs, one at the live end (bottom) and other one at the free end (top) of the specimen using LVDT holders.
8. Apply the load at the displacement rate of 2 mm/min.
9. Obtain the recorded data from the DAQ system.

CALCULATIONS

1. Calculate the bond stress using the following formulation

$$\tau = \frac{\text{applied load}}{\text{surface area of the bonded strand}}$$

2. Plot the bond stress vs slip at live end.
3. Determine the bond yield stress of the specimen.
4. Compute the bond strength as 90% of the bond yield stress from the bond stress – slip behaviour.
5. Bond strength of stressed strands in concrete can be computed using the taut strands by the bond yield stress method.

APPENDIX C – THE LOAD – SLIP RESPONSE AT LIVE AND FREE ENDS OF THE SPECIMENS

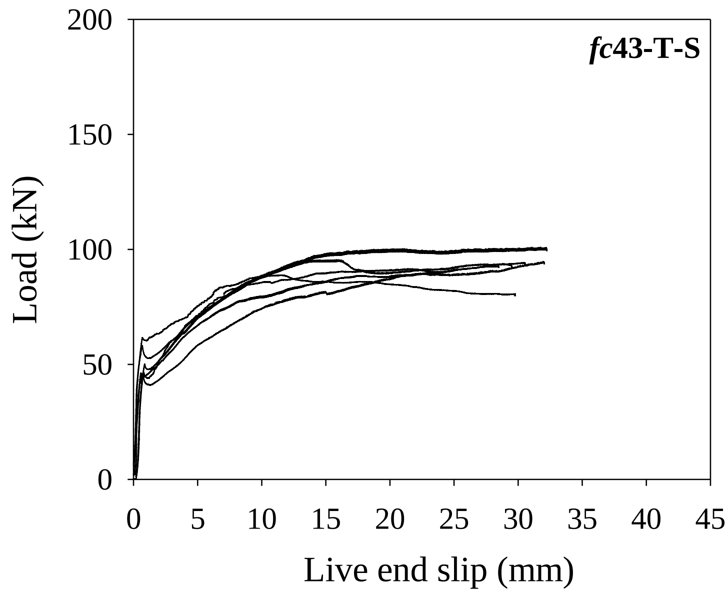

Figure C 1 Load – slip behaviour of taut strands with l_e = 450 mm in f_c = 43 MPa at live end

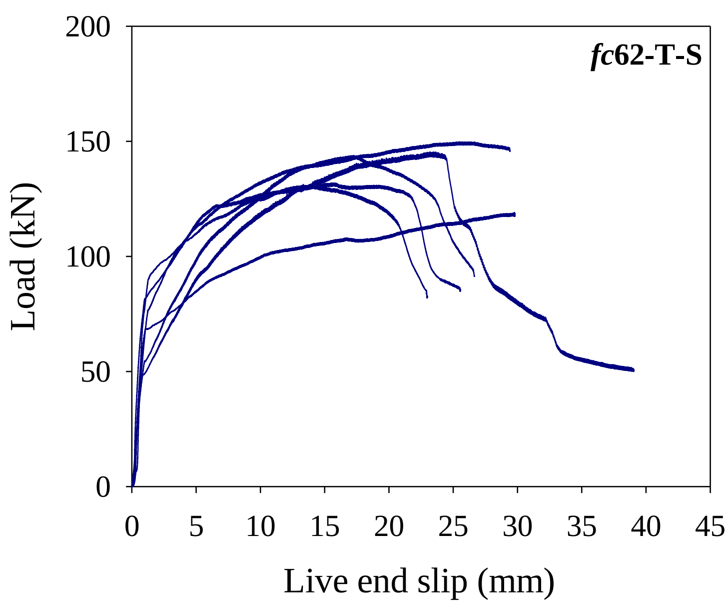

Figure C 2 Load – slip behaviour of taut strands with l_e = 450 mm in f_c = 62 MPa at live end

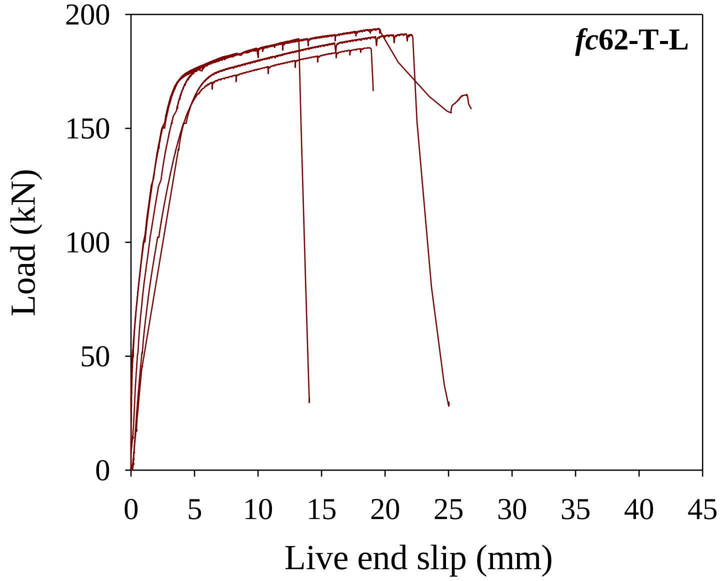

Figure C 3 Load – slip behaviour of taut strands with l_e = 950 mm in f_c = 62 MPa at live end

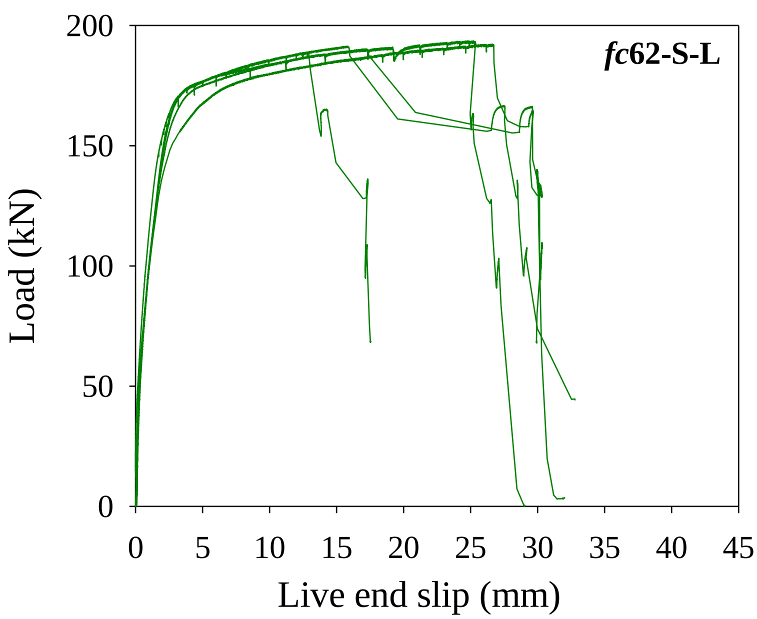

Figure C 4 Load – slip behaviour of stressed strands with l_e = 950 mm in f_c = 62 MPa at live end

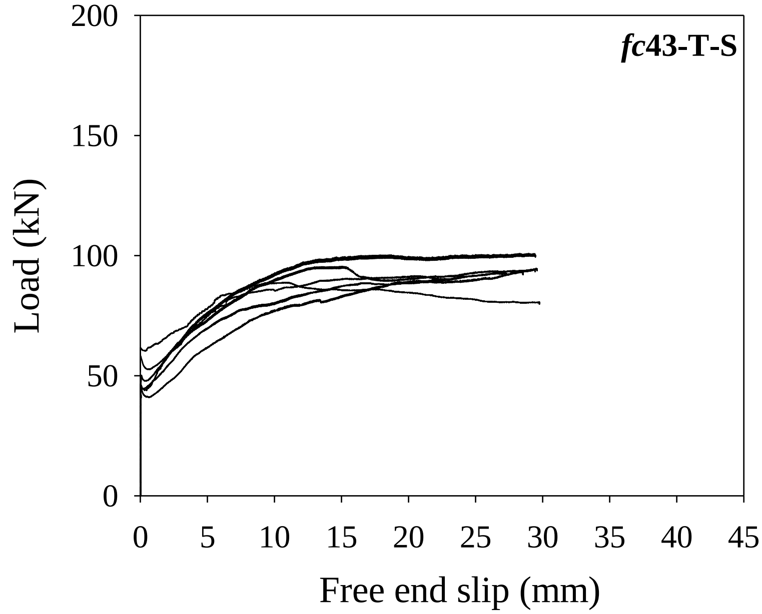

Figure C 5 Load – slip behaviour of taut strands with l_e = 450 mm in f_c = 43 MPa at free end

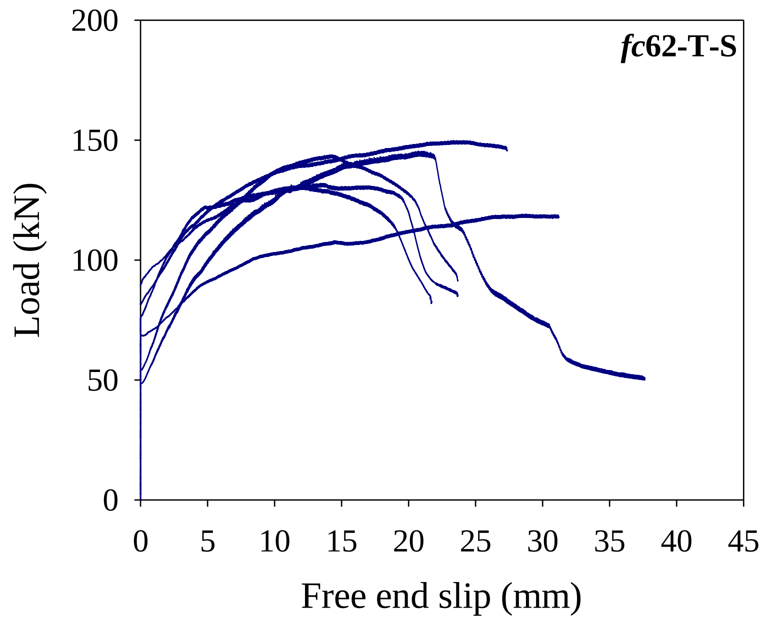

Figure C 6 Load – slip behaviour of taut strands with l_e = 450 mm in f_c = 62 MPa at free end

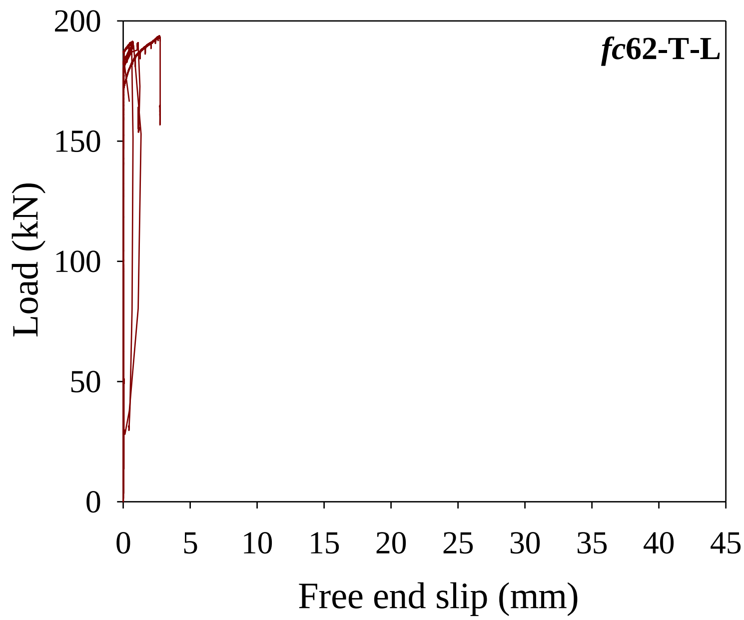

Figure C 7 Load – slip behaviour of taut strands with l_e = 950 mm in f_c = 62 MPa at free end

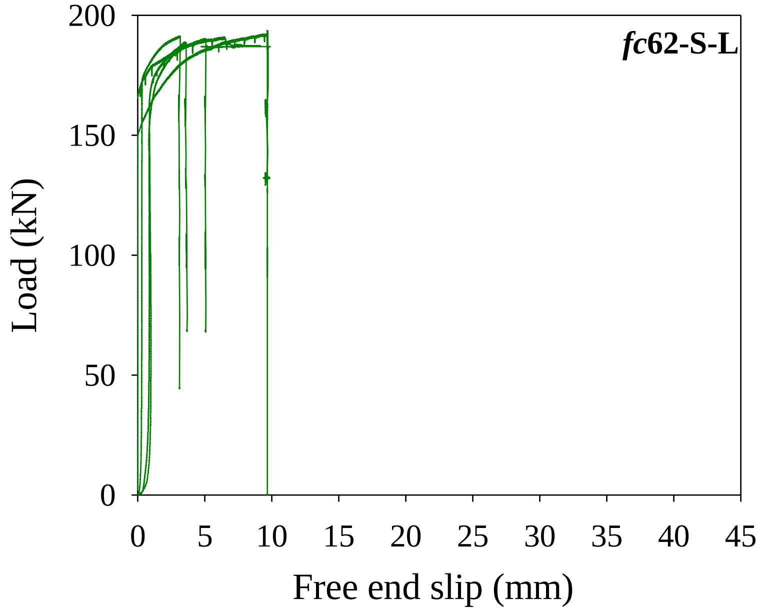

Figure C 8 Load – slip behaviour of stressed strands with l_e = 950 mm in f_c = 62 MPa at free end

APPENDIX D - THE BOND STRESS – SLIP RESPONSE AT LIVE AND FREE ENDS OF THE SPECIMENS

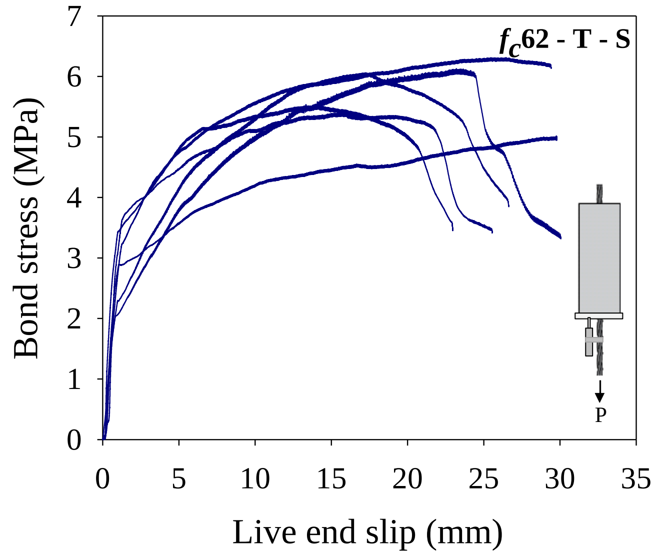

Figure D 1 Bond stress – slip behaviour of taut strands with l_e = 450 mm in f_c = 43 MPa at live end

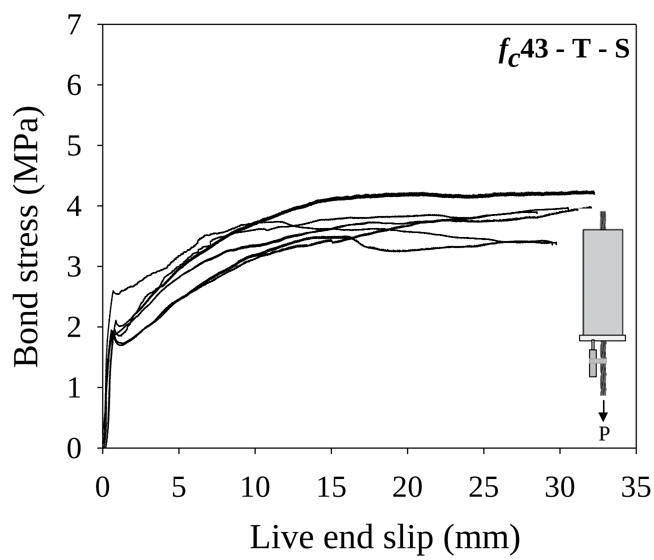

Figure D 2 Bond stress – slip behaviour of taut strands with l_e = 450 mm in f_c = 62 MPa at live end

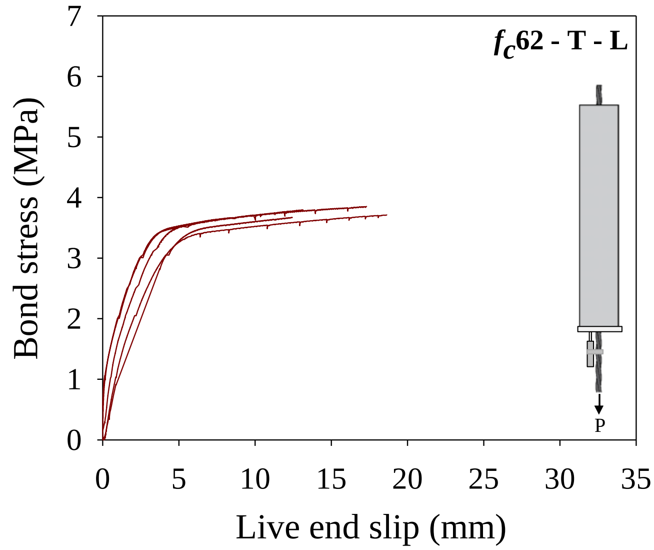

Figure D 3 Bond stress – slip behaviour of taut strands with l_e = 950 mm in f_c = 62 MPa at live end

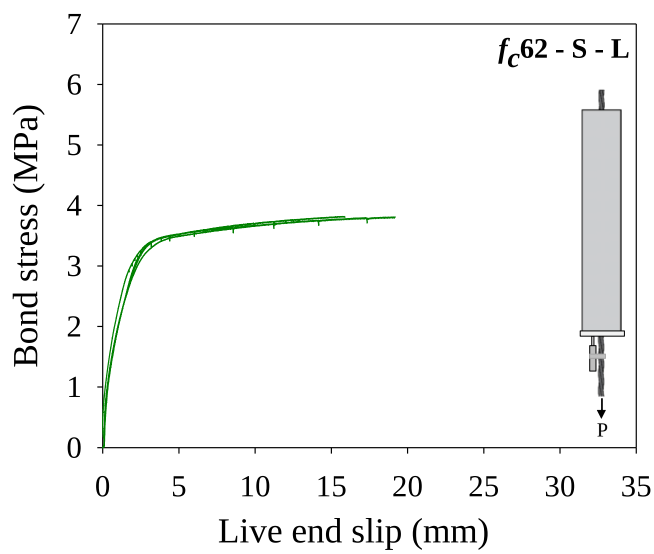

Figure D 4 Bond stress – slip behaviour of stressed strands with l_e = 950 mm in f_c = 62 MPa at live end

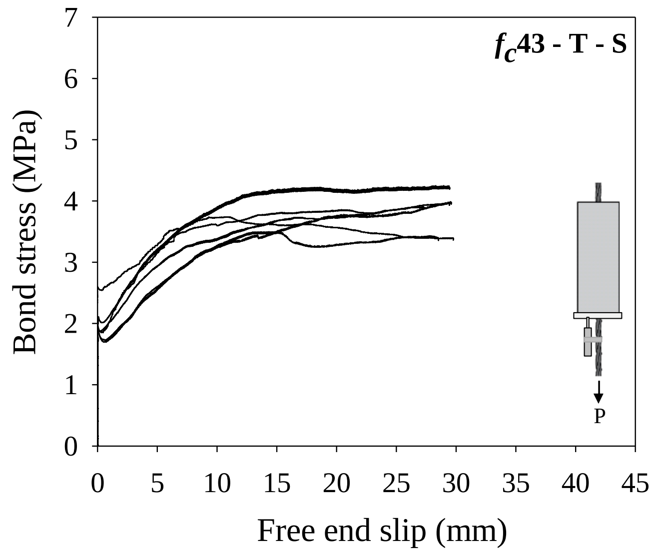

Figure D 5 Bond stress – slip behaviour of taut strands with l_e = 450 mm in f_c = 43 MPa at free end

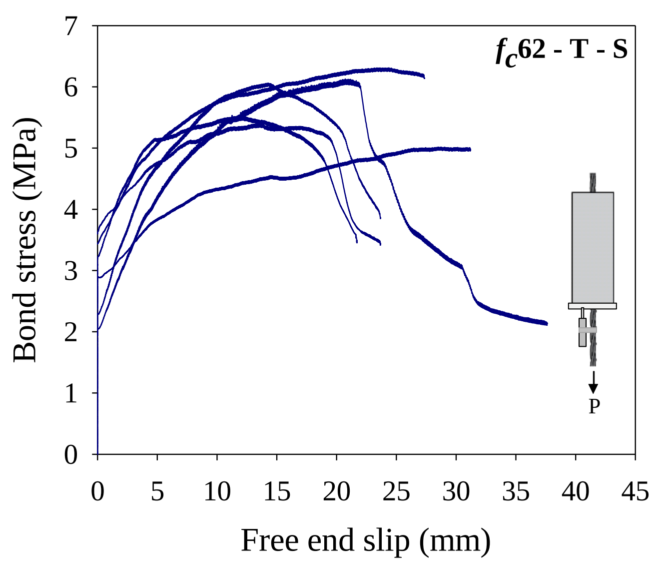

Figure D 6 Bond stress – slip behaviour of taut strands with l_e = 450 mm in f_c = 62 MPa at free end

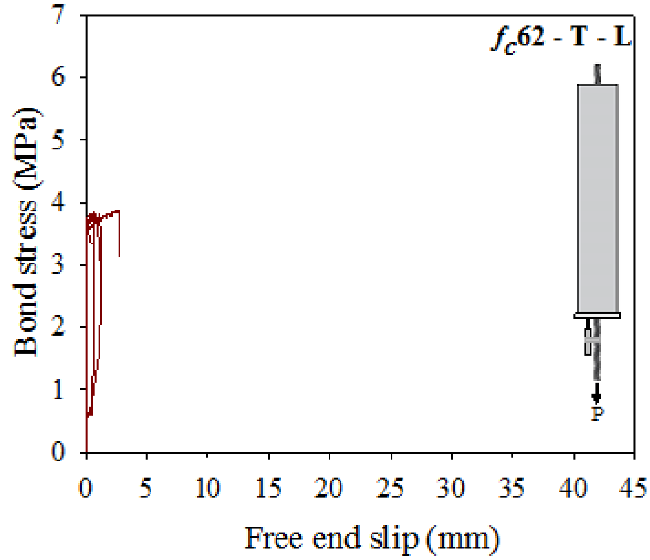

Figure D 7 Bond stress – slip behaviour of taut strands with l_e = 950 mm in f_c = 62 MPa at free end

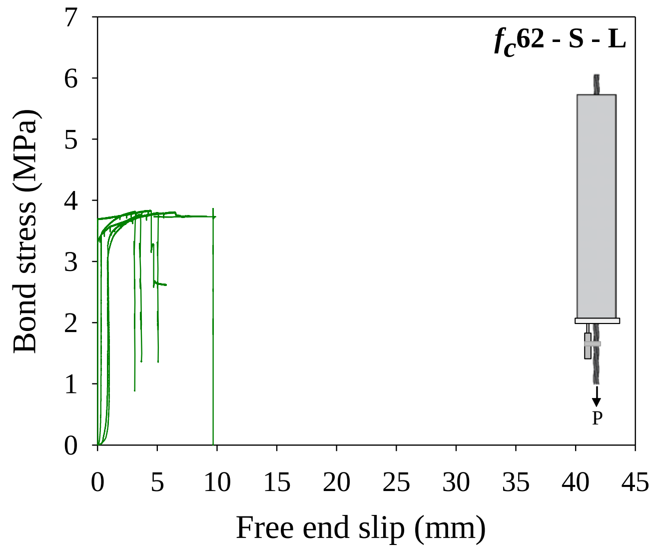

Figure D 8 Bond stress – slip behaviour of stressed strands with l_e = 950 mm in f_c = 62 MPa at free end

LIST OF PUBLICATIONS BASED ON THIS THESIS

REFEREED JOURNALS

1. **Mohandoss P.,** Pillai R. G., and Sengupta A.K. "Transmission length of the pretensioned concrete system: comparison of codes and test data", *Magazine of Concrete Research*, ICE Publications, April 2018, DOI: 10.1680/jmacr.17.00553 [Journal impact factor: 1.488].

2. **Mohandoss P.,** Pillai R. G., and Sengupta A.K. "Effect of compressive strength of concrete on transmission length of pretensioned concrete system"

   (to be re-submitted to *Engineering Structures, Elsevier*)

3. **Mohondoss P.,** Pillai R. G., and Gettu R. "Determination of bond strength in pretensioned concrete systems using 90% yield stress method".

   (Draft ready to be submitted to *Materials and Structures, Springer*)

INTERNATIONAL CONFERENCE PAPERS

* Indicates presenter

1. **Mohandoss P.***, Pillai R.G., and Gettu R., "Effect of Prestress on the Bond strength of Pretensioned Concrete systems", International Conference on Advances in Construction Materials and Systems, 3rd RAIKAR RILEM WEEK and ICACMS, December 15 – 16, 2018.

2. **Mohandoss P.*** and Pillai R.G., "Effect of Prestress on the Bond strength of Pretensioned Concrete systems", International Conference on Advances in Construction Materials and Systems, 71st RILEM WEEK and ICACMS, September 3 - 8, 2017.

3. **Mohandoss P.***, Pillai R.G., and Sengupta A. K., "Comparison of prediction models for transmission length and shear capacity of pretensioned concrete systems", 4th Asian conference on Ecstasy in Concrete (ACECON), Kolkata, India, October 08-10, 2015.

NATIONAL CONFERENCE PAPER

* Indicates presenter

1. **Mohandoss P.*** and Pillai R.G, “Bond performance of pretensioned concrete system”, 10th Structural engineering convention (SEC), Chennai, India, December 21-23, 2016.

SPECIAL PUBLICATION

1. **Mohandoss P**, Kompella K. S., and Pillai R. P., “Bond performance of pre-tensioned concrete system”, Proceedings of SEC 2016, Recent advances in Structural Engineering, Volume 1, Chapter 22, Springer publication, DOI: 10.1007/978-981-13-0362-3_22.

INTERNATIONAL CONFERENCE PRESENTATIONS

* Indicates presenter

1. **Mohandoss P.***, Pillai R. G., Gettu R., and Sengupta A. K. “Assessment of the bond strength of pretensioned strands in concrete”, Concrete Research in India, Mumbai, India, December 14, 2018. (Poster presentation)
2. **Mohandoss P.***, Pillai R. G., Gettu R., and Sengupta A. K. “Strand-Concrete Bond in Pretensioned Concrete Systems (PTC)-Mechanisms and Laboratory Testing” the ACI 123 Concrete Research Poster Session at the Spring 2018 ACI Convention and Exposition in Salt Lake City, UT, USA, 24 – 28th March, 2018. (Poster presentation)
3. **Mohandoss P.***, Kompella S. K., Gettu N., and Pillai R. G., “A Study on the bond performance of pre-tensioned concrete system”, International Conference on Advances in Construction Materials and Systems, 71st RILEM WEEK and ICACMS, 3rd – 8th September 2017. (Poster presentation)
4. **Mohandoss P.***, Kompella S. K., Maheswari S. K., Nair S. A. O., and Pillai R. G., “Factors influencing the bond behaviour of pretensioned concrete system” Gordon research conference (GRC), Hong Kong, China, July 31st – August 8th, 2016. (Poster presentation)
5. **Mohandoss P.***, Pillai R. G., Gettu R., and Sengupta A. K. “Effect of compressive strength of concrete on transmission length of pretensioned concrete” the ACI Open Topic Session at the Spring 2018 ACI Convention and Exposition in Salt Lake City, UT, USA, 24 – 28th March, 2018 (Oral Presentation)

6. Kompella S. K.*, **Mohandoss P**., Gettu N., and Pillai R. G., “Enhancing the bond strength of prestressed concrete sleepers”, Concrete Research in India, Research Scholar Symposium, Mumbai, India, December 14 -15, 2018. (Poster presentation)
7. Kompella S. K.*, Gettu N., **Mohandoss P**., and Pillai R. G., “A study on the performance of bond in pre-tensioned concrete railroad ties (sleepers)”, the concrete convention and exposition, American concrete institute, Detroit, USA, 26-30th March, 2017. (Oral presentation)

DOCTORAL COMMITTEE

CHAIRPERSON	Dr. K. Ramamurthy Professor and Head Department of Civil Engineering
GUIDE	Dr. Radhakrishna G. Pillai Associate Professor Department of Civil Engineering
MEMBERS	Dr.Ravindra Gettu Professor Department of Civil Engineering
	Dr. Amlan Kumar Sengupta Professor Department of Civil Engineering
	Dr. Srinivasan Chandrasekaran Professor Department of Ocean Engineering

CURRICULUM VITAE

Name	:	Prabha Mohandoss
Date of birth	:	June 24, 1990

Educational qualifications

2011	:	**Bachelor of Engineering (B.E.)**
Institution	:	Thiagarajar College of Engineering Madurai, Tamil Nadu, India
Specialization	:	Civil Engineering
2013	:	**Master of Engineering (M.E.)**
Institution	:	Anna University: Regional Centre Madurai, India
Specialization	:	Structural Engineering
2018	:	**Doctor of Philosophy (Ph.D.)**
Institution	:	Indian Institute of Technology Madras Chennai, India
Specialization	:	Bond performance of steel-concrete systems Civil Engineering